Statistical Analysis of Neuroimaging Data

Hongtu Zhu, Ph.D

Department of Biostatistics and
Biomedical Research Imaging Center,
University of North Carolina at Chapel Hill

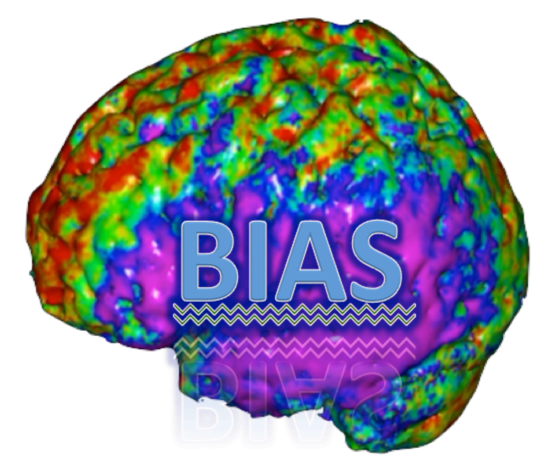

Outline

Imaging Science

Imaging Modalities

Data

Projects

Imaging Science

Imaging Science
From Wikipedia, the free encyclopedia

Imaging Science

is a multidisciplinary field concerned with the generation, collection, duplication, analysis, modification, and visualization of images.

As an evolving field, it includes research and researchers from

Physics, Mathematics, Statistics, Electrical Engineering, Computer Vision, Computer Science and Perceptual Psychology.

Three key components of imaging science

- **Image acquisition:** studies the physical mechanisms and mathematical models and algorithms by which imaging devices generate image observations.
- **Image interpretation/application:** is to see, monitor, and Interpret the targeted world/patterns being imaged.
- **Image processing:** is any linear or nonlinear operator that operates on the images and produces targeted patterns.

What is image?

(i) In computer science an image is an exact replica of the contents of a storage device (a hard disk drive or CD-ROM for example) stored on a second storage device.
(ii) is an optically formed duplicate or other reproduction of an object formed by a lens or mirror.



Mathematics. Image is the point or set of points in the range corresponding to a designated point in the domain of a given function.

As $\tilde{x} \in \Omega \subseteq R^k \quad f(\tilde{x}) \in M \subseteq R^m \quad f : \Omega \to M \subseteq R^m$

Ω is a compact set.

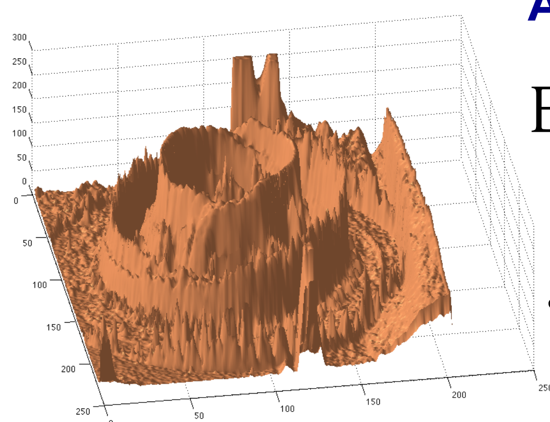

Additional Conditions:

Each component of $f(\tilde{x})$ is nonnegative.

$$\int_\Omega \| f(\tilde{x}) \|^k \, d\tilde{x} < \infty \quad \text{for any } k > 0$$

Digitized Images $f : \Omega_0 \to \{0, 1, \cdots, M_0\}$

- **Sampling (grid points):** $\Omega_0 \in \Omega$

  An ordered array or a triangular array or etc;

  A set of small cells of the same shape and size (pixels, voxels).

  Sometime, it involves interpolation.

  Sampling Rate ensure that all the relevant information contained in the image is largely retained by sampling.

- **Quantization:** is a process of assigning the function value at each sampling point to one of the finite set of integers.

$$0, 1, 2, \cdots, 2^m \text{ for } m = 5 \sim 12, \text{that is } M_0 = 2^{\mathrm{m}}$$

General Digital Image

$$f(x,y,z,t,s):\Omega \rightarrow \{0,1,\cdots,M_0\}$$

- Spatial parameters

  (x,y,z)
- Time parameters

  t
- Spectral parameters

  s
- A limited range of values

  M_0

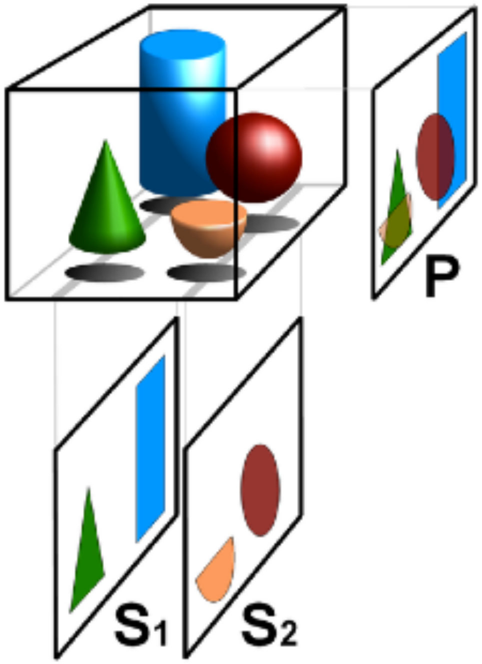

- Spatial resolution
- Temporal resolution
- Spectral resolution

  Range of wave-length

  Number of color
- Gray scale resolution

Imaging Modalities

Imaging Devices

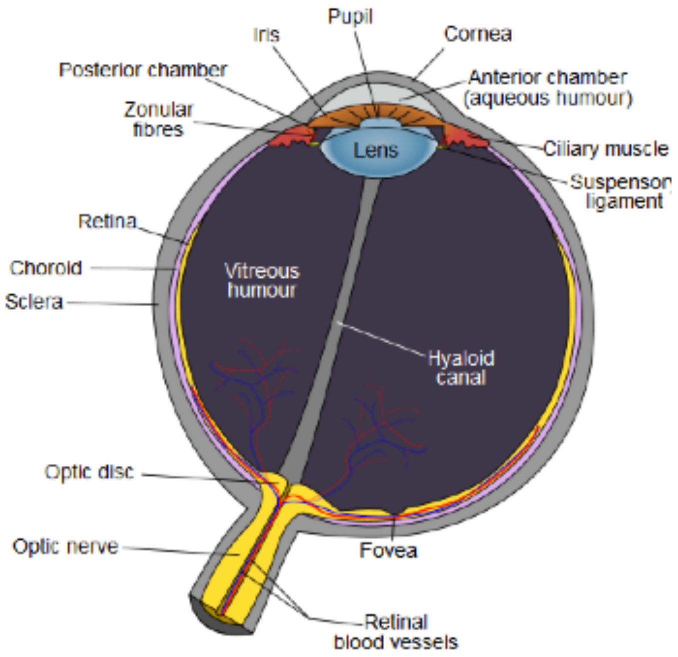

Figure 5.13 PET scanner. A movable table shifts the patient through the circular hole in the gantry. The external design is similar to that of a CT scanner and to some extent to that of an MRI scanner. (Courtesy of the Department of Nuclear Medicine.)

Targets

- Electromagnetic waves (most technologies)
- Sound (ultrasound)
- Particles (electron microscopy)
- Mechanical contact forces (scanning probe microscopy)

Electromagnetic Waves

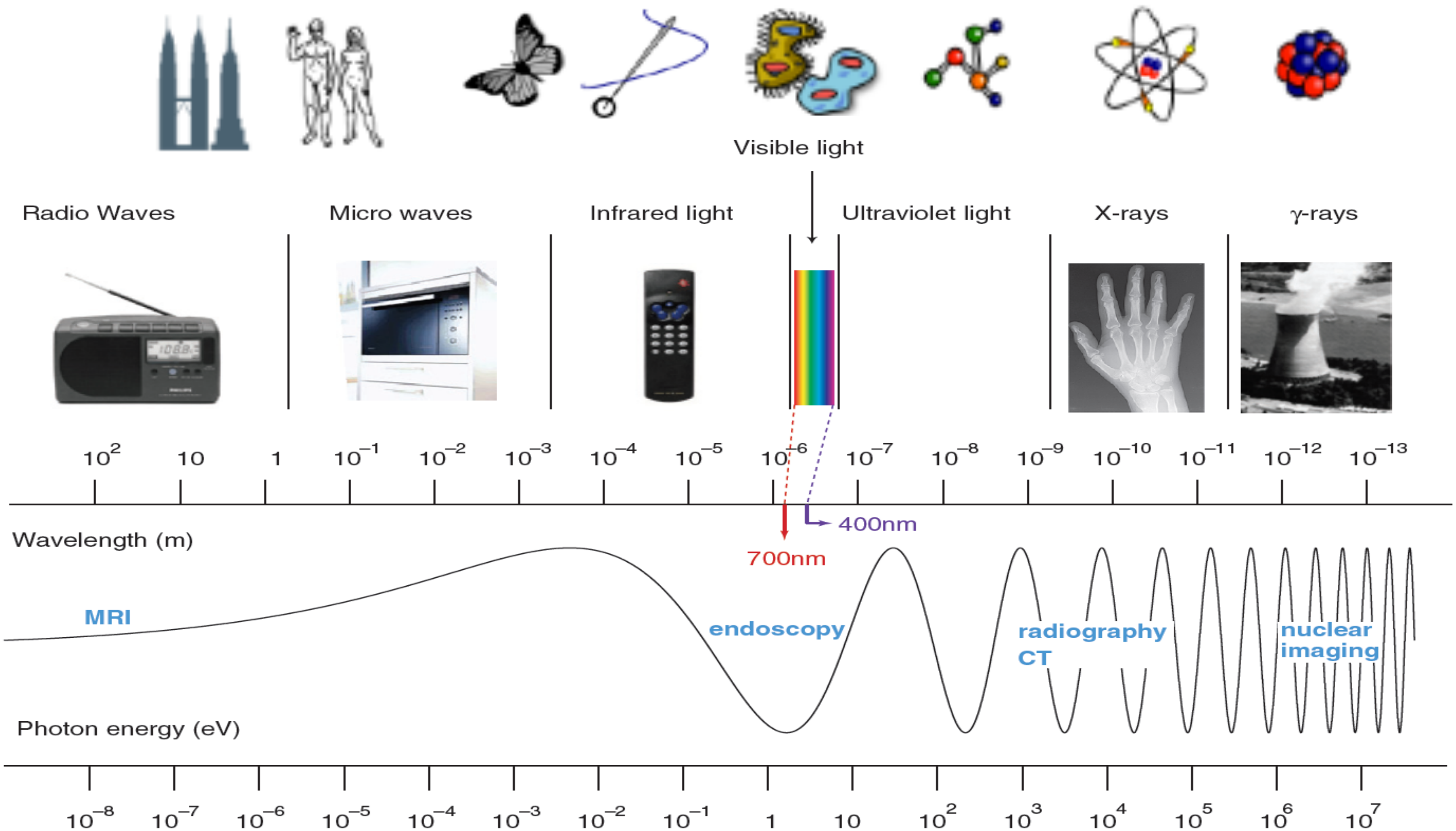

Figure 2.1 The electromagnetic spectrum.

nm (nanometer, E-9m)

Electromagnetic Imaging

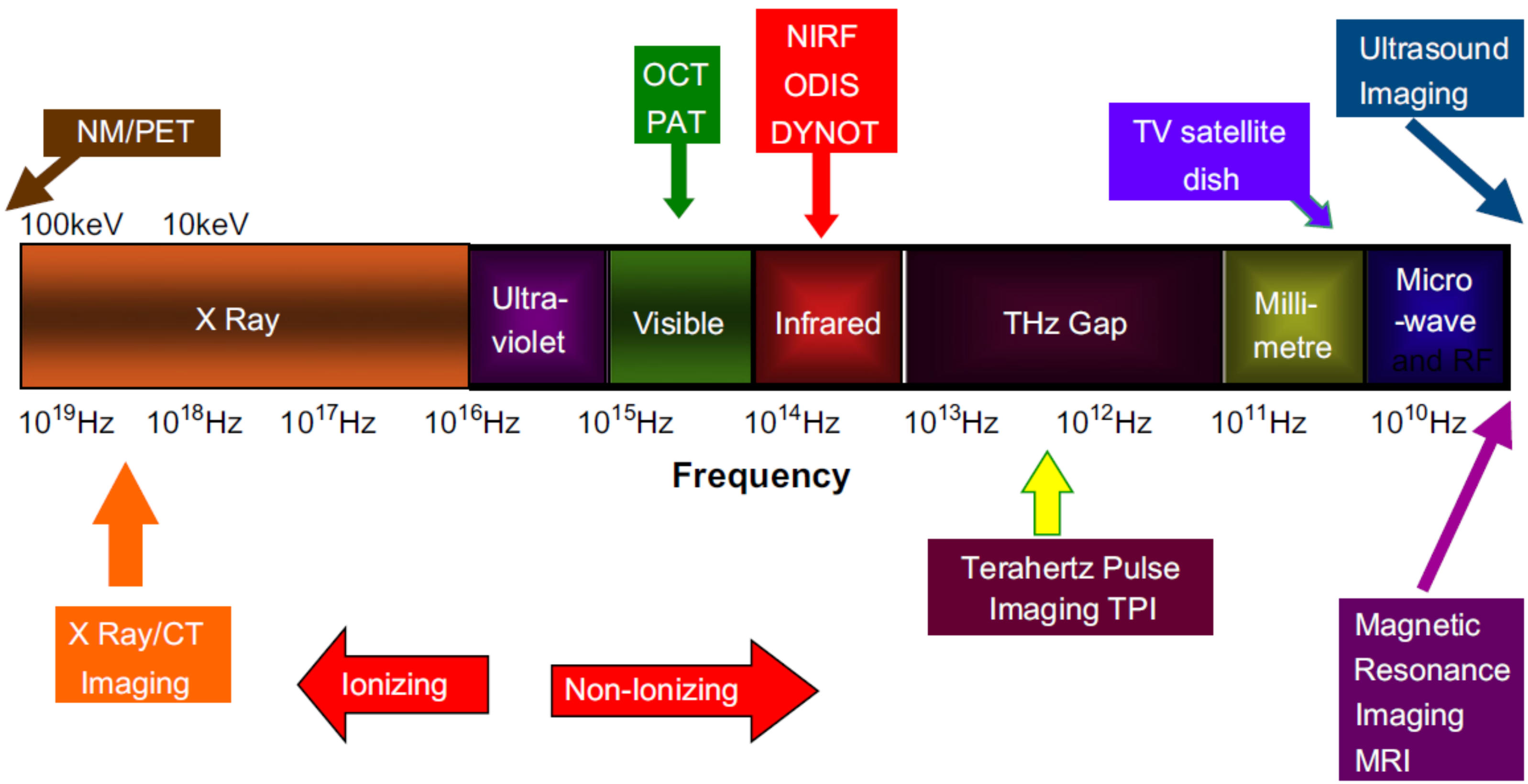

Figure 4 – Frequency spectrum of electromagnetic radiation imaging technologies.

Electromagnetic Imaging

- Radio range: radio astronomy, MRI
- Microwave range: RADAR
- Visible range: Standard camera, light microscopy
- X-ray range: CT, micro-CT
- Gamma range: Gamma camera

Medical imaging
From Wikipedia, the free encyclopedia

- Medical imaging is the technique and process used to create images of the human body (or parts and function thereof) for clinical purposes (medical procedures seeking to reveal, diagnose or examine disease) or medical science (including the study of normal anatomy and physiology).
- 2010, 5 billion medical imaging studies were done worldwide.

X-rays are ionizing waves consisting of photons traveling at the speed of light with energy E=hf

- X-rays produced by a tube.
- Filtered to removed undesired energy.
- Restriction to illuminate organ of interest
- Grid removes scattered radiation.
- Recording of image on electronic plate (or film).

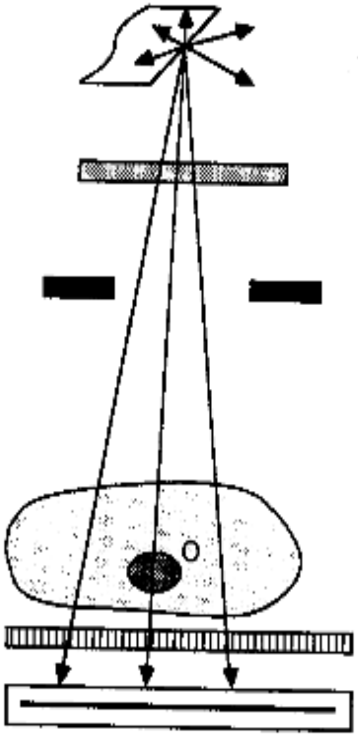

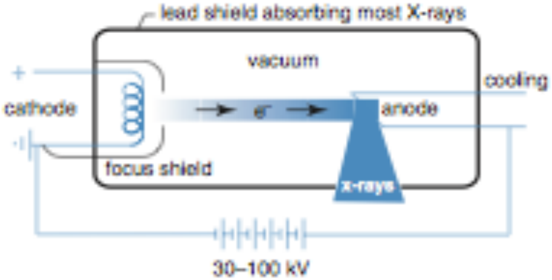

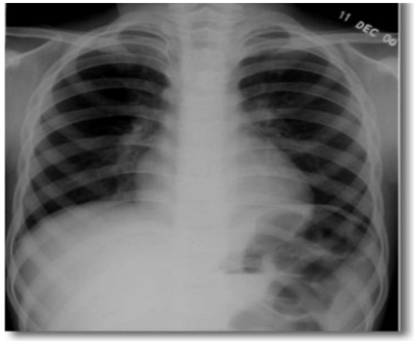

Computed Tomography (3D X-rays) is a imaging method employing tomography created by computer. Digital geometry processing is used to generate a 3D image of the inside of an object from a large series of 2D X-ray images taken around a single axis of rotation.

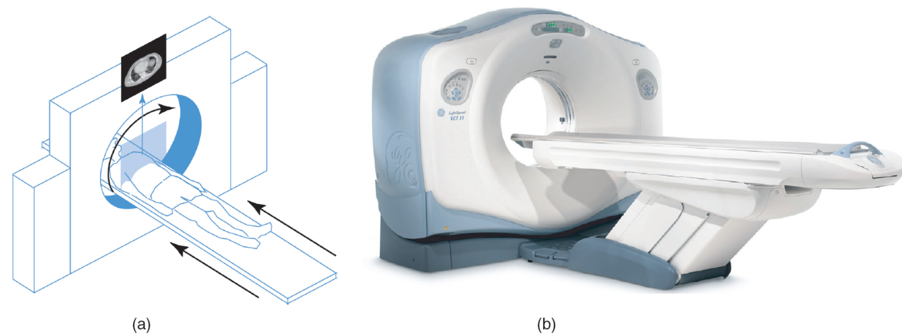

Figure 3.1 **(a)** Schematic representation, and **(b)** photograph of a CT scanner. (Courtesy of GE Healthcare.)

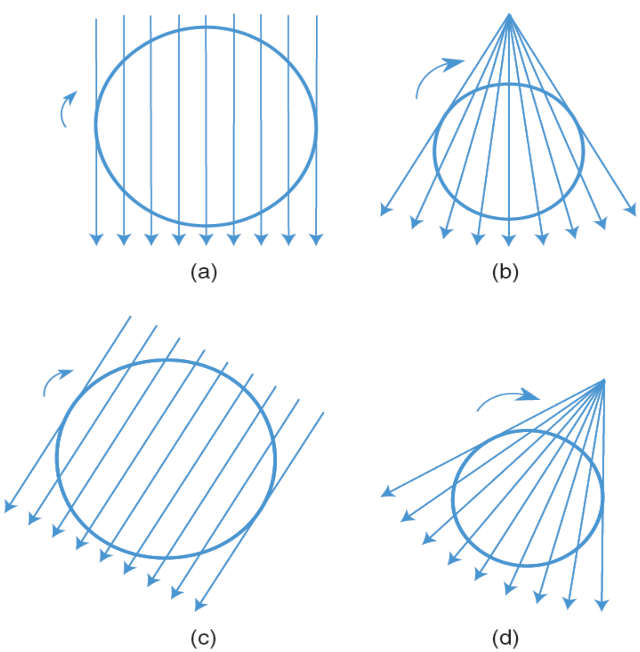

Figure 3.2 Basic scanning procedure in CT. A set of lines is scanned covering the entire field of view: **(a)** parallel-beam geometry and **(b)** fan-beam geometry. This process is repeated for a large number of angles (**c** and **d**).

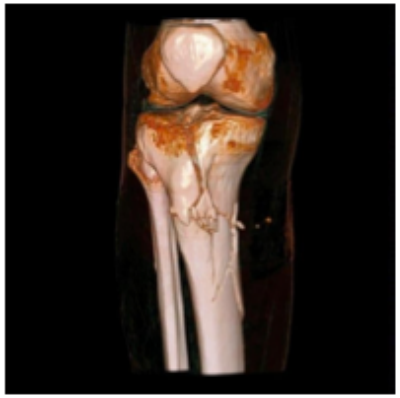

SPECT and PET

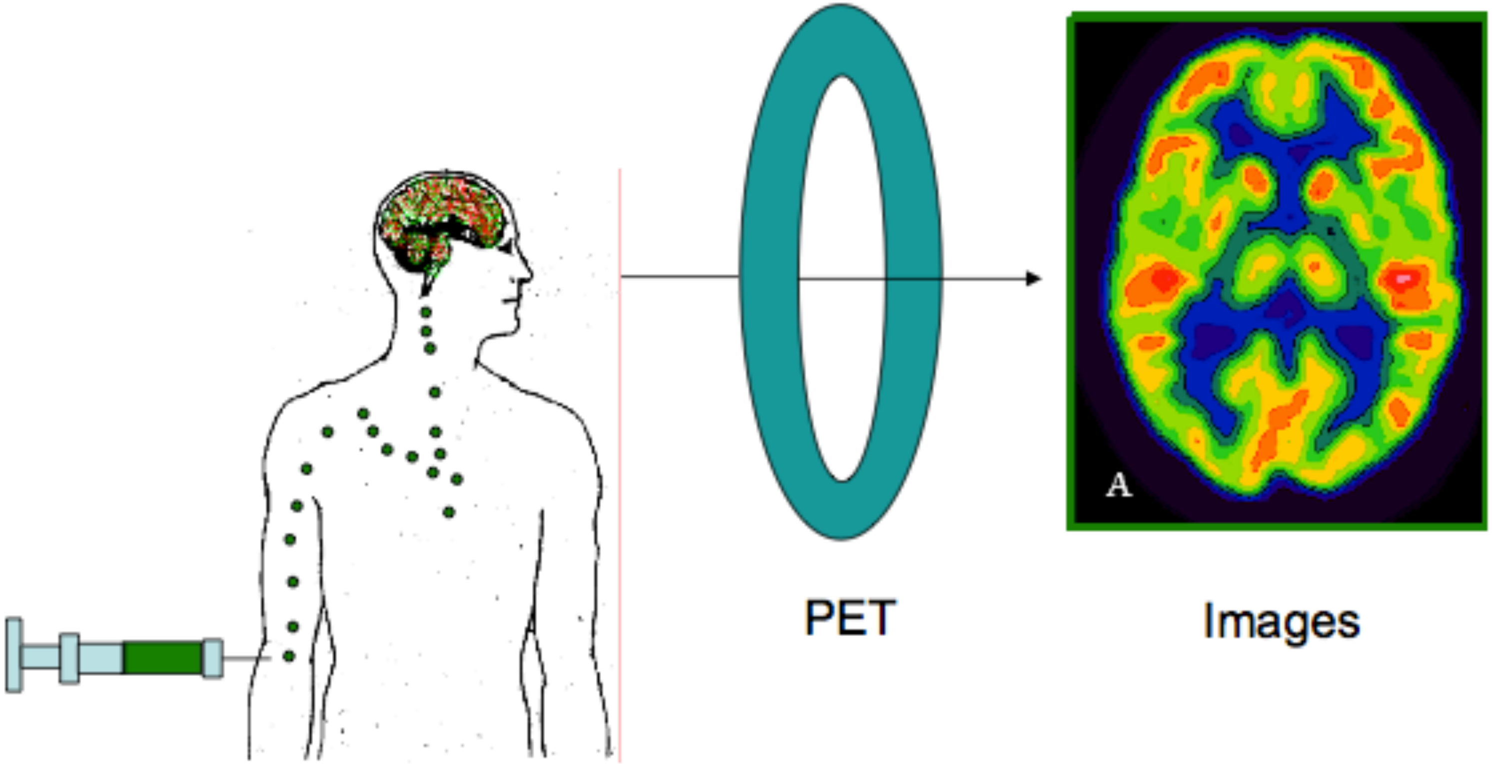

SPECT=Single-Photon Emission Computed Tomography

is a nuclear medicine tomographic imaging technique using gamma rays for measuring the blood flow to the brain.

Radio-labeled chemical (ECD or HMPAO) is quickly injected at time of seizure onset to detect the region of increased blood flow, which is associated with seizure activity.

By comparing the ictal scan (imaged during seizure) and the interictal scan (imaged without seizure), the regions of activation in the brain are detected to locate the seizure origin.

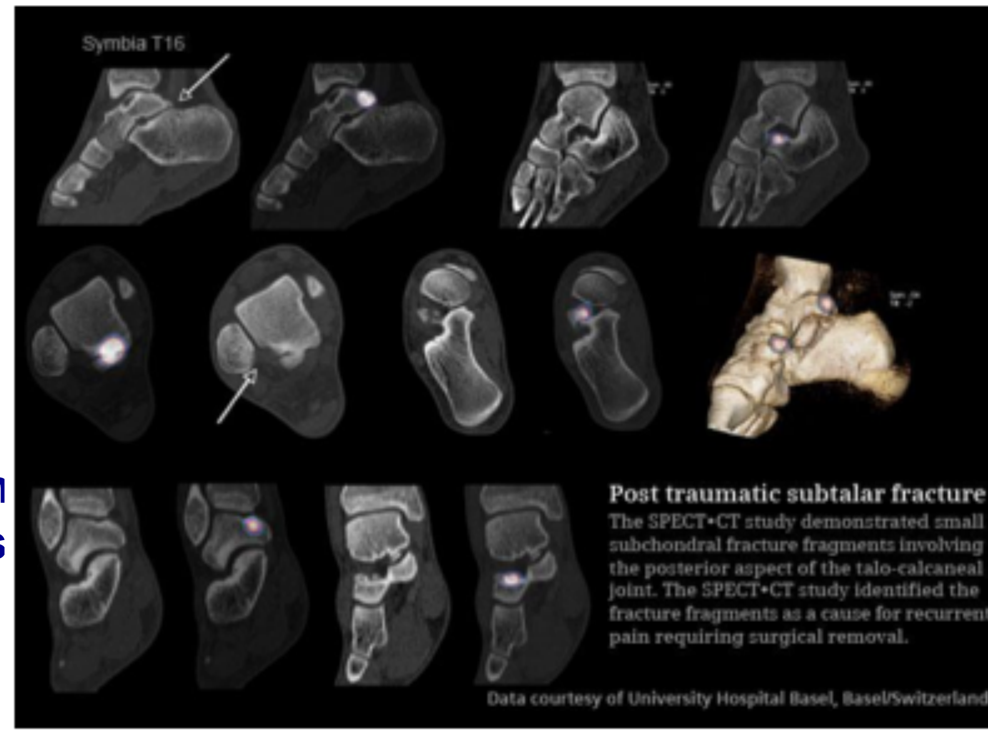

http://www.youtube.com/watch?v=l6V6VLxQlkY

PET=Positron Emission Tomography is a functional imaging technique to extensively study the relationship between energy consumption and neuronal activity. It uses positron-emitting radioactive tracers that are attached to molecules that enter biological pathways of interest.

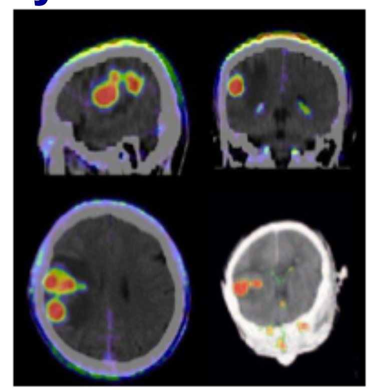

FDG: Fluorodeoxyglucose (similar to Glucose).

Brain uses glucose as major source of energy. Normal brain picks up FDG in a large amount.

In epilepsy, the brain cell (neuron) does not function right or the neurons are lost due to a variety of reasons.

FDG-PET scan detects the regions of brain where the Glucose uptake is low (hypo-metabolism), which is often associated with the site of seizure origin.

PET measures

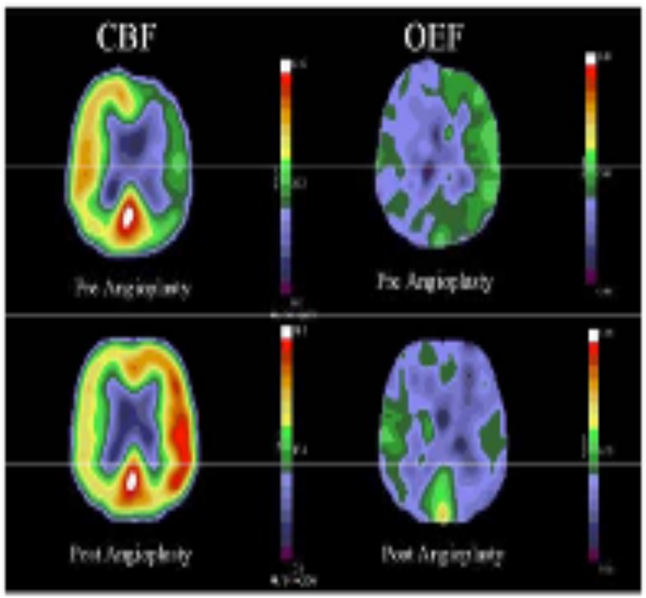

Reduced Cerebral Blood Flow (CBF) and elevated compensatory Oxygen Extraction (OEF) before and after carotid artery angioplasty (stroke risk)

PET tracers

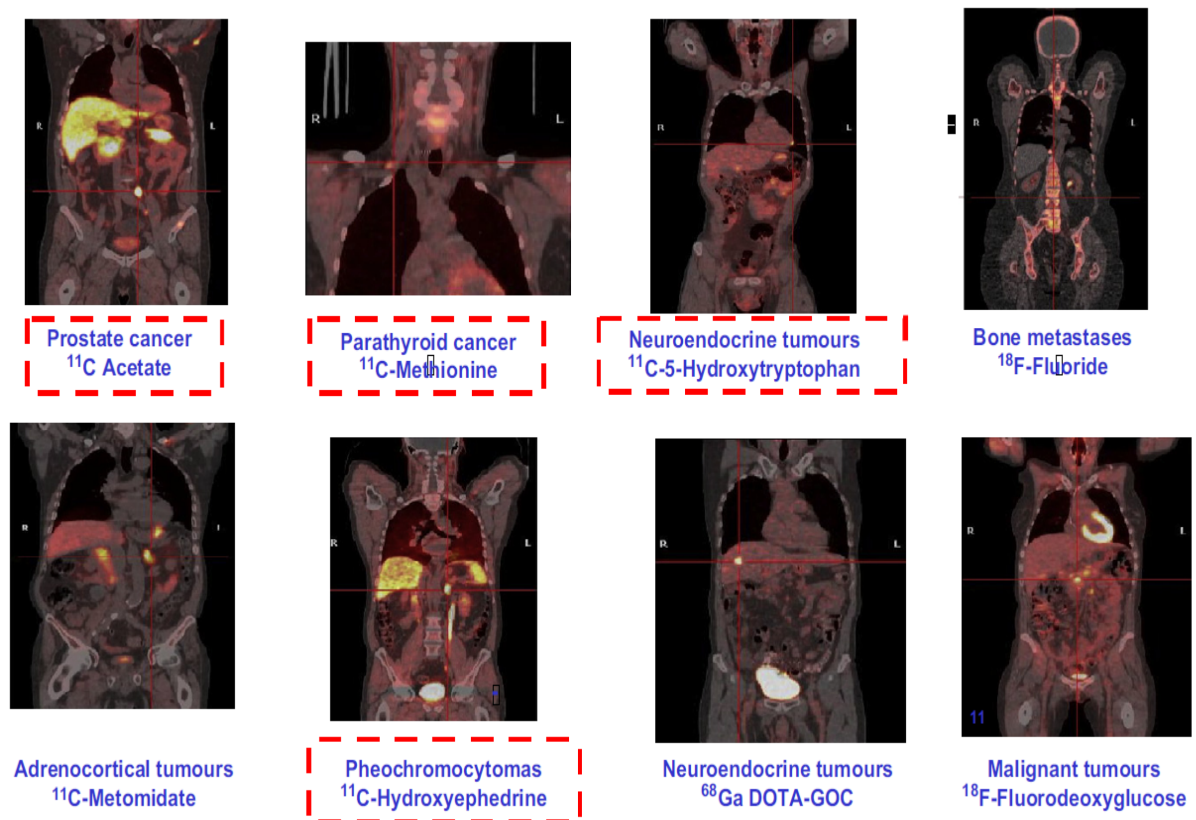

Figure 13 – Examples of PET tracers in oncology where endogenous substances are framed (courtesy of Imanet Uppsala).

PET and SPECT

PET and SPECT scan is different from CT, MRI or Ultrasound, which detect structure changes and anatomy, can provide physiological and molecular information of brain.

PET and SPECT are clinically indicated for pre-surgical localization of seizure origin. They are covered by most insurance providers.

They provide valuable seizure localization information in addition to MRI scan, EEG and clinical assessment to the surgeons.

Ultrasound imaging involves exposing part of the body to high-frequency sound waves to produce pictures of the inside of the body.

- Because ultrasound images are captured in real-time, they can show the structure and movement of the body's internal organs, as well as blood flowing through blood vessels.

- When a sound wave strikes an object, it bounces back, or echoes. By measuring these echo waves it is possible to determine how far away the object is and its size, shape, and consistency (whether the object is solid, filled with fluid, or both).

- In medicine, ultrasound is used to detect changes in appearance of organs, tissues, and vessels or detect abnormal masses, such as tumors.

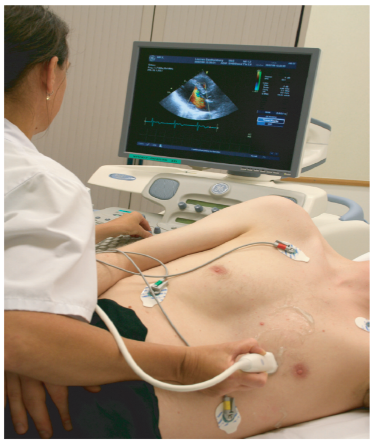

Figure 6.34 Example of a commercial echocardiographic scanner. (Courtesy of the Department of Cardiology.)

Fetus at 14 weeks

Fetus at 29 weeks

2D transducer: general appearance

Magnetic Resonance Imaging (MRI) is to visualize detailed internal structures. The good contrast is provides between the different soft tissues of the body make it useful in brain, muscles, heart, and cancer.
No ionizing radiation.

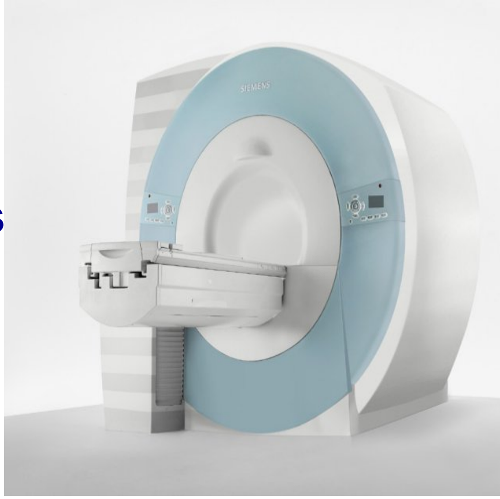

It uses a powerful magnetic field to align the magnetization of some atoms in the body, then uses radio frequency fields to systematically alter the alignment of this magnetization. This causes the nuclei to produce a rotating magnetic field detectable by the scanner.

Paul Lauterbur and Peter Mansfield were awarded the 2003 Nobel Prize in Physiology or Medicine for their "discoveries concerning magnetic resonance imaging".

http://www.youtube.com/watch?v=6_2D3Lh1v74&feature=related

Magnetic Resonance Imaging (MRI)

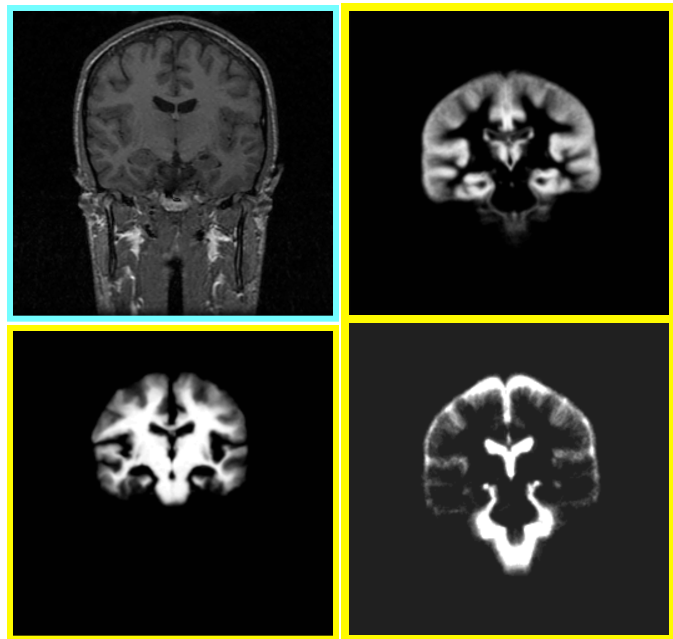

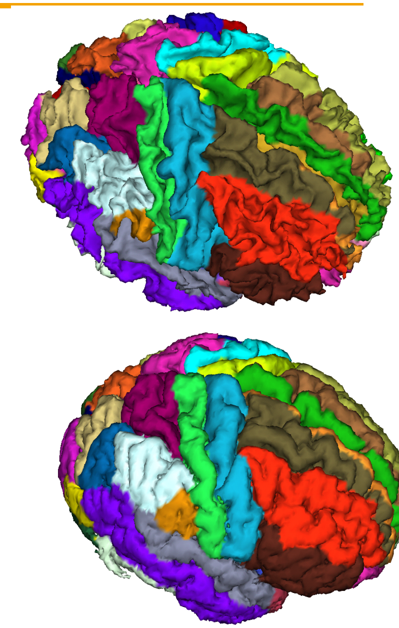

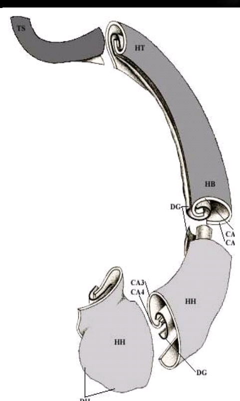

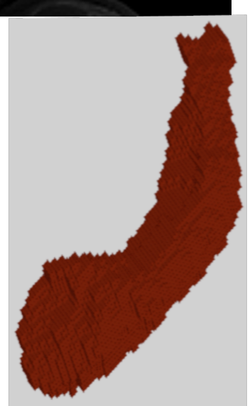

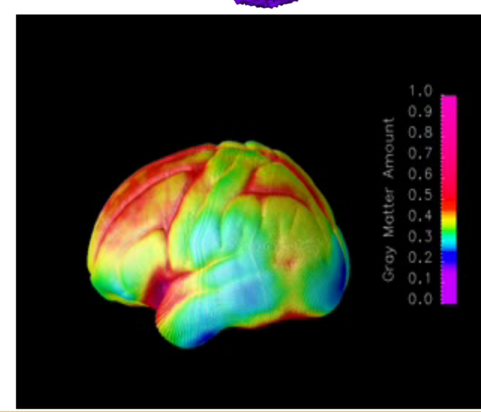

Functional MRI measures the hemodynamic response (change in blood flow) related to neural activity in the brain or spinal cord of humans or other animals. Since the early 1990s, fMRI has come to dominate the brain mapping field due to low invasiveness, absence of radiation exposure, and relatively wide availability.

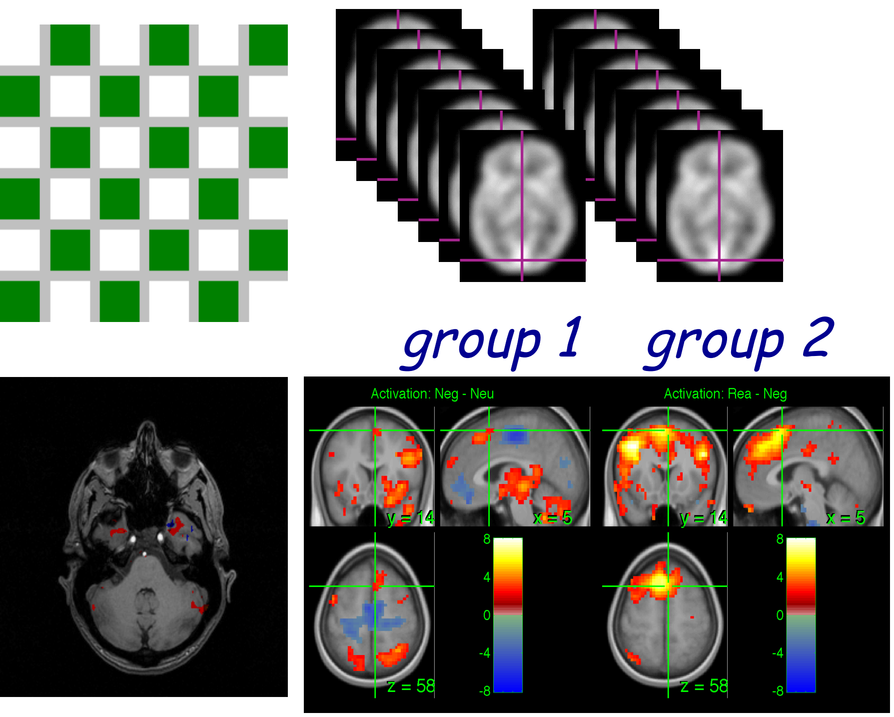

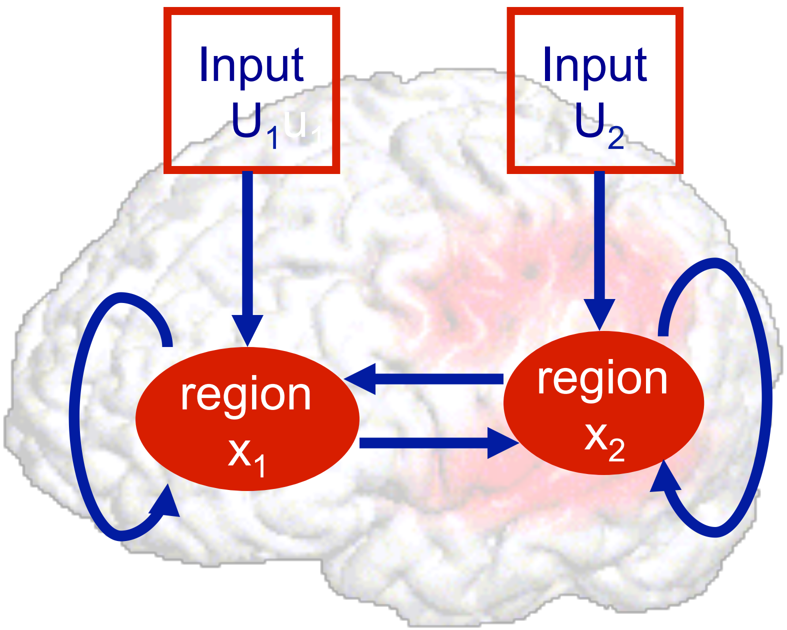

Diffusion MRI can provide information about damage to parts of the nervous system and about white matter connections among brain regions.

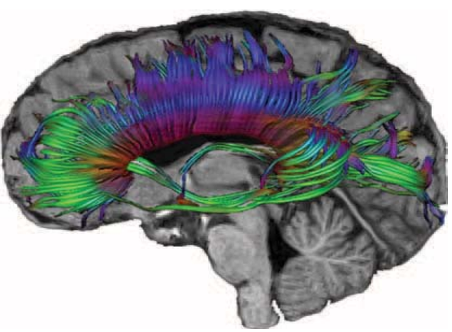

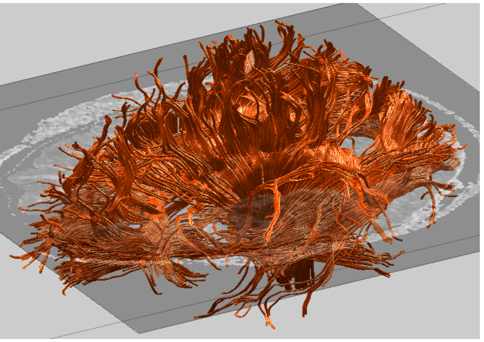

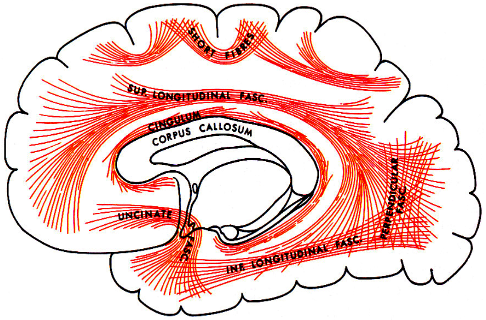

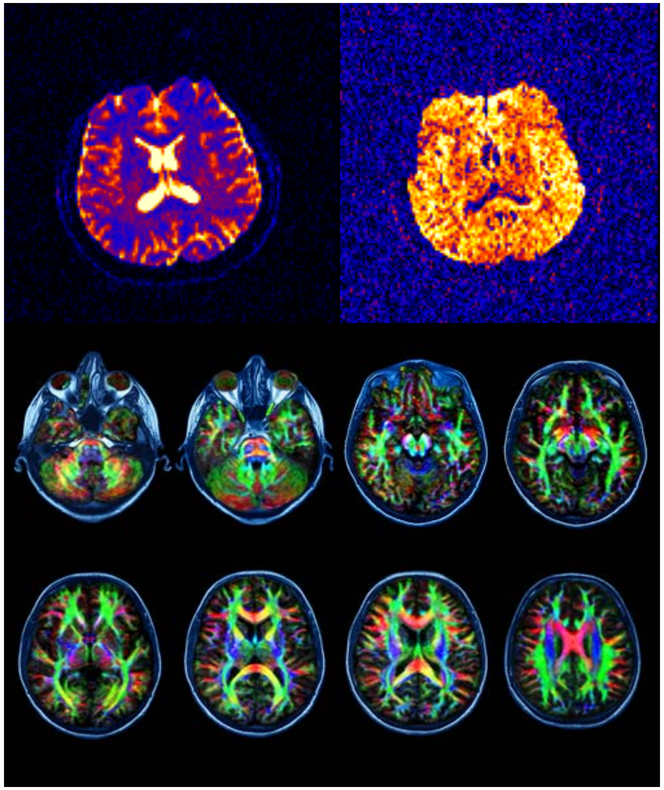

http://www.youtube.com/watch?v=XwUn64d5Ddk&feature=related

Molecular Imaging originated from the field of radiopharmacology to better understand the molecular pathways inside organisms.

- Molecular imaging uses biomarkers to help image particular targets or pathways. Probes interact chemically with their surroundings and in turn alter the image according to molecular changes occurring with the area of interest.

- This process is markedly different from previous methods of imaging which primarily imaged differences in qualities such as density or water content.

- This ability to image fine molecular changes opens up an incredible number of exciting possibilities for medical application, including early detection and treatment of disease and basic pharmaceutical development.

- Molecular imaging allows for quantitative tests, imparting a greater degree of objectivity to the study of these areas.

Molecular imaging & therapy

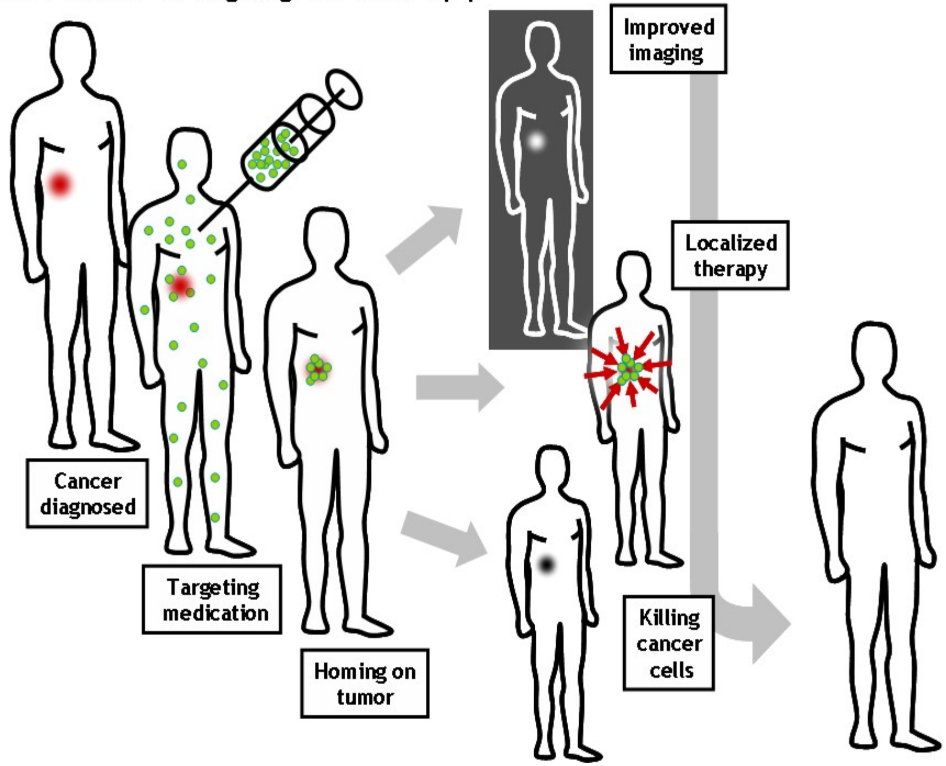

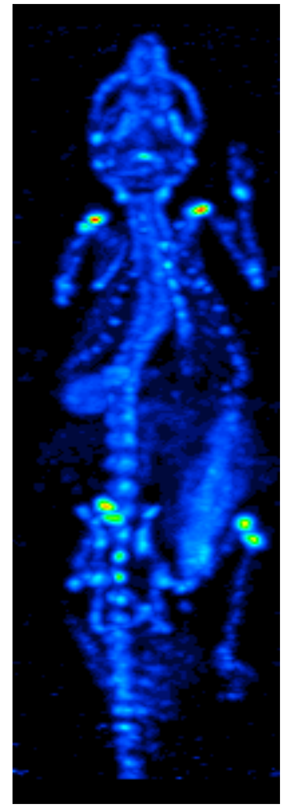

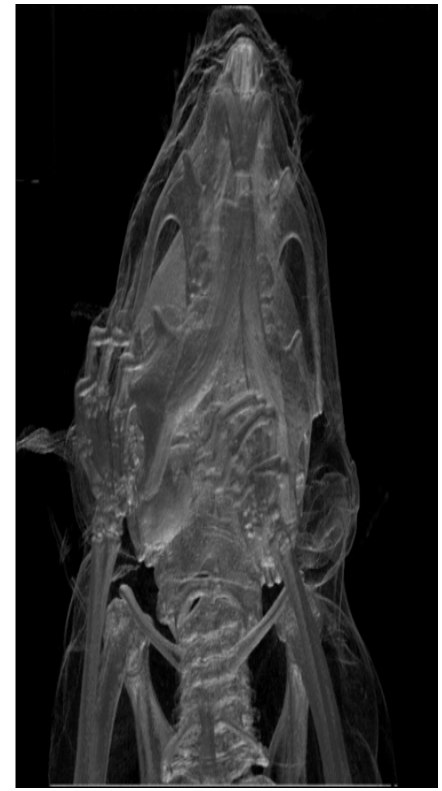

Data

Large Neuroimaging Data

- NIH normal brain development
- 1000 Functional Connectome Project
- Alzheimer's Disease Neuroimaging Initiative
- National Database for Autism Research (NDAR)
- Human Connectome Project

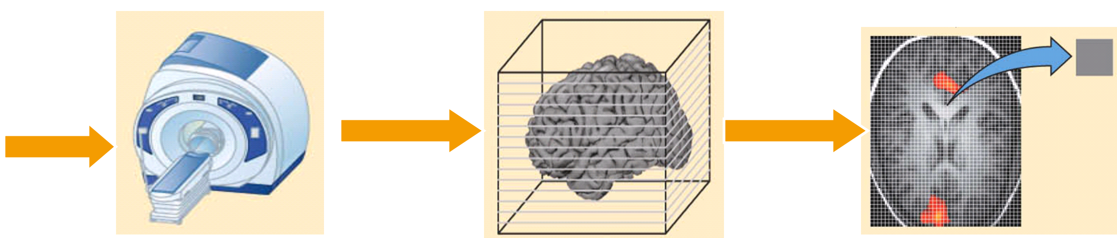

www.guysandstthomas.nhs.uk/.../T/Twins400.jpg

Complex Study Design:

cross-sectional studies;

clustered studies including

longitudinal and twin/familial studies;

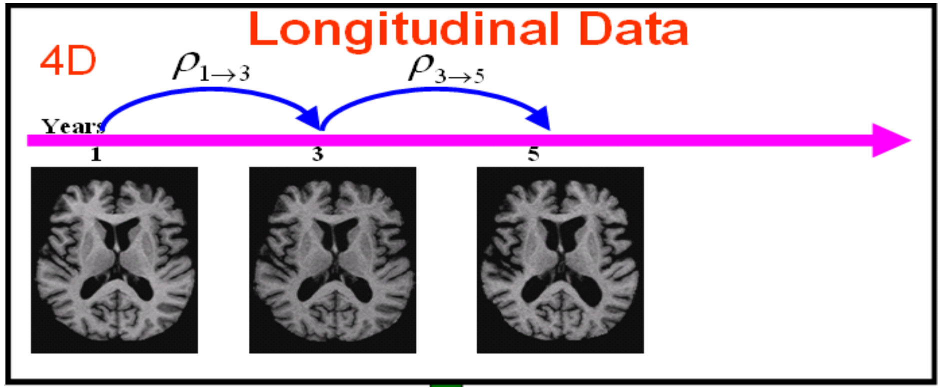

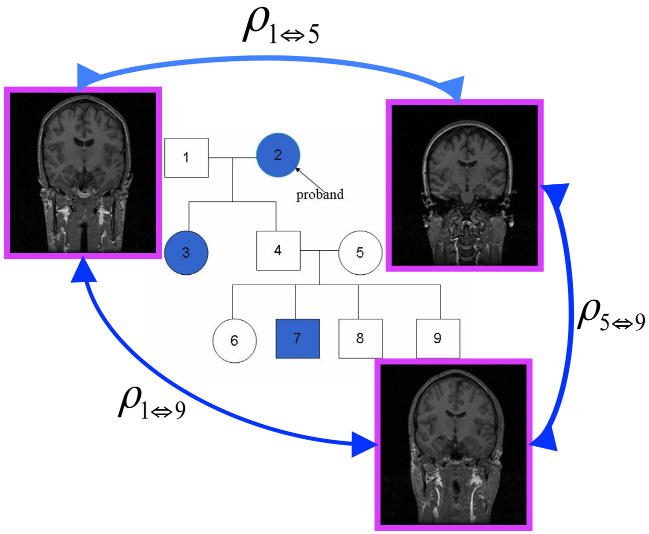

Complex Data Structure

Multivariate Imaging Measures

Smoothed Functional Imaging Measures

Whole-brain Imaging Measures

Time Series Imaging Measures

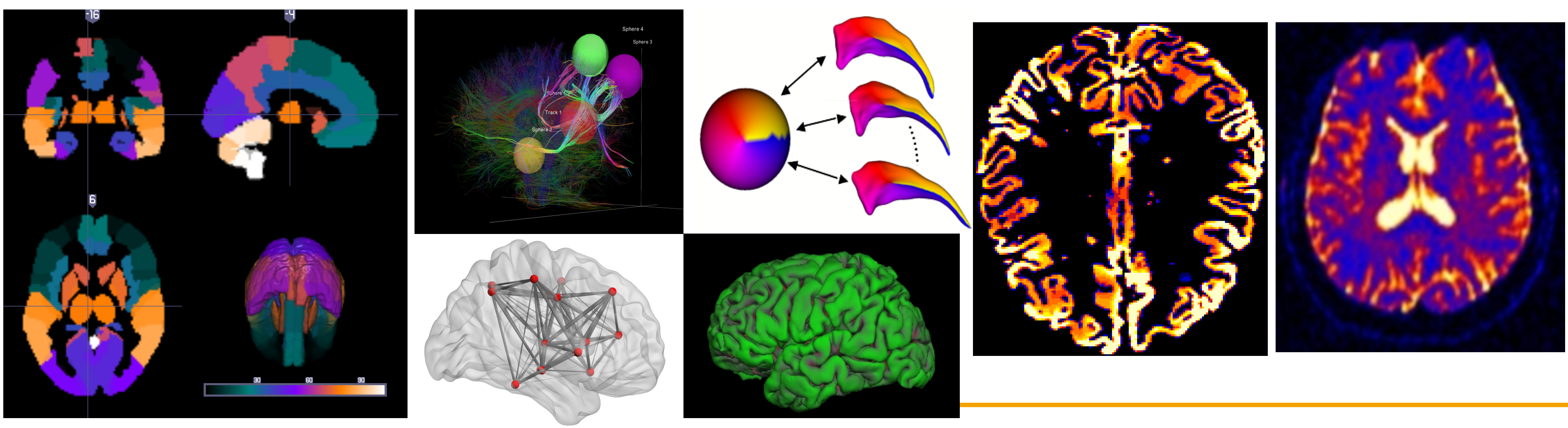

Anatomical Connectivity: a pattern of anatomical links;
Functional Connectivity: statistical dependencies;
Effective Connectivity: causal interactions

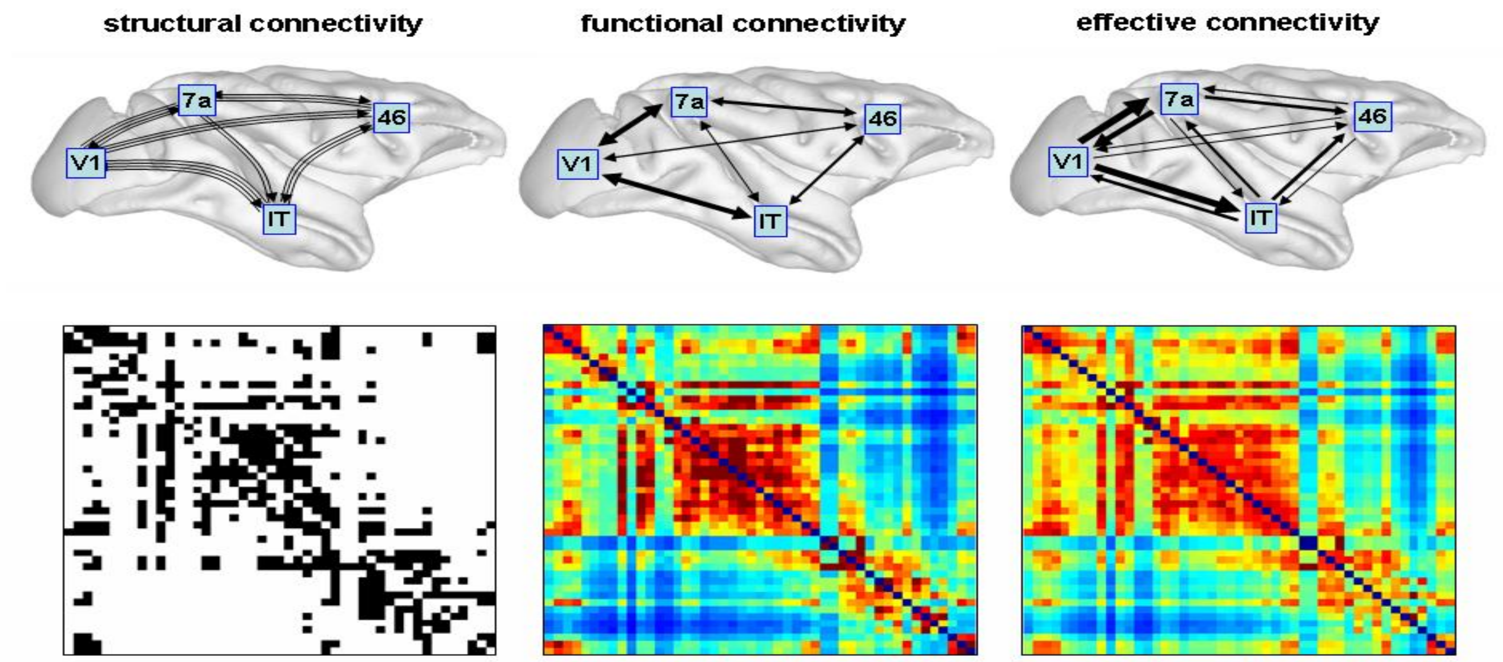

http://www.scholarpedia.org/article/Brain_connectivity

Brain connectivity refers to AC, FC, and EC between **distinct units** within a nervous system. It is crucial to elucidating how neurons and neural networks process information.

The units include Individual Neurons, Neuronal Populations, Anatomically ROIs.

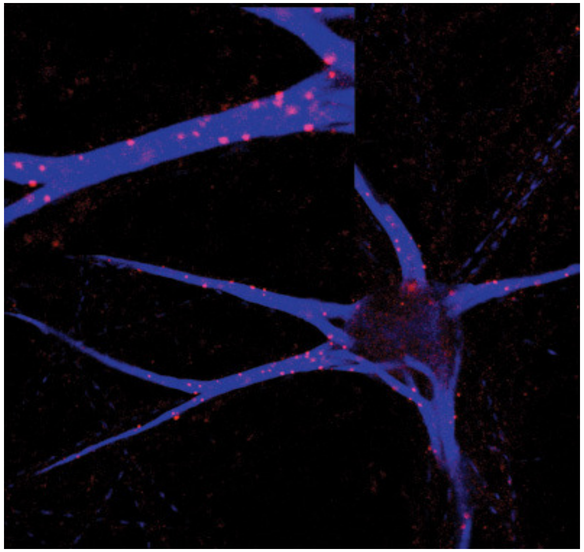

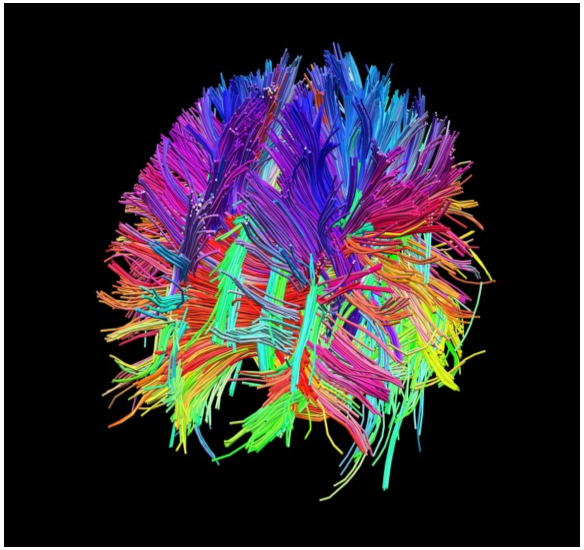

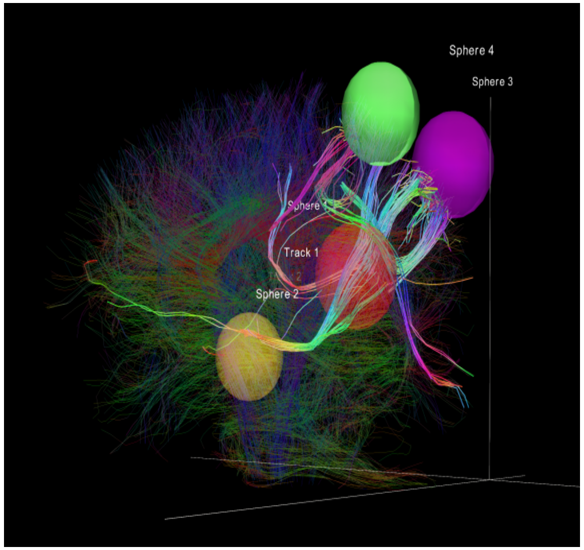

http://www.humanconnectomeproject.org/informatics/

- **Raw time series**
- **Connectivity strength (Correlation or Partial Correlation)**
- **Directed and undirected graphs**
- **Covariates (e.g., age, gender, diagnostic)**

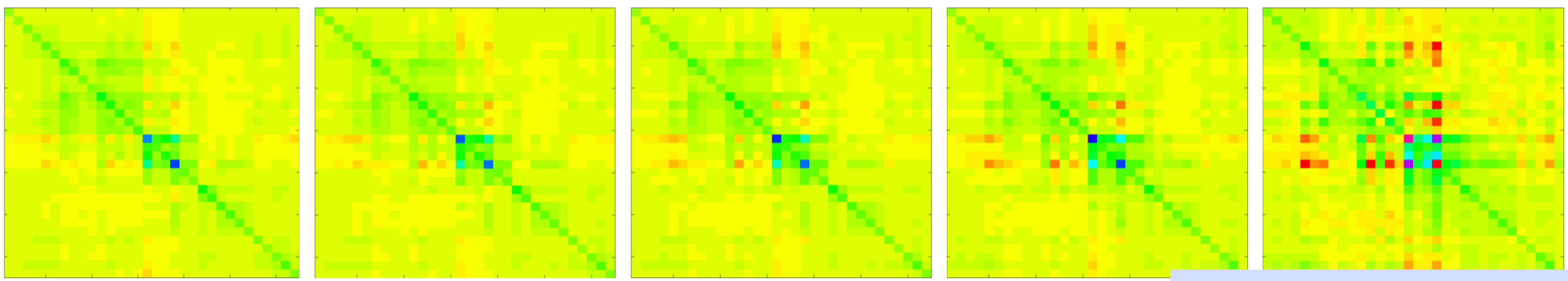

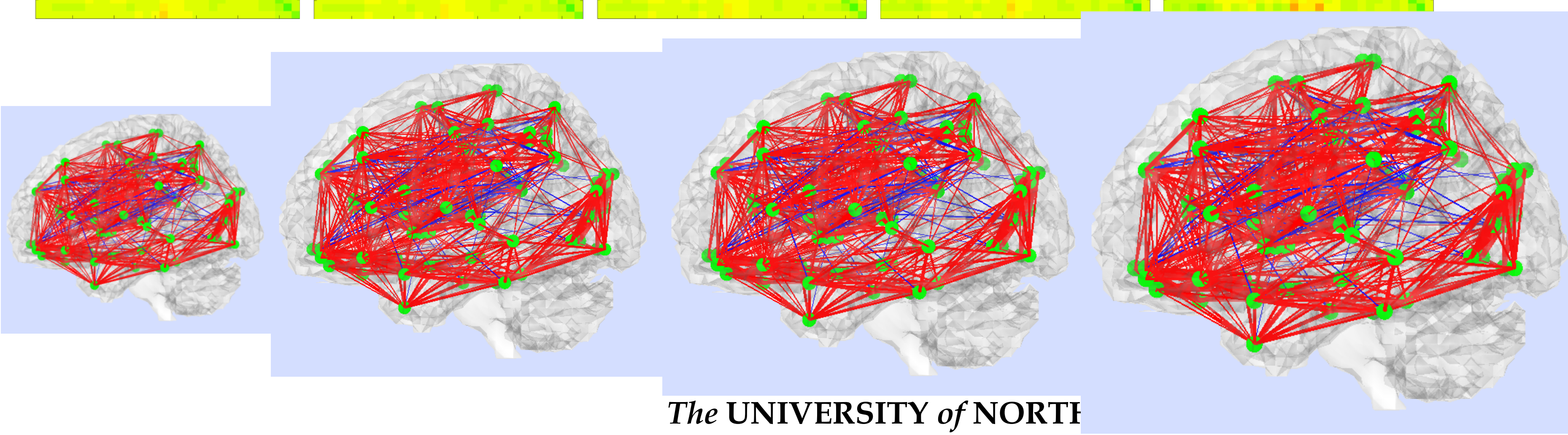

Multiple Data Types

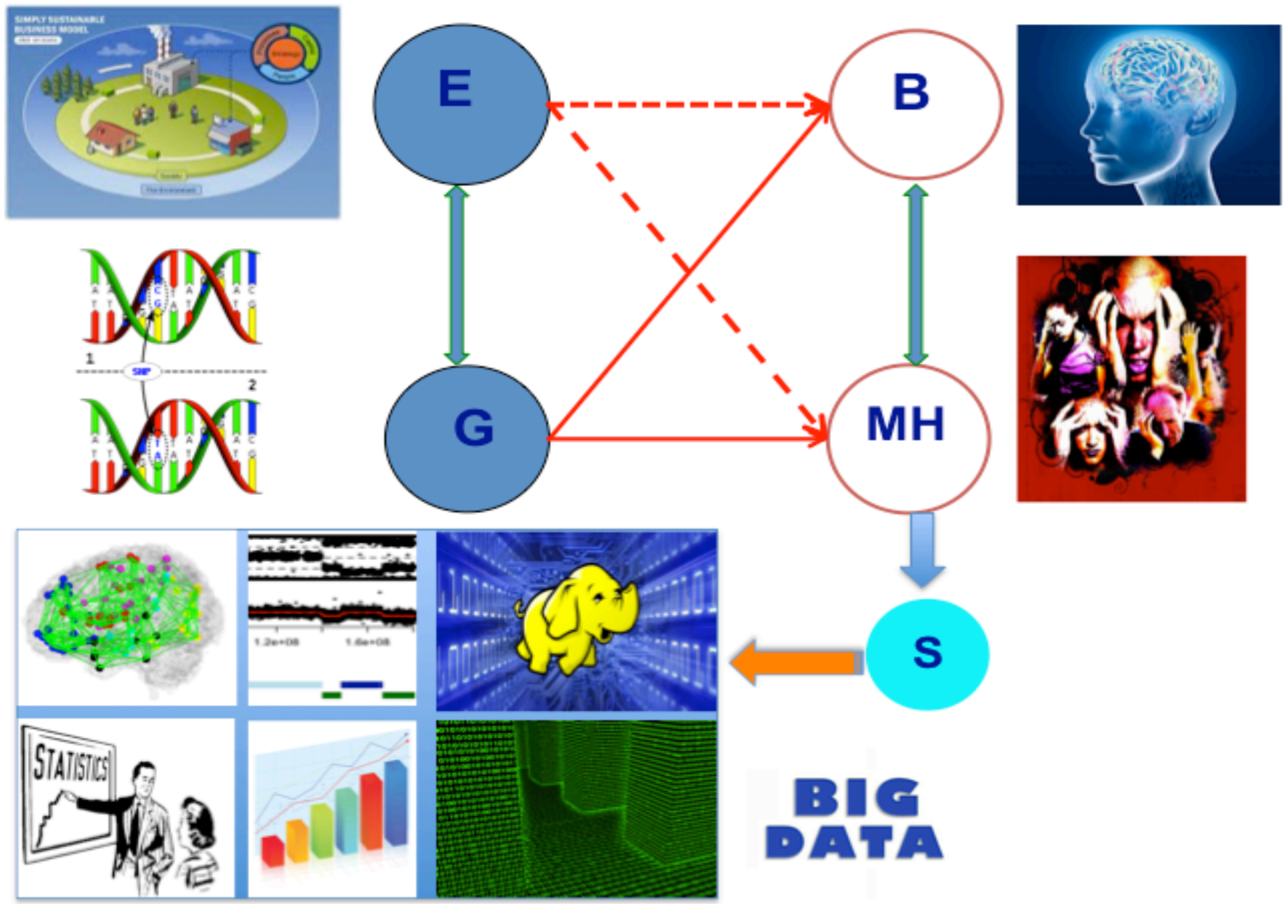

Projects

UNC Biostatistics and Imaging Analysis Lab

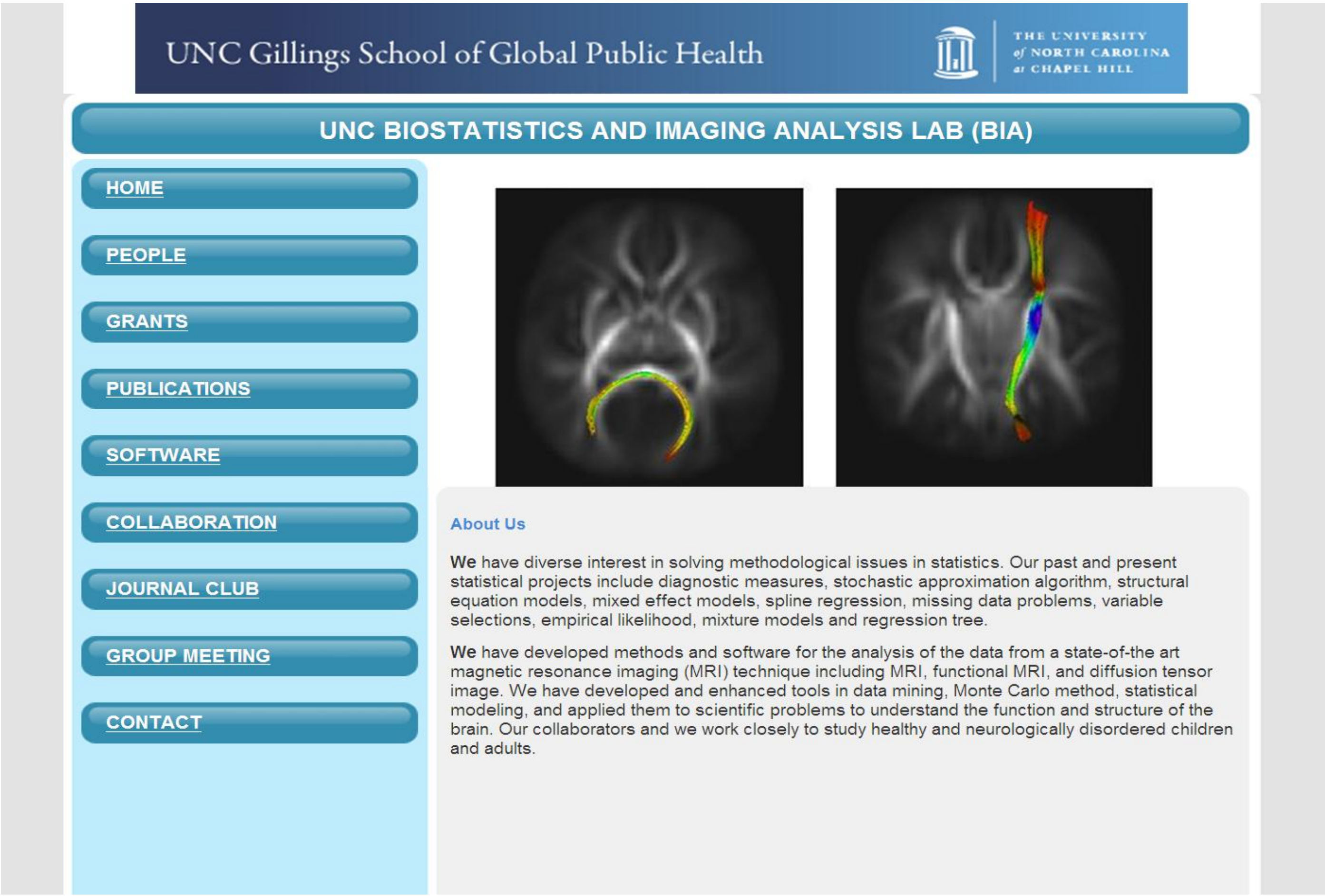

Raw Images

- Image Reconstruction
- Image Segmentation
- Image Registration
- Image Smoothing

Multiple Comparisons

Statistical Modelling

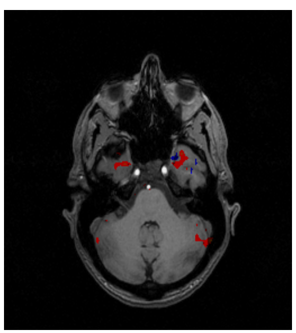

Project I: Corpus Callosum Shape for ADHD Diagnosis

Attention Deficit Hyperactivity Disorder

ADHD affects at least 5-10% of school-age children and is associated with substantial lifelong impairment, with annual direct costs exceeding $36 billion/year in the US.

- Despite a voluminous empirical literature, the scientific community remains without a comprehensive model of the pathophysiology of ADHD.
- The clinical community remains without **objective biological tools** capable of informing the diagnosis of ADHD for an individual or guiding clinicians in their decision-making regarding treatment.

www.google.com

ADHD 200

PI: Michael P. Milham, M.D., Ph.D.

The ADHD-200 Sample is a grassroots initiative, dedicated to accelerating the scientific community's understanding of the neural basis of ADHD through the implementation of open data-sharing and discovery-based science.

776 resting-state fMRI and anatomical MRI datasets aggregated across 8 independent imaging sites, **491** of which were obtained from typically developing individuals and **285** in children and adolescents with ADHD (ages: 7-21 years old).

Phenotypic information includes: diagnostic status, dimensional ADHD symptom measures, age, sex, intelligence quotient (IQ), and lifetime medication status.

ADHD 200 Global Competition

Imaging-Based Diagnostic Classification Contest

The team from Johns Hopkins University scored 119 out of 195 points, with one point awarded per correct diagnosis (typically developing, ADHD primarily inattentive type, or ADHD combined type).

while the intent of the competition was imaging-based classification, the team of the **University of Alberta** scored 124 points using all available phenotypic data while excluding imaging data – **5 more points than the winning imaging-based classification approach**.

Percentage prediction accuracy ranged between **43.08% and 61.54%** (mean = 56.02%) when using a two-class classifier to classify TDC vs. ADHD, disregarding the ADHD subtypes.

Data Processing

Corpus Callosum

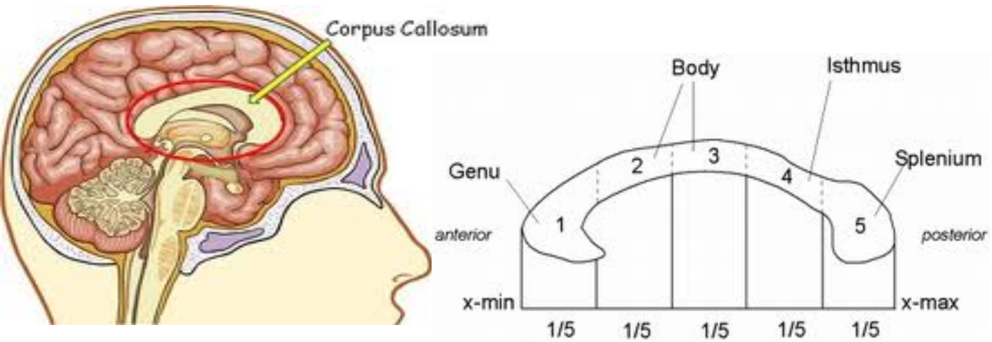

CC Segmentation

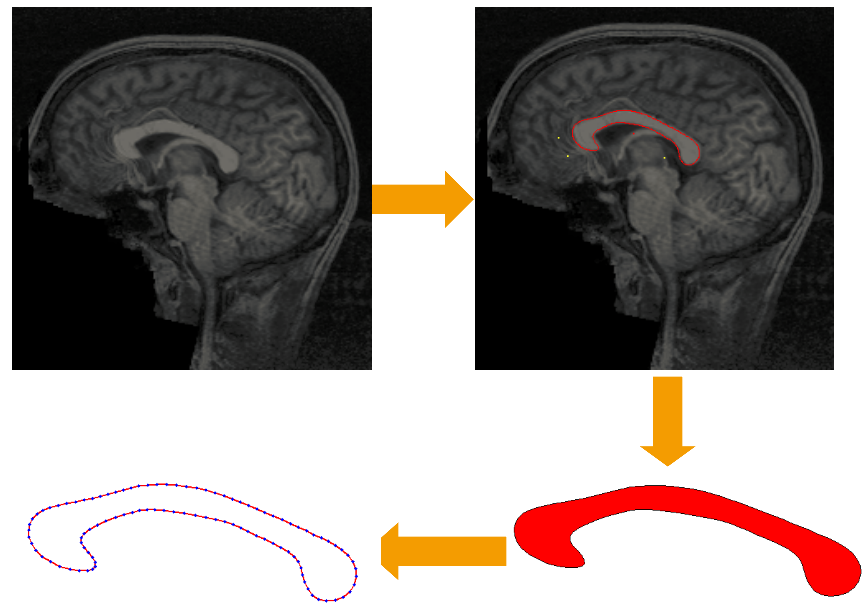

CC is a wide, flat bundle of neural fibers beneath the cortex in the eutherian brain at the longitudinal fissue. It connects the left and right cerebral hemispheres and facilitates interhemispheric commucation. It is the largest white matter structure in the brain.

wiki

Simulation Studies

Setting: 2 Clusters.
Generated from NC and ADHD subjects respectively

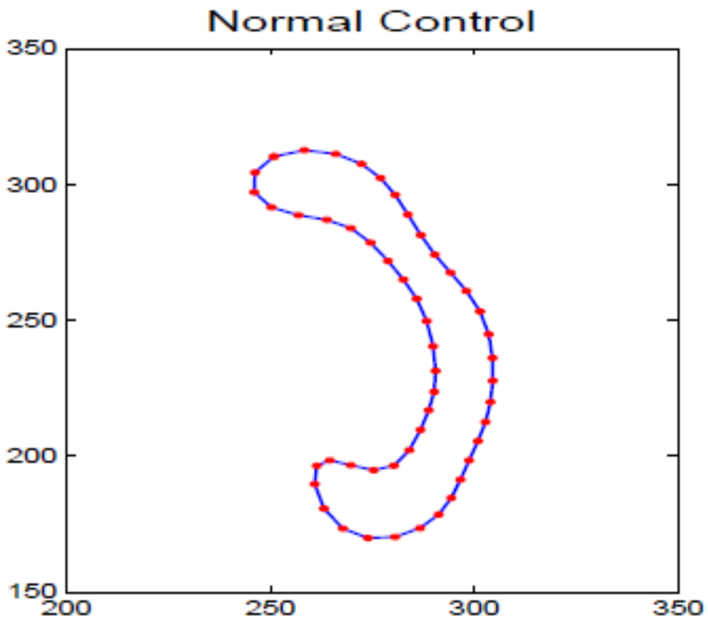

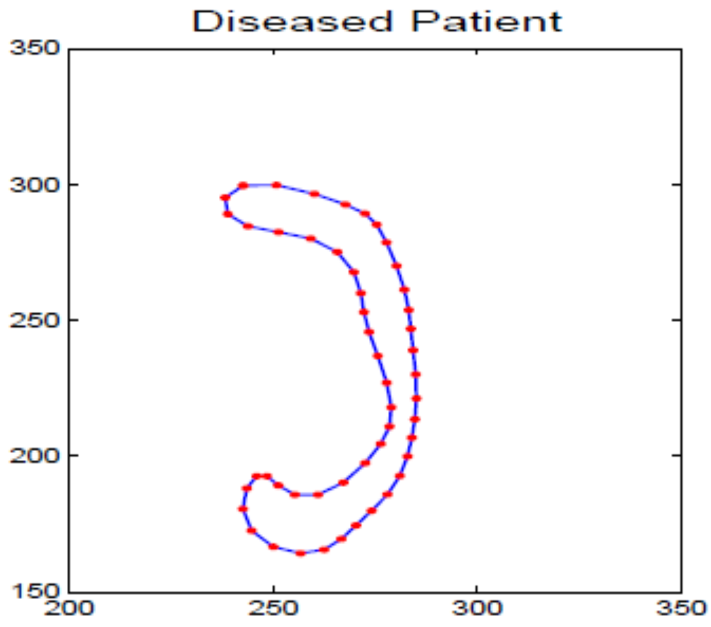

Simulation Studies

Performance of MOS and penalized MOSFA models for different simulation cases

		Case 1: $c_1 = 2, c_2 = 1$		
Model	Cluster	$m_0 = 30$	$m_0 = 60$	$m_0 = 90$
	1	0	25	29
MOS	2	200	172	22
	3	0	3	149
	RI(aRI)*	1(1)	0.95(0.92)	0.59(0.17)
	1	0	0	0
penalized	2	200	198	195
MOSFA	3	0	2	5
	RI(aRI)	1(0.99)	1(0.99)	0.96(0.92)
		Case 2: $c_1 = 5, c_2 = 2$		
Model	Cluster	$m_0 = 30$	$m_0 = 60$	$m_0 = 90$
	1	32	46	56
MOS	2	139	102	31
	3	29	52	113
	RI(aRI)	0.86(0.74)	0.76(0.54)	0.61(0.20)
	1	0	12	23
penalized	2	188	160	141
MOSFA	3	12	28	36
	RI(aRI)	0.99(0.98)	0.92(0.91)	0.88(0.85)

Real Data Analysis

Four clusters: First three clusters contain 167 NC and 3 ADHD subjects while the last one contains 4 NC and 67 ADHD subjects.

Cluster 1

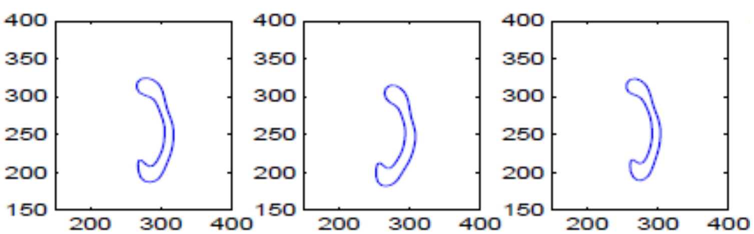

Cluster 2

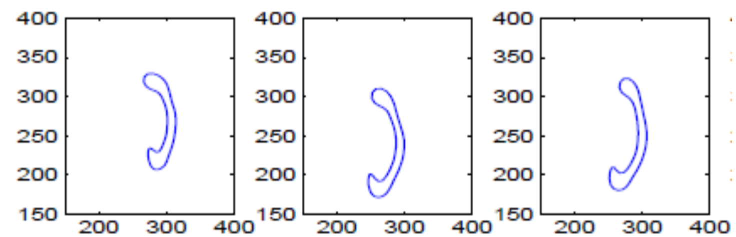

Cluster 3

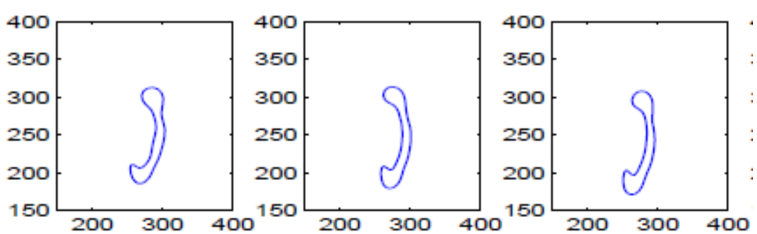

Cluster 4

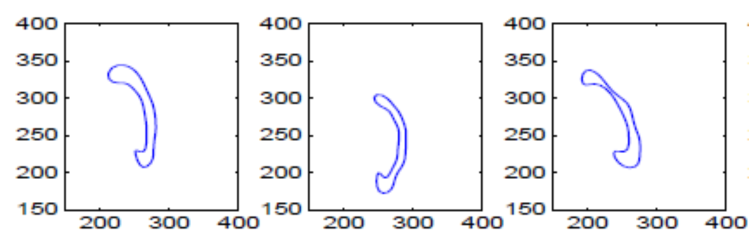

Real Data Analysis

Shapes placed equidistant along the geodesic paths in four clusters

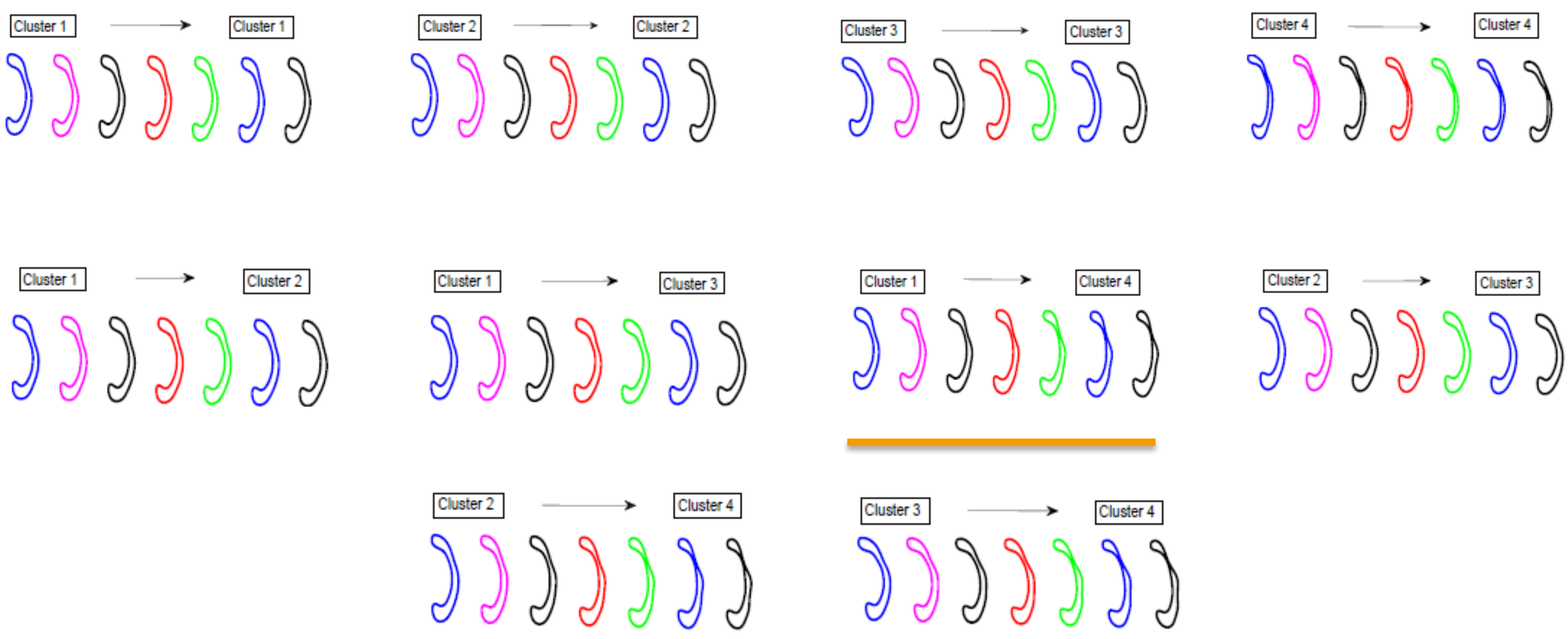

Real Data Analysis

Geodesic distance between each pair of shapes

Distance	Cluster 1	Cluster 2	Cluster 3	Cluster 4
Cluster 1	0.0805	0.0840	0.0862	0.1295
Cluster 2	-	0.0398	0.0731	0.1295
Cluster 3	-	-	0.0510	0.1496
Cluster 4	-	-	-	0.0989

Mean shape difference test among different clusters

	Cluster 2	Cluster 3	Cluster 4
Cluster 1	0.0552	0.0881	0.6431
	(0.3284)	(0.1343)	(0.0050)
Cluster 2	-	0.0044	0.0474
		(0.5808)	(0.0040)
Cluster 3	-	-	0.0218
			(0.0349)

Project II: Functional Imaging Data Reconstruction

Motivation

Functional MRI measures the hemodynamic response (change in blood flow) related to neural activity in the brain or spinal cord of humans or other animals. Since the early 1990s, fMRI has come to dominate the brain mapping field due to low invasiveness, absence of radiation exposure, and relatively wide availability.

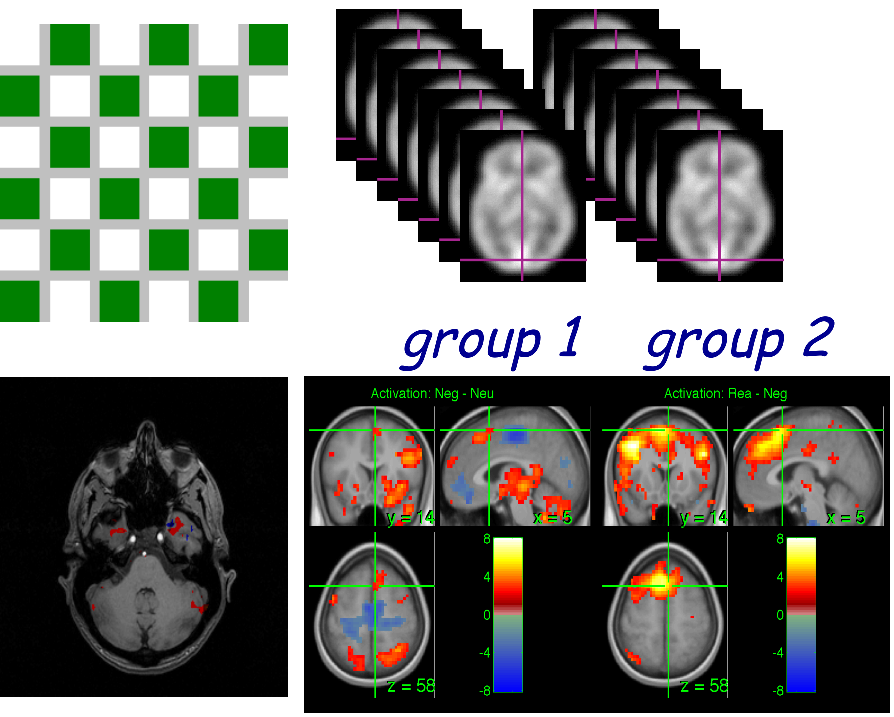

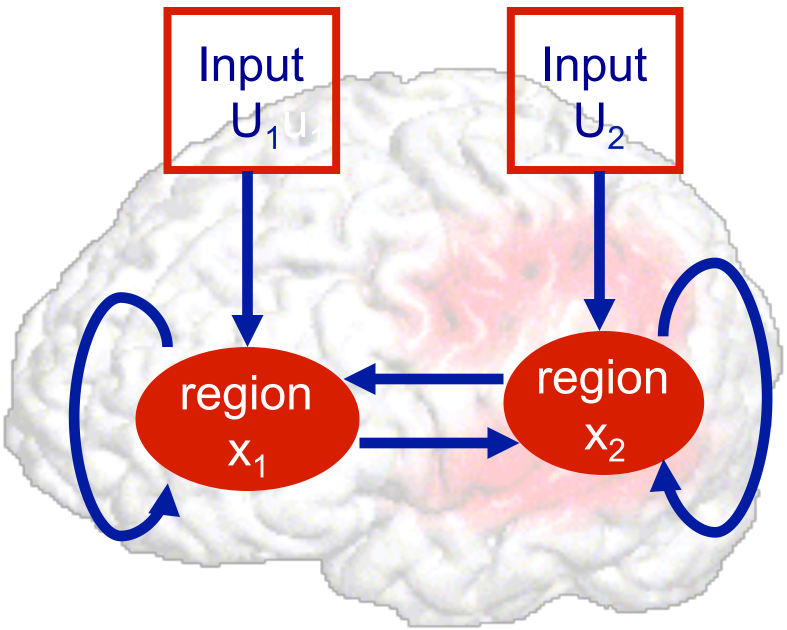

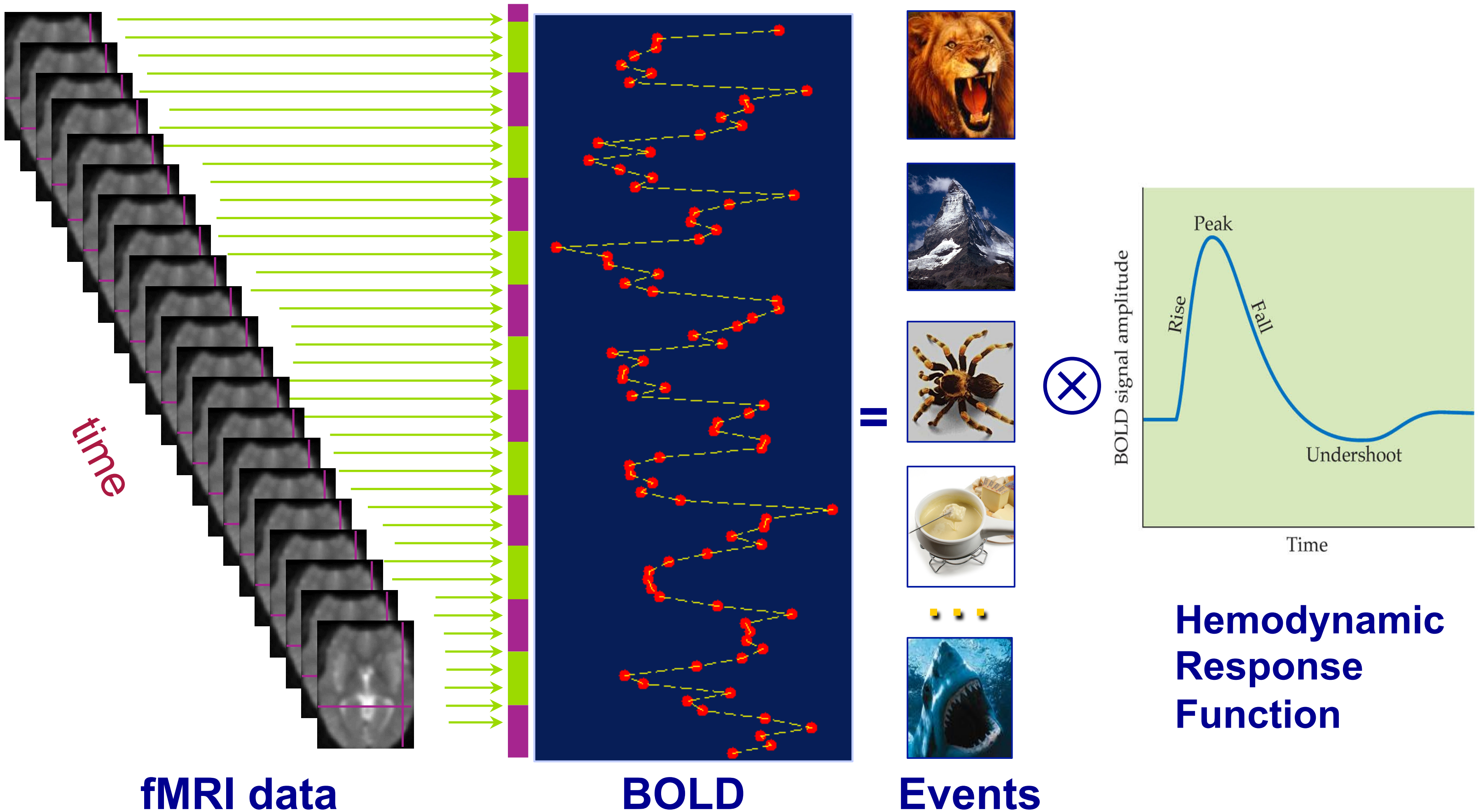
time
=
Peak
Rise
Fall
Undershoot
BOLD signal amplitude
Time
Hemodynamic Response Function
fMRI data
BOLD
Events

- The most common approach towards fMRI uses the Blood Oxygenation Level Dependent (BOLD) contrast.
- fMRI measurements are of amount of deoxyhemoglobin per voxel.
- BOLD response in fMRI is a complex, nonlinear function of the results of neuronal and vascular changes.
- HRF has multiple components
  - Changes delayed by 1-2 sec (lags activity)
  - Initial dip (not always seen)
  - Influx of Hb greater than needed for activity
  - 5-6 sec time to peak
  - Undershoot follows ~6s later

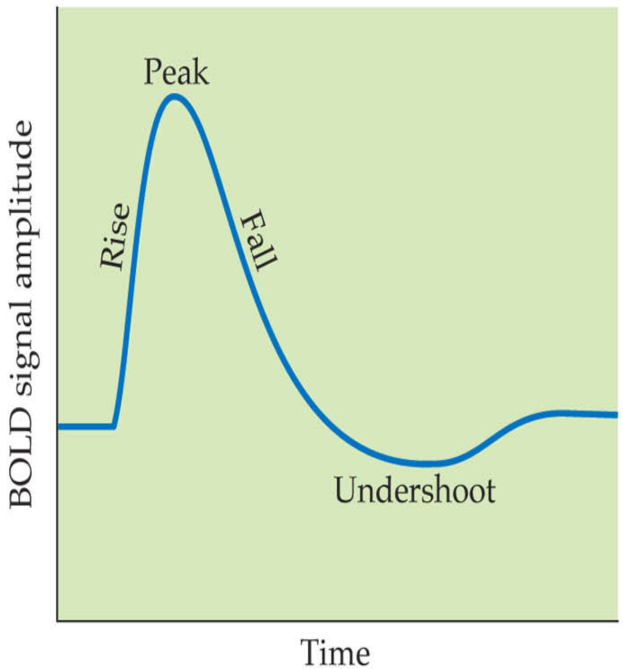

A Linear Time Invariant System

is characterized by the following properties:

- **Scaling** – if the input is scaled by a factor *b* then the BOLD response will also be scaled by a factor *b*.
- **Superposition** – the response to two different stimuli applied together is equal to the sum of the individual responses.
- **Time-invariance** – if a stimulus is shifted by a time *t*, then the response is shifted by *t*.

Convolution model

$$X(t) \otimes h(t) = \sum \beta_i f_i(t) + \varepsilon(t) = \mathrm{BOLD}(t)$$

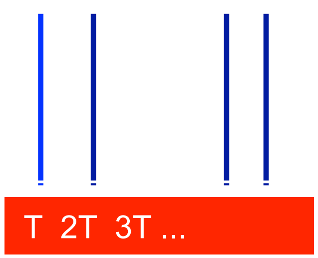

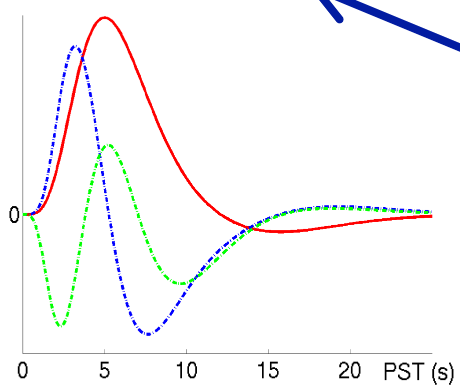

Basis Functions

Convolution

	Block Design	Event-Related
Experimental Stimulus Function	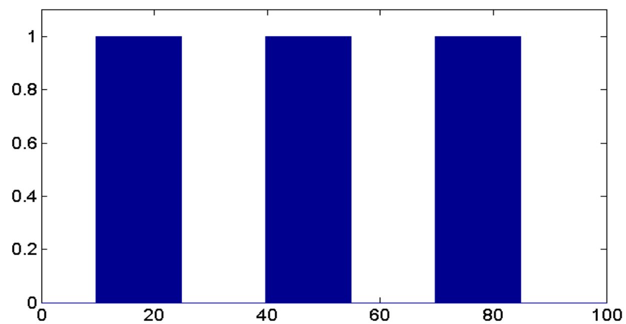	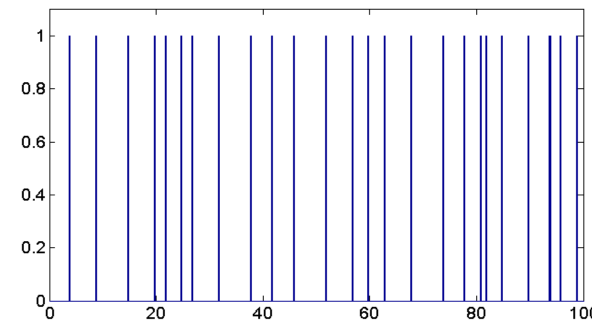
Hemodynamic Response Function	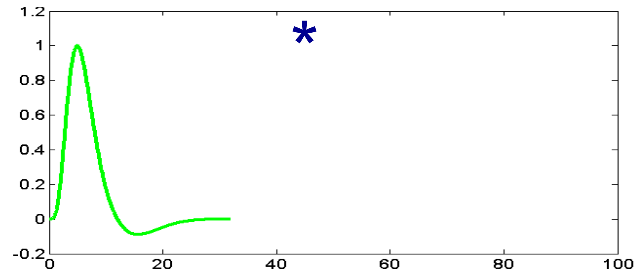	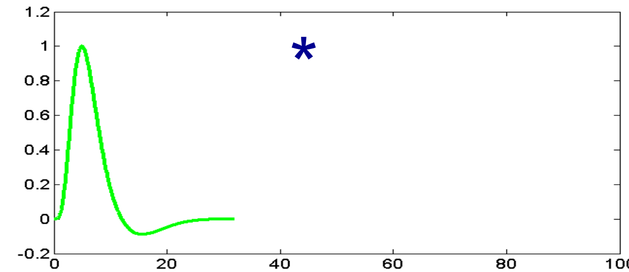
Predicted Response	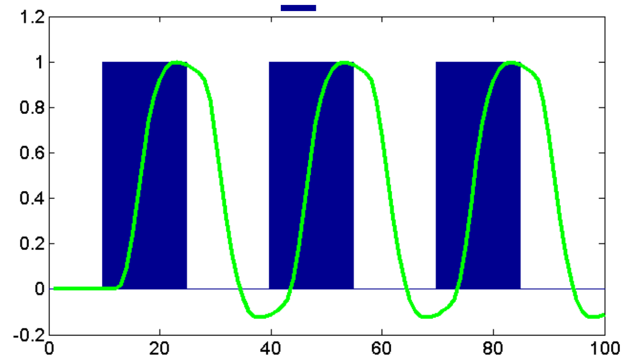	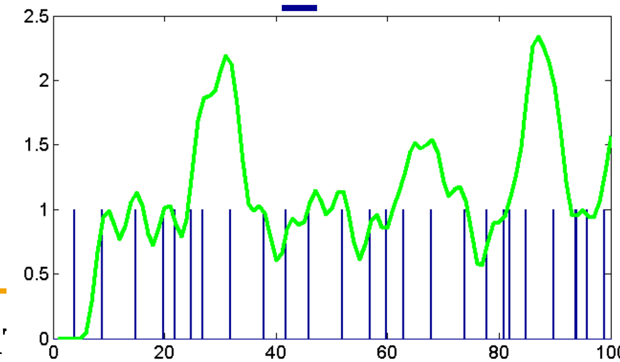

Stimulus (“Neural”) HRF Predicted Data

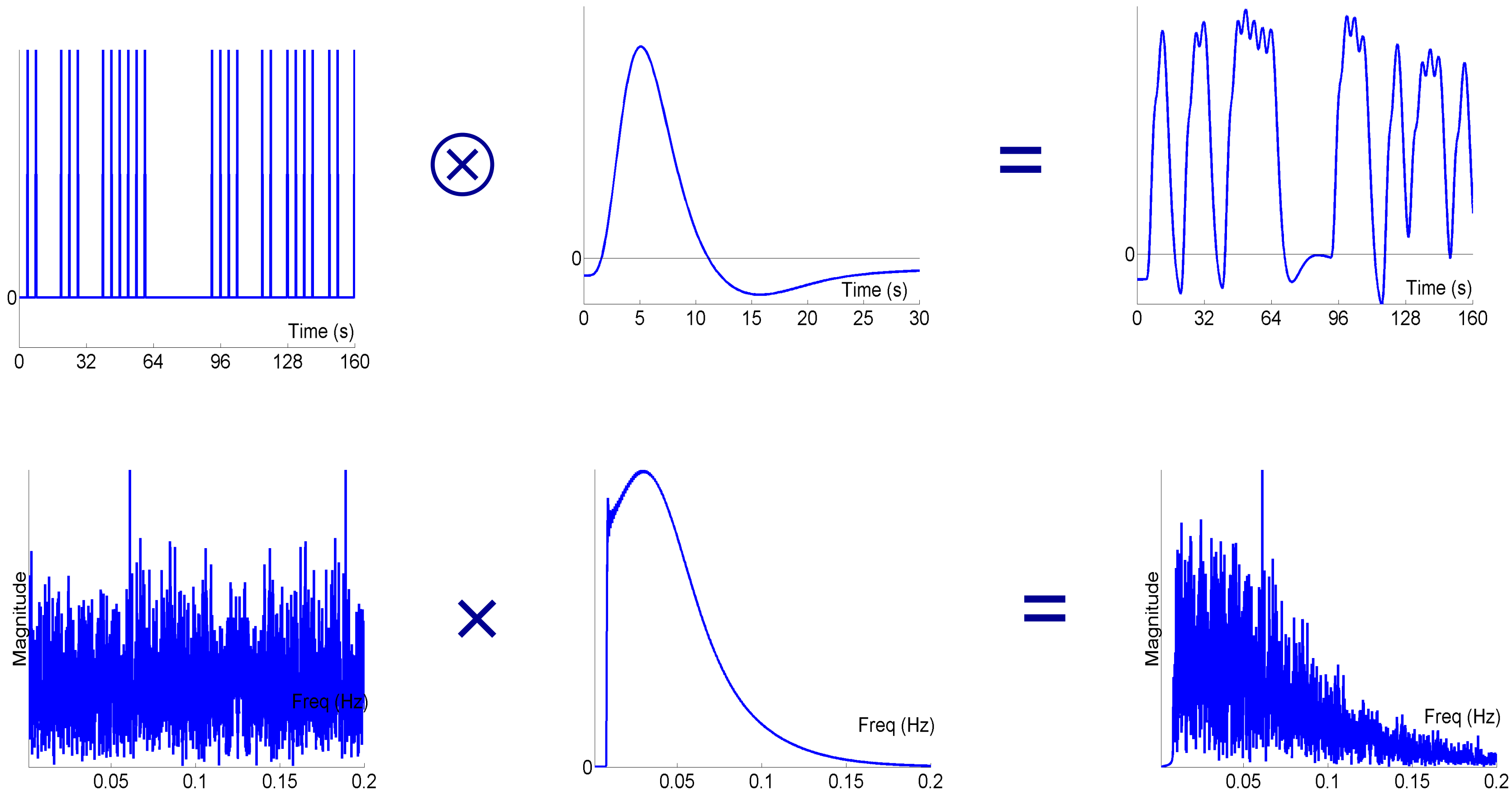

Timing of Brain Events

- **The ability to estimate features of the hemodynamic response plays an important role in using fMRI to study mental processes.**
    - ♦ **the amplitude of the HRF may provide information about the strength of neuronal activity.**
    - ♦ **the onset of the HRF may provide information about the timing of neuronal activity.**
    - ♦ **the duration of the HRF may provide information about the duration of neuronal activity.**

Simulation

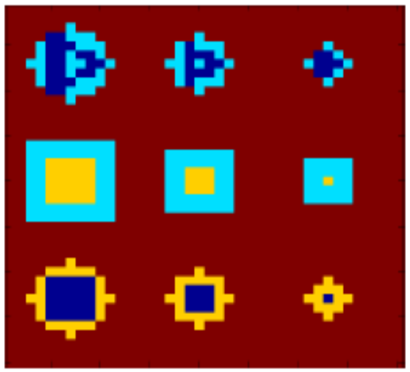

(a.1)

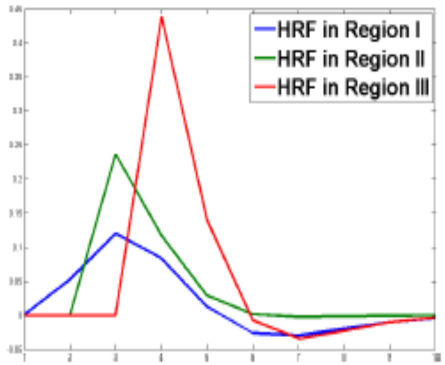

(a.2)

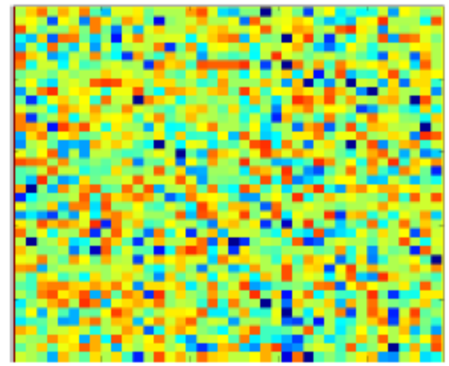

(a.3)

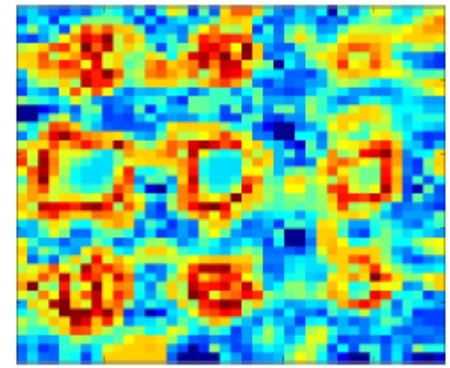

(a.4)

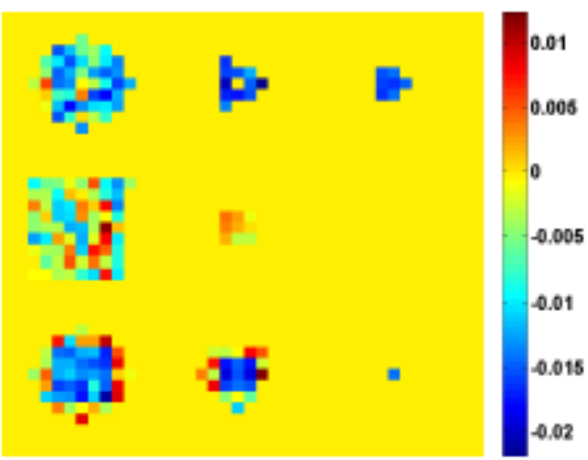

(a.1)

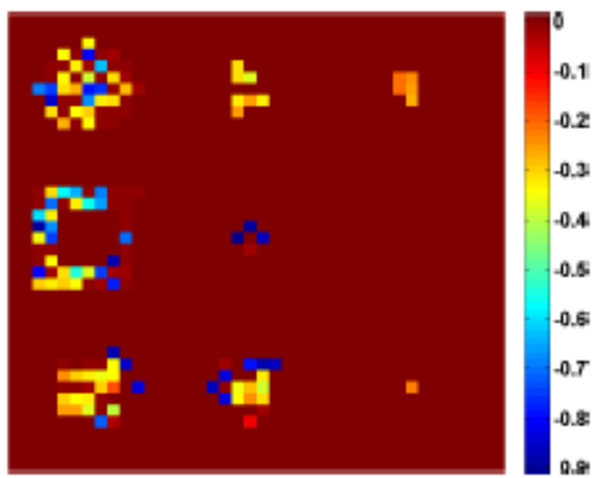

(a.2)

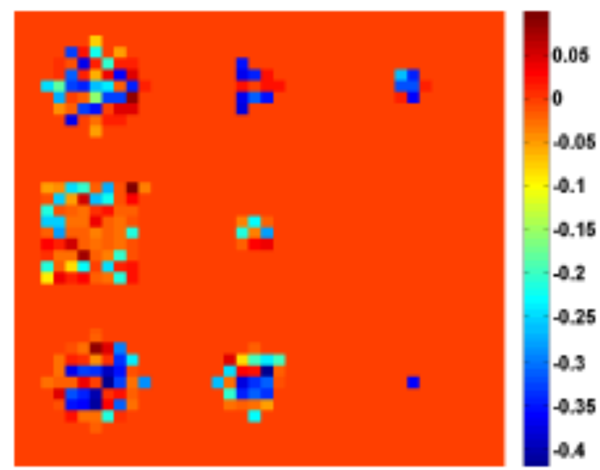

(a.3)

Simulation Set-up

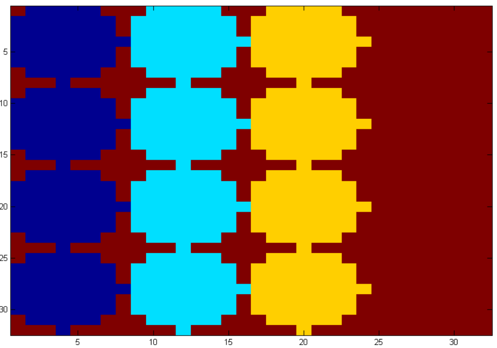

(i)

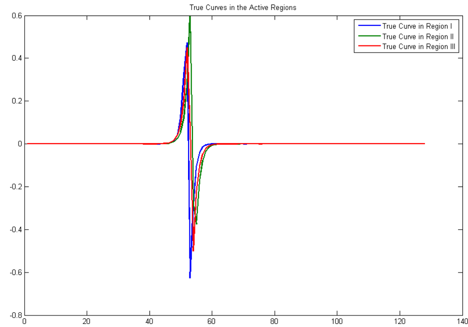

(ii)

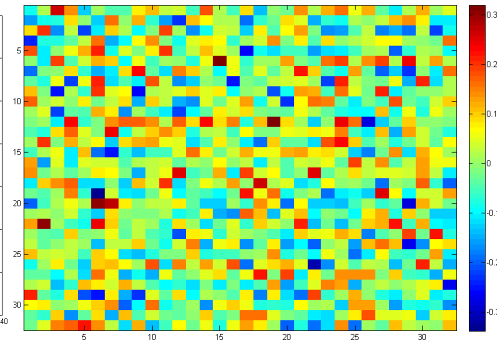

(iii)

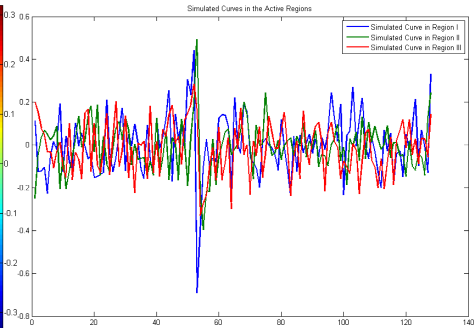

(iv)

(i) A temporal cut of the true images;

(iii) A temporal cut of the simulated images

(ii) The true curves

(iv) The simulated curves

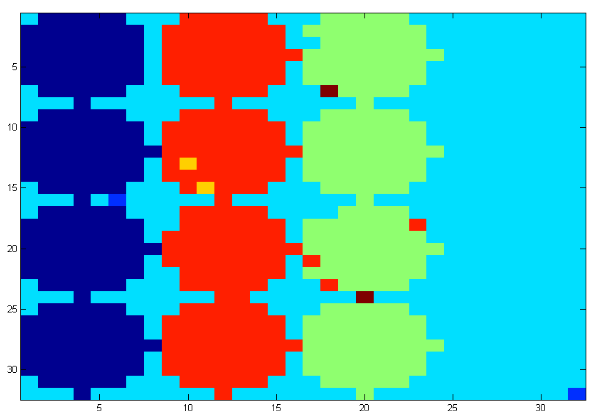

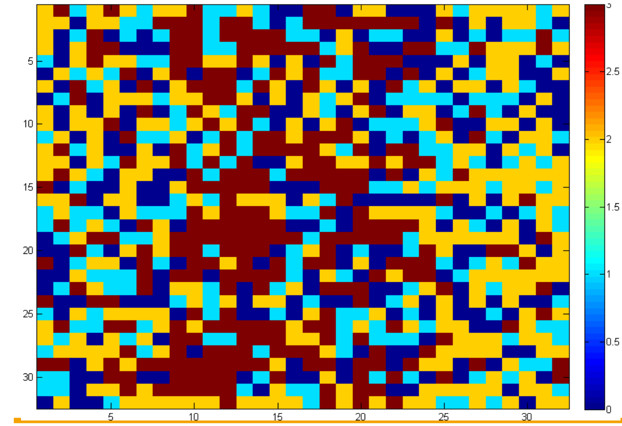

Real fMRI data

PI: Kelly Giovanello

- This data set is from a memory related experiment to compare the neural correlates of relational memory during implicit (non-strategic) versus explicit (conscious, strategic) retrieval.
- There are four different sequences of stimuli.
- We use SPM8 to preprocess the images including the realignment, timing slicing, segmentation, coregistration, normalization and spatial smoothing.

Data Analysis Results

We focus on some significant regions of interest (ROI) detected by SPM to study the HRFs of the voxels by our method. The results are verified by sFIR and GAM.


(1)

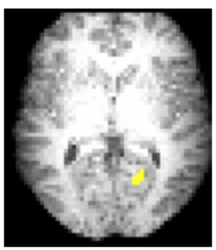
(2)

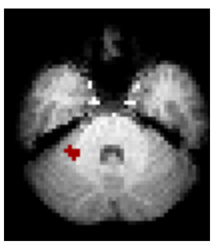
(3)

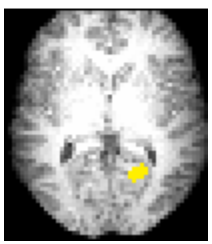
(4)

(1)-(4) The slices containing ROIs (colored ones) of the F maps for the 1st-4th stimulus sequences, respectively.

Data Analysis Results (Cont.)

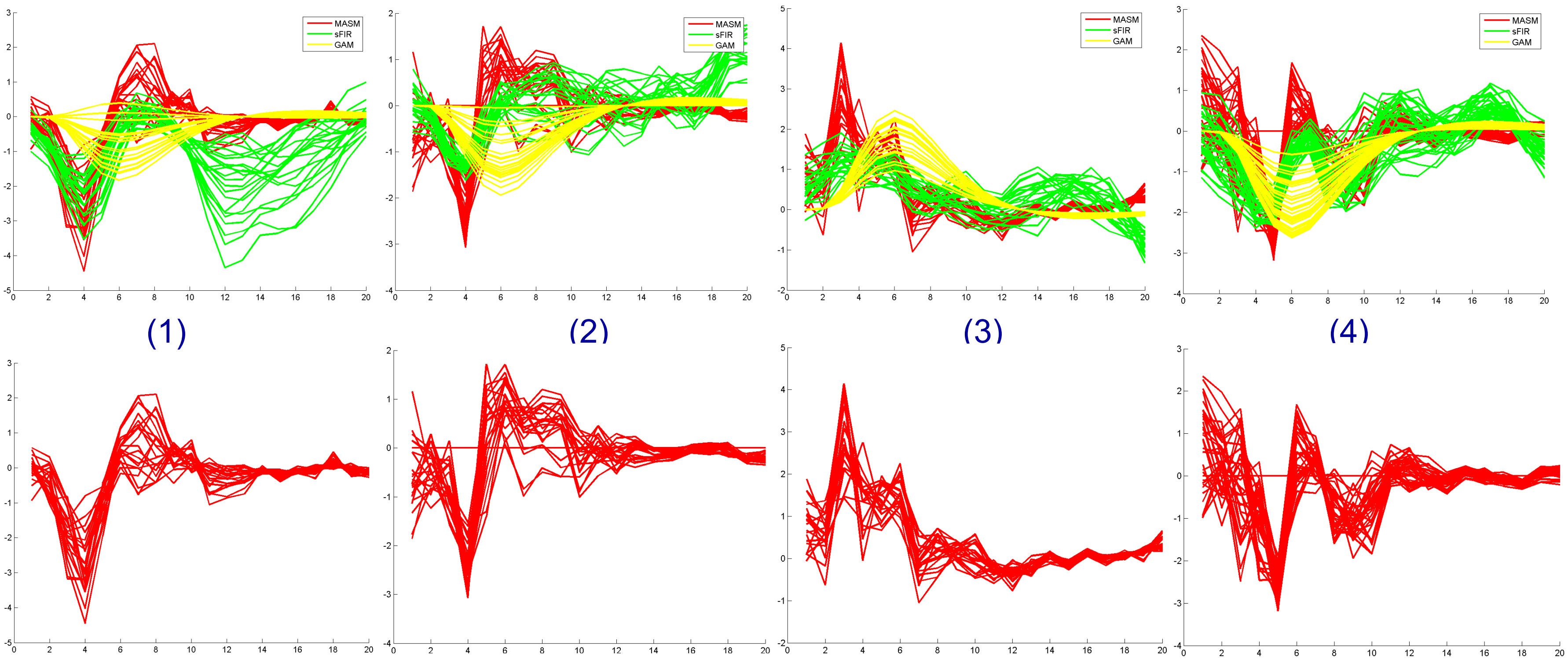

(1) (2) (3) (4)

(5) (6) (7) (8)

(1)-(4) Estimated HRFs at the significant ROIs corresponding each condition from MASM (red), sFIR(green) and GAM(yellow); (5)-(8) Estimated HRFs from only MASM in the each ROI.

Clustering Results

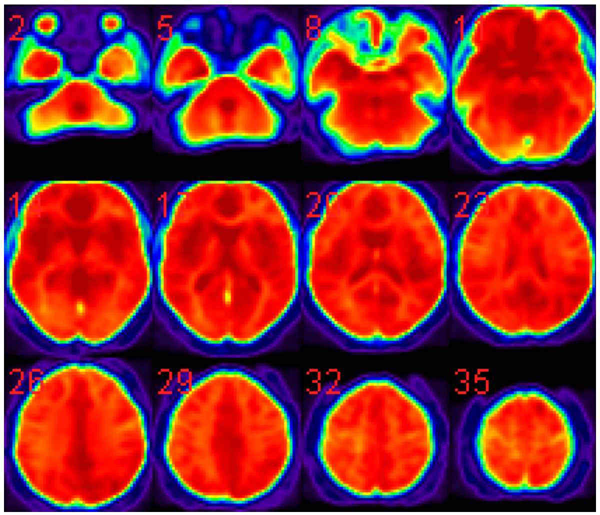

Slices from raw images

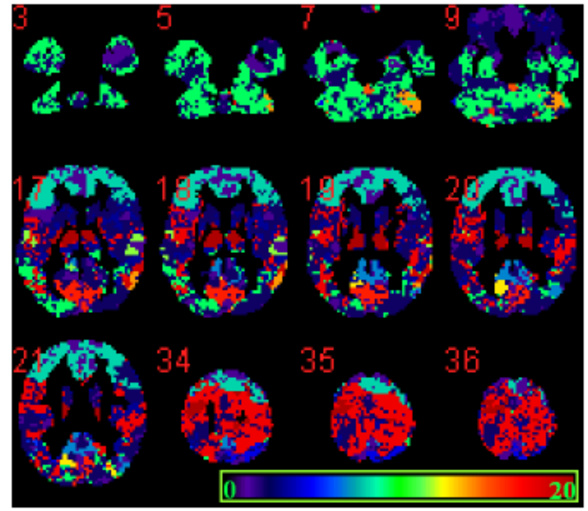

Clustered pattern

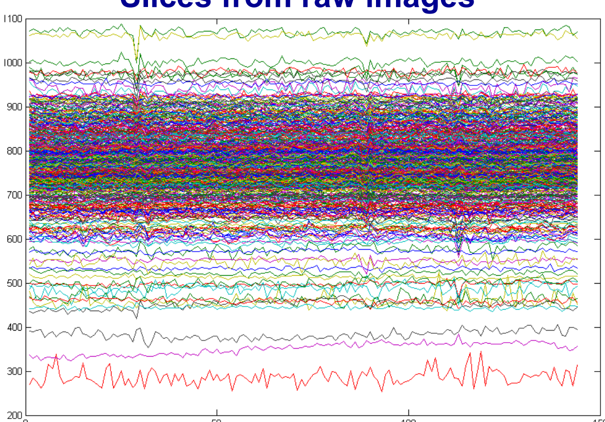

Sample of original curves

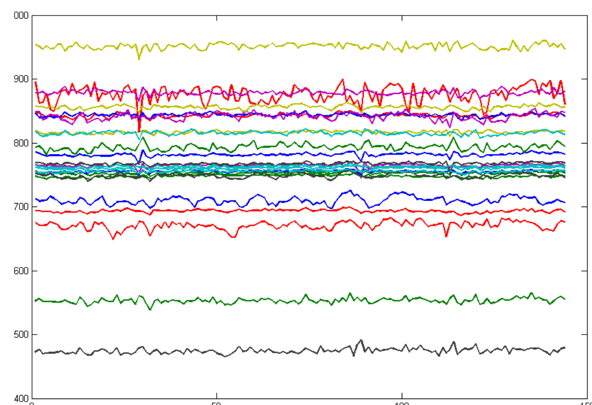

Mean curves of clusters

An Application –Functional Connectivity

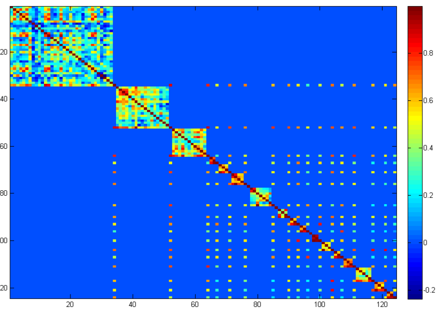

Original Correlation Matrix

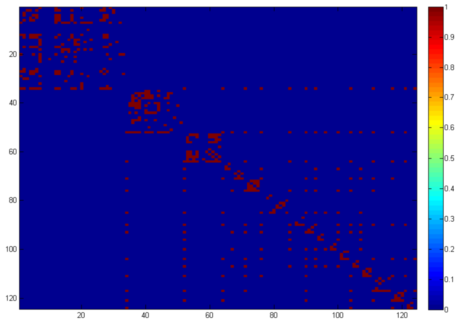

Threshold at 0.5

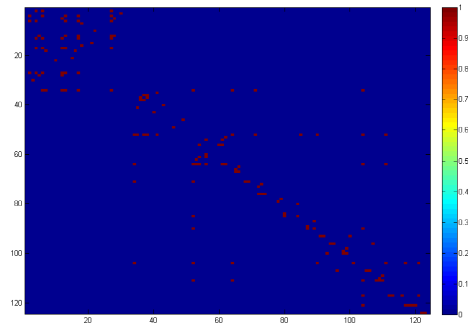

Threshold at 0.7

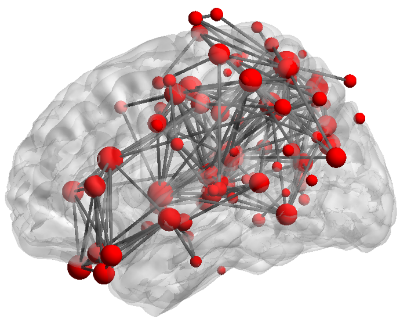

Sagital View Threshold 0.5

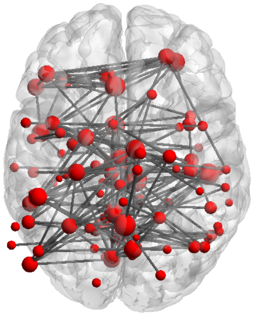

Axial View Threshold 0.5

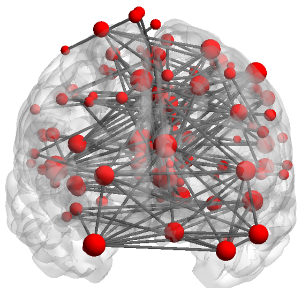

Coronal View Threshold 0.5

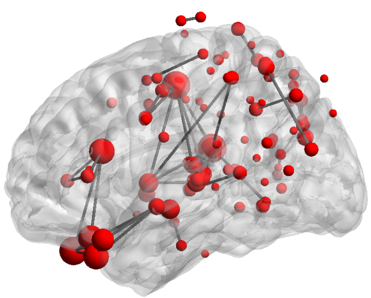

Sagital View Threshold 0.7

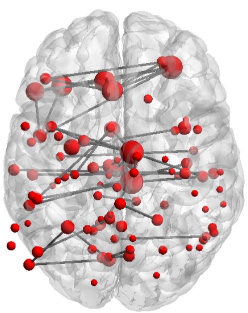

Axial View Threshold 0.7

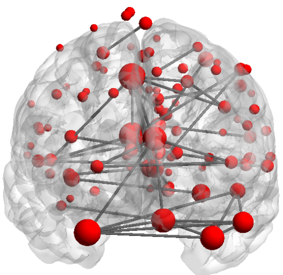

Coronal View Threshold 0.7

Project III: White Matter Tract Statistics for Brain Development

Real Data

- PI: Dr. John H. Gilmore from Dept of Psychiatry at UNC-CH
- Healthy/High risk full-term infants
- Diffusion Tensor Images
- 5 diffusive outcomes: FA, MD, $\lambda_1, \lambda_2, \lambda_3$ along multiple major fiber tracts

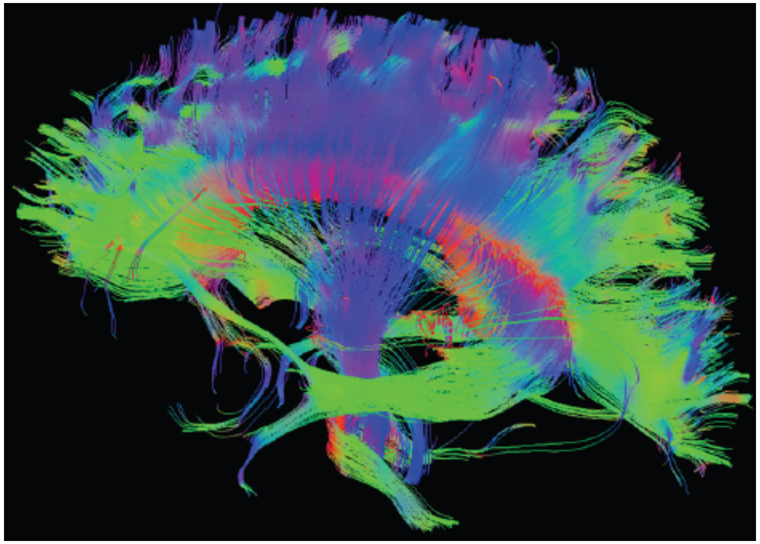

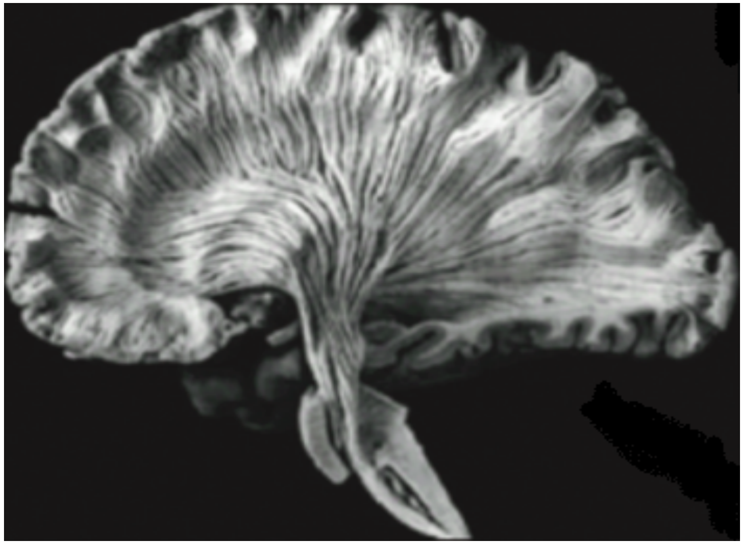

DTI Fiber Tract Data

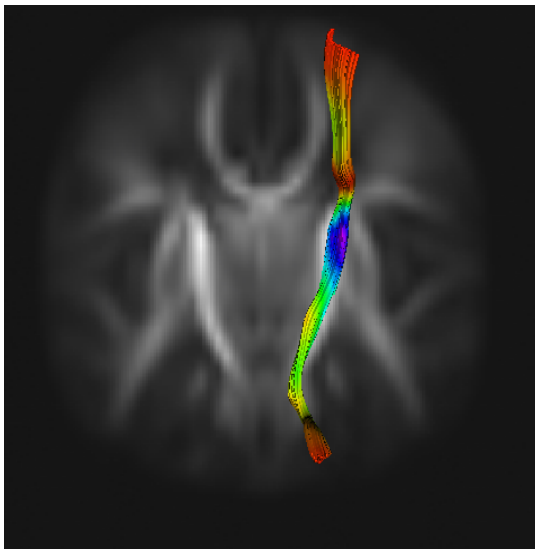

Data

- **Diffusion properties (e.g., FA, RA)**

$$Y_i(s_j) = (y_{i,1}(s_j), \cdots, y_{i,m}(s_j))^T$$

- **Grids** $\{s_1, \cdots, s_{n_G}\}$

- **Covariates (e.g., age, gender, diagnostic)**

$$x_1, \cdots, x_n$$

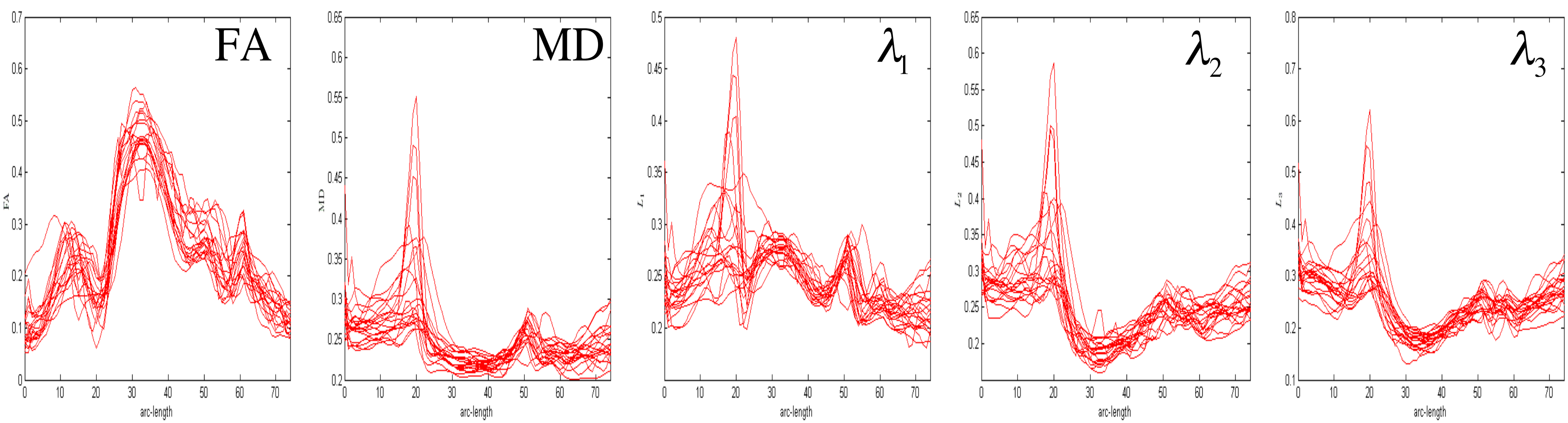

FADTTS Path Diagram

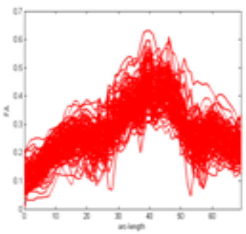

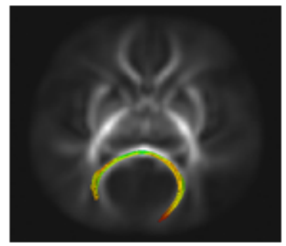

Multivariate varying coefficient model

$$y_{i,k}(s) = \mathbf{x}_i^T B_k(s) + \eta_{i,k}(s) + \epsilon_{i,k}(s)$$

Weighted least square estimation

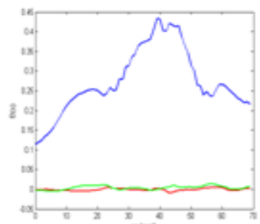

$$B_k(s_j) = B_k(s) + \dot{B}_k(s)(s_j - s)$$

Functional principal component analysis

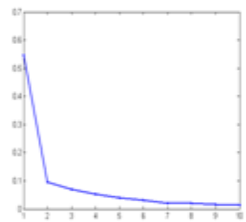

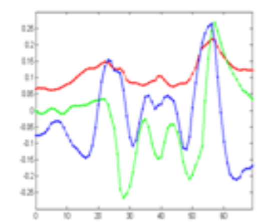

$$\hat{\Sigma}_{\eta,kk}(s,t) = \sum_{l=1} \hat{\lambda}_{k,l}\hat{\psi}_{k,l}(s)\hat{\psi}_{k,l}(t)$$

Confidence bands

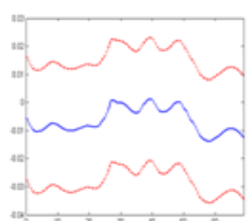

Resampling methods

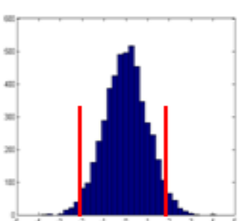

$$P(\sup_{s\in[0,L_0]} |G_{kl}(s)| \le C_{kl}(\alpha)) = 1 - \alpha$$

Hypothesis test

$$H_0 : \mathbf{C}\mathrm{vec}(B(s)) = \mathbf{b}_0(s)$$

$$H_1 : \mathbf{C}\mathrm{vec}(B(s)) \neq \mathbf{b}_0(s)$$

Resampling methods

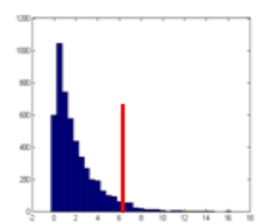

$$S_n = n\int_0^{L_0} \mathbf{d}(s)^T[\mathbf{C}(\hat{\Sigma}_\eta(s,s)\otimes\hat{\Omega}_X^{-1})\mathbf{C}^T]^{-1}\mathbf{d}(s)ds \quad p = G^{-1}\sum_{g=1}^{G} 1(S_n^{(g)} \ge S_n)$$

Real Data

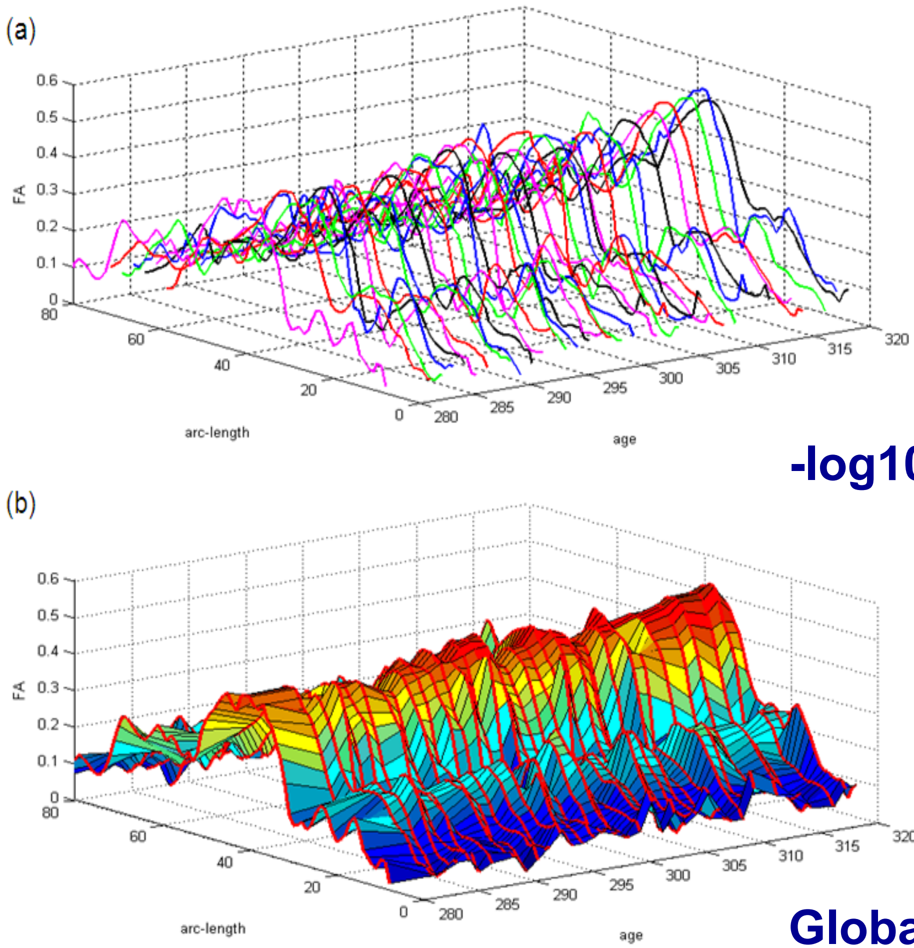

Local p-value

(c)

-log10(p)

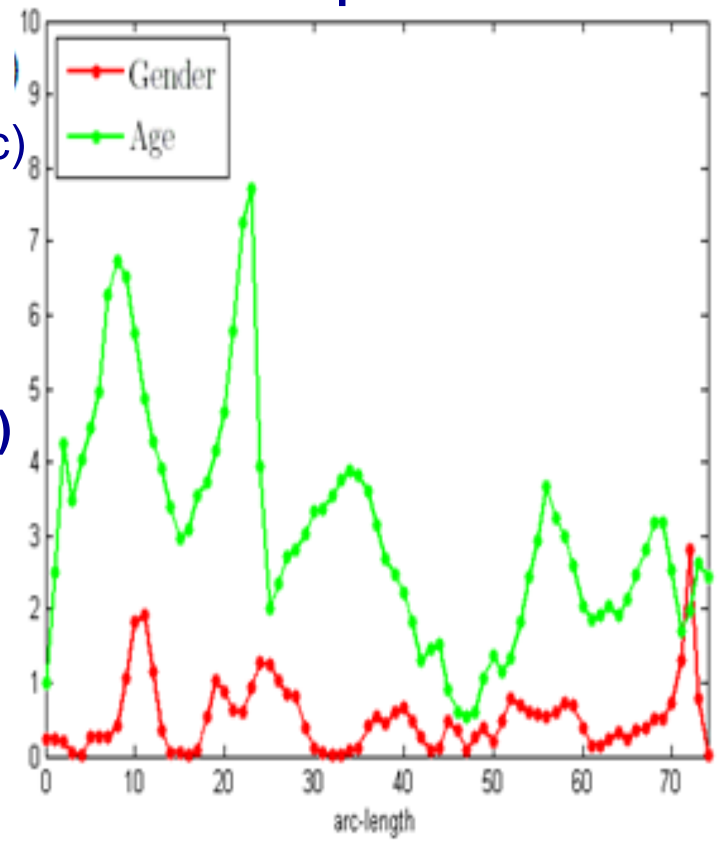

Global p-value: Age (<0.001), Gender (0.341)

Confidence Bands

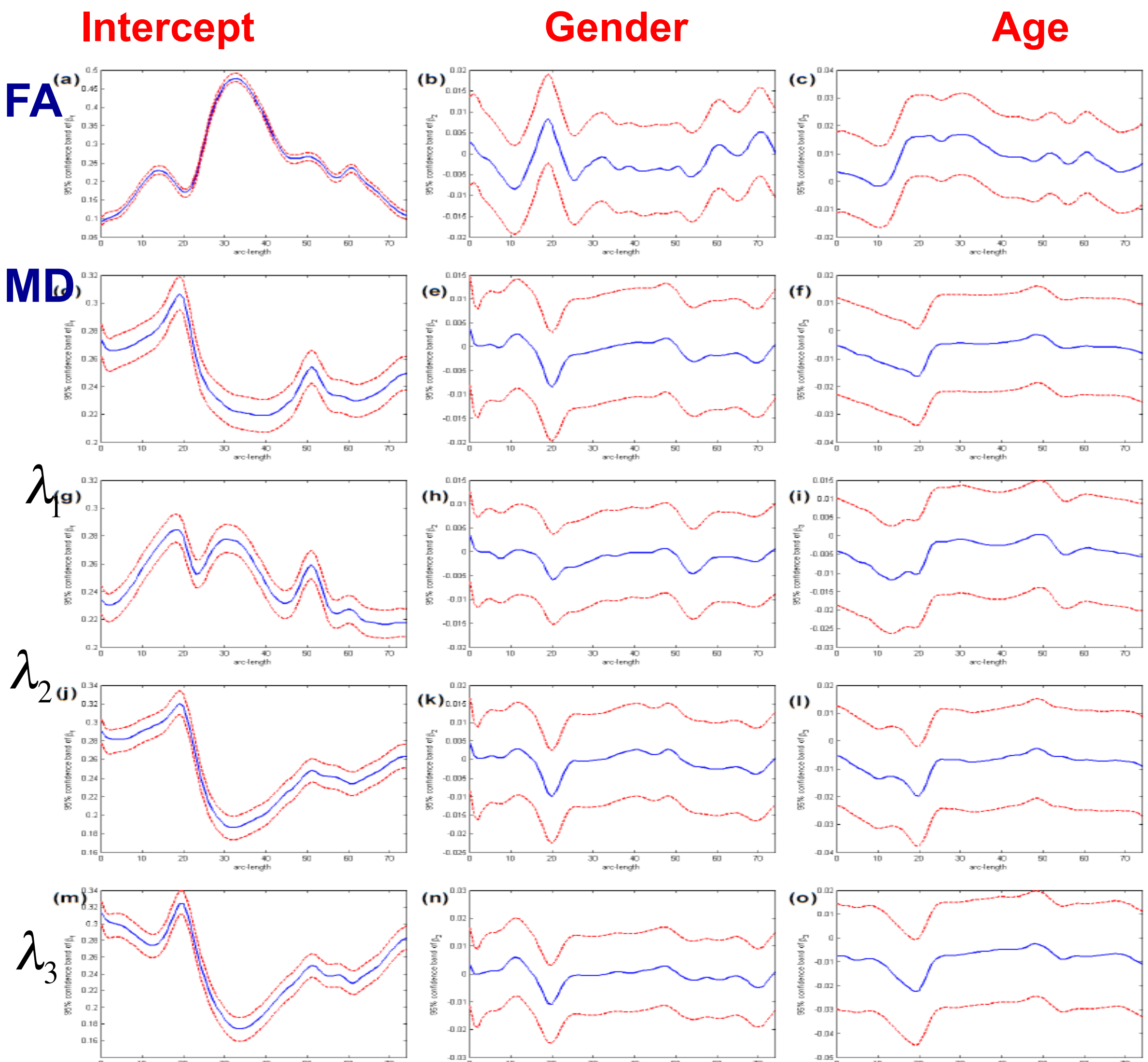

Functional Principal Component Analysis

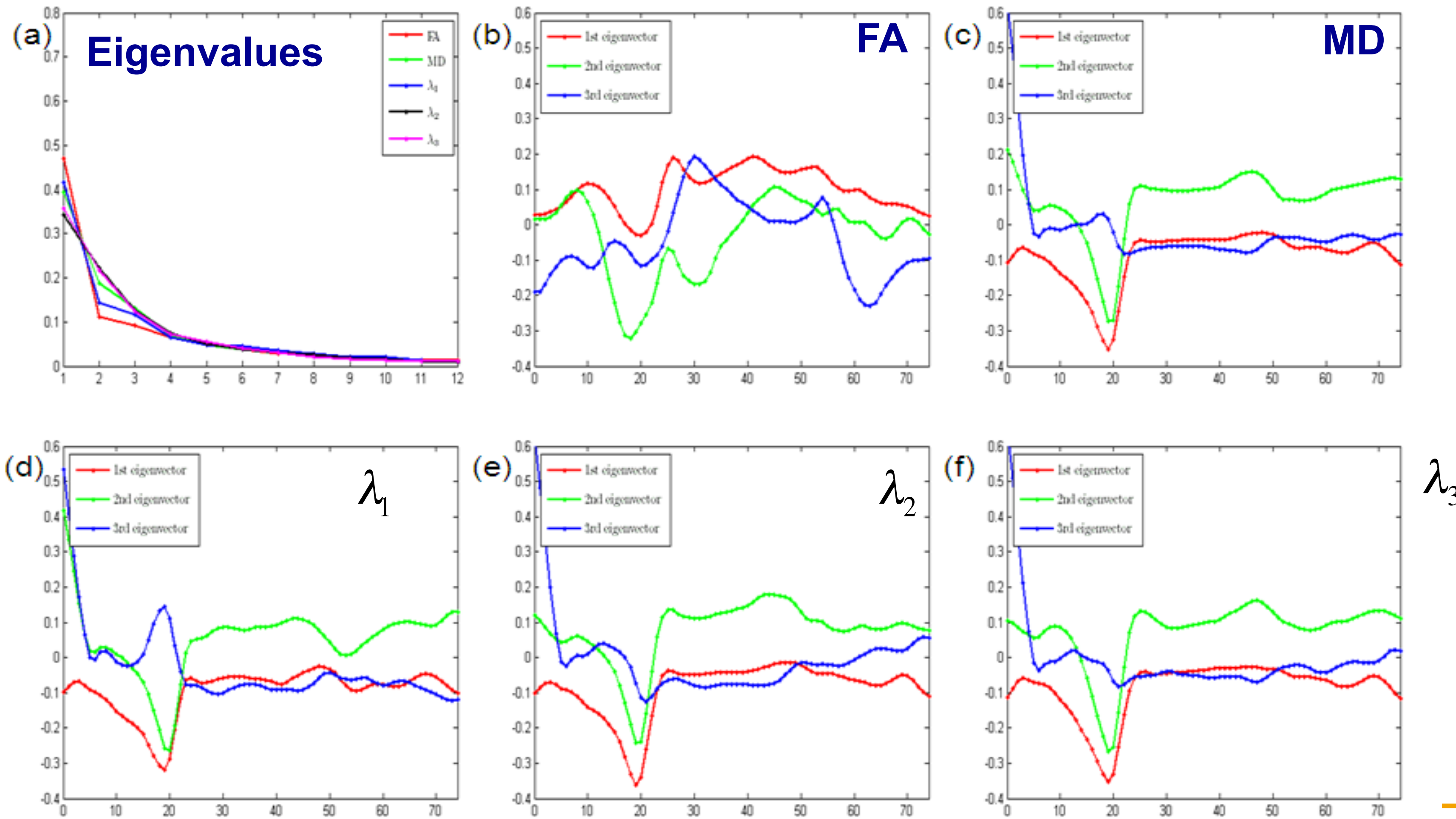

Longitudinal Fiber Tracts

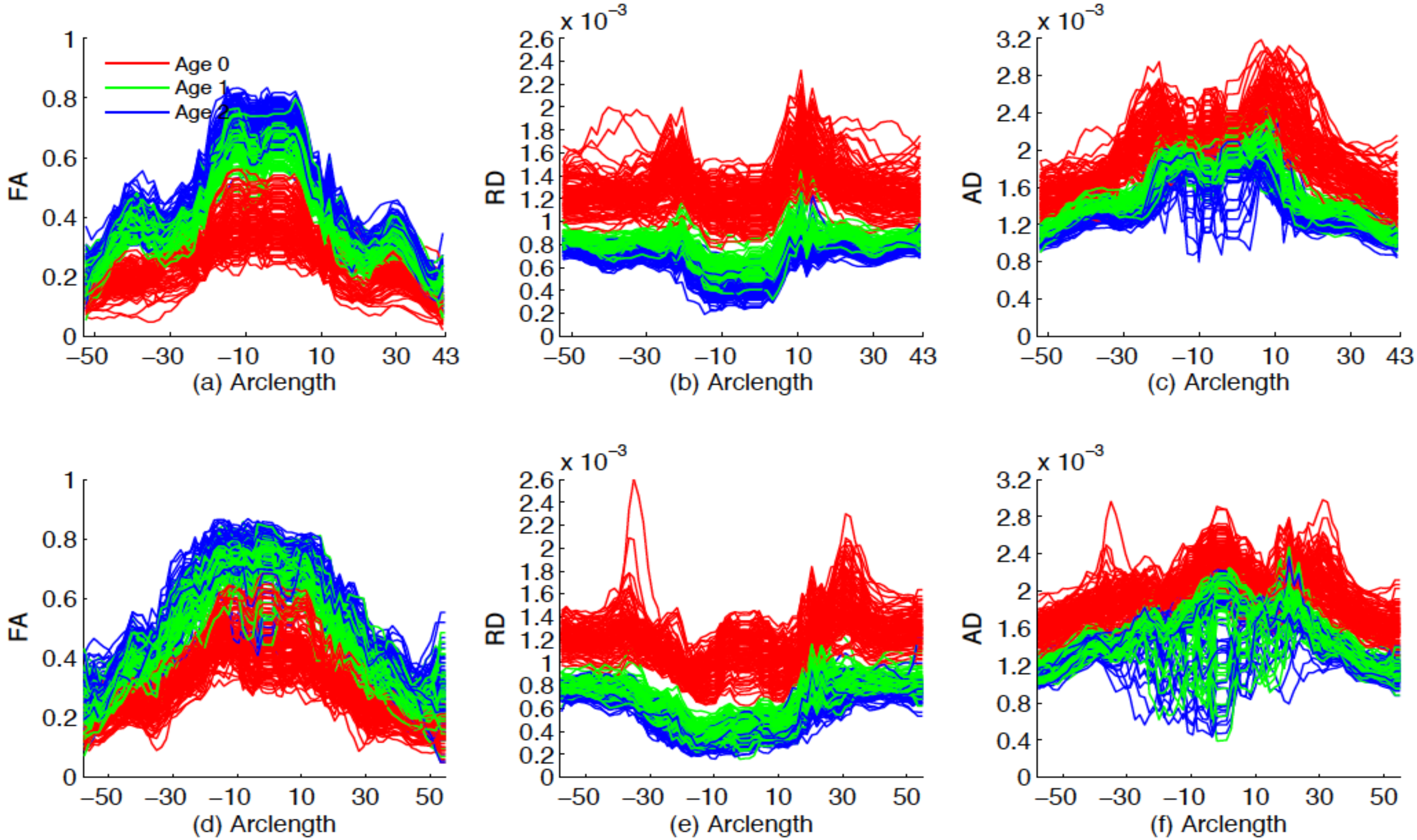

Longitudinal Functional Mixed Effects Model

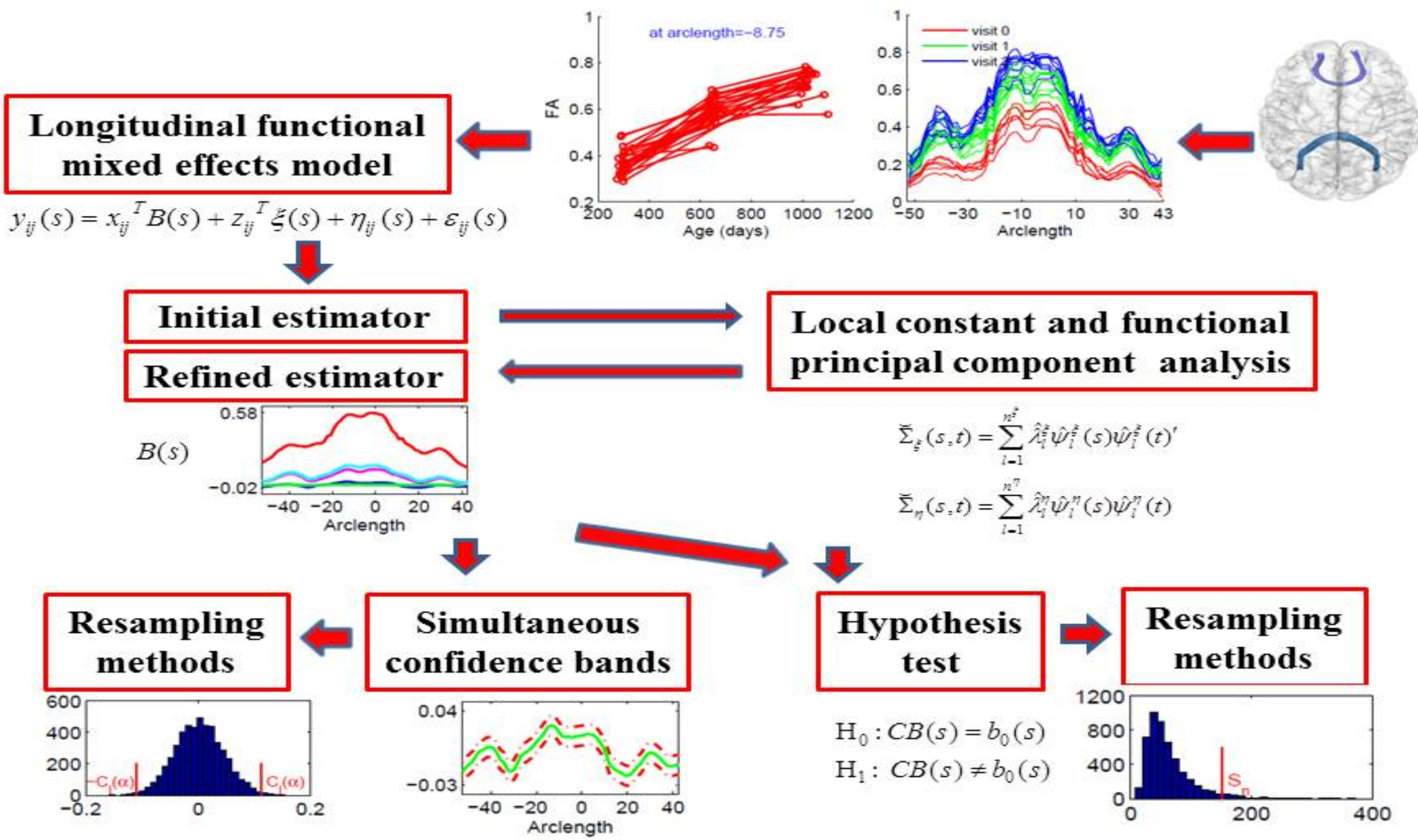

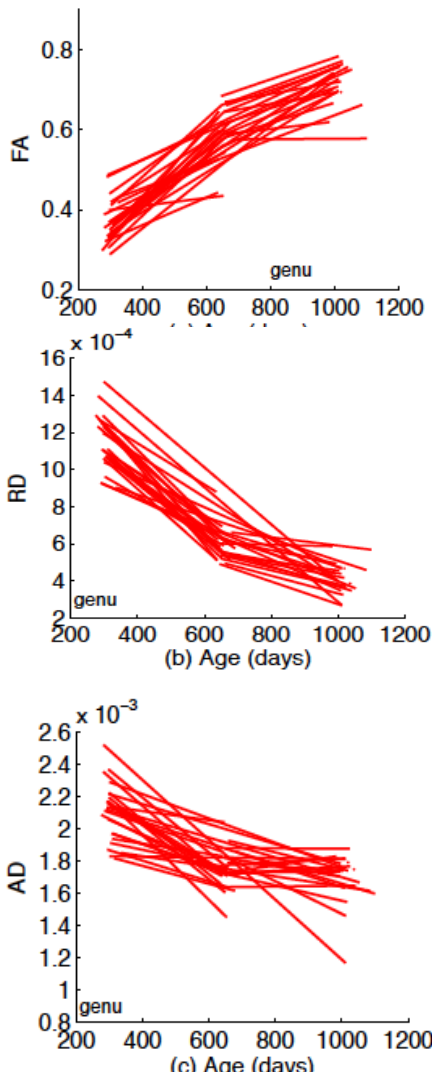

FA
genu
RD
x 10^-4
genu
(b) Age (days)
AD
x 10^-3
genu
(c) Age (days)

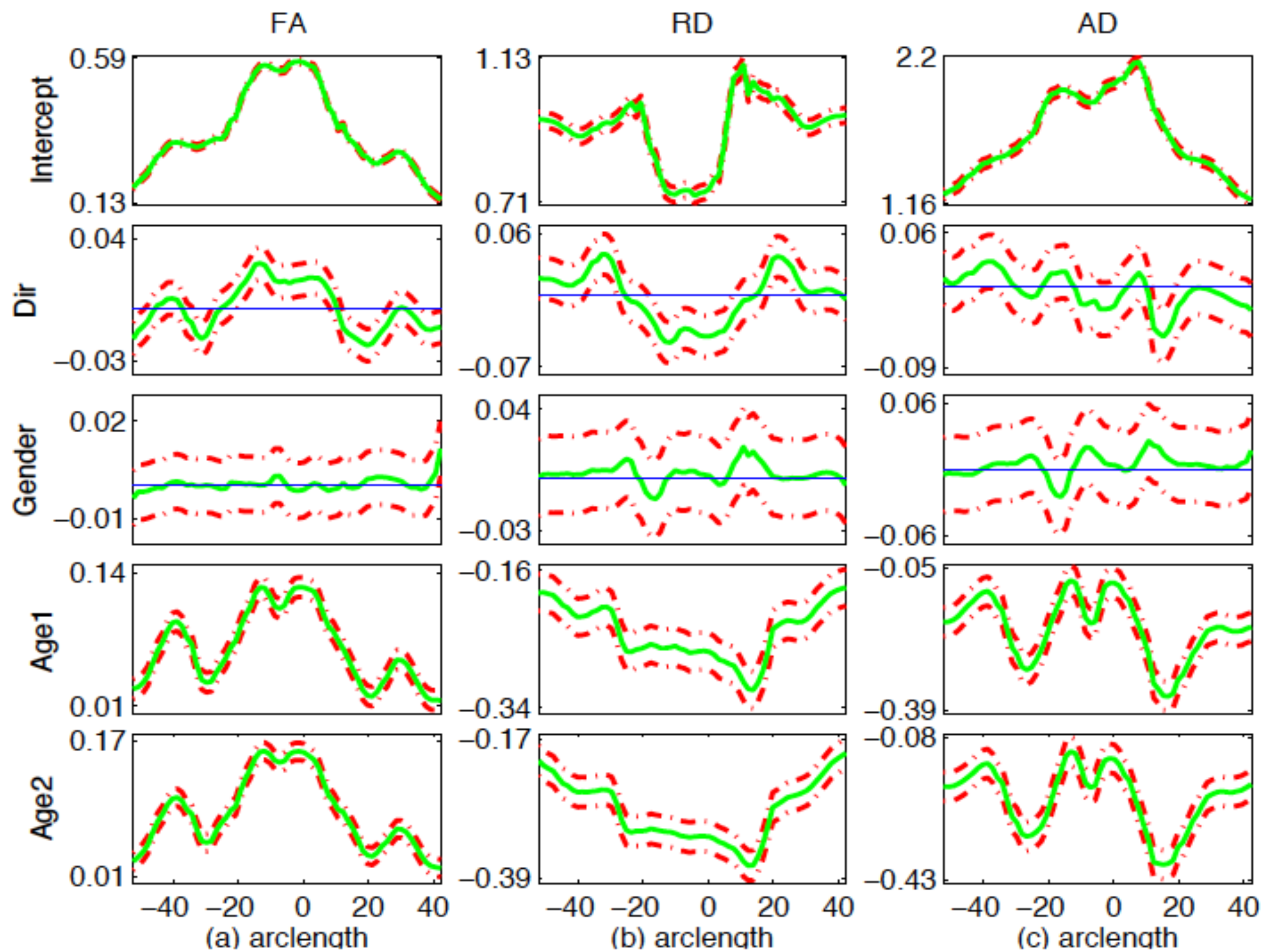

FA
RD
AD
Intercept
Dir
Gender
Age1
Age2
(a) arclength
(b) arclength
(c) arclength

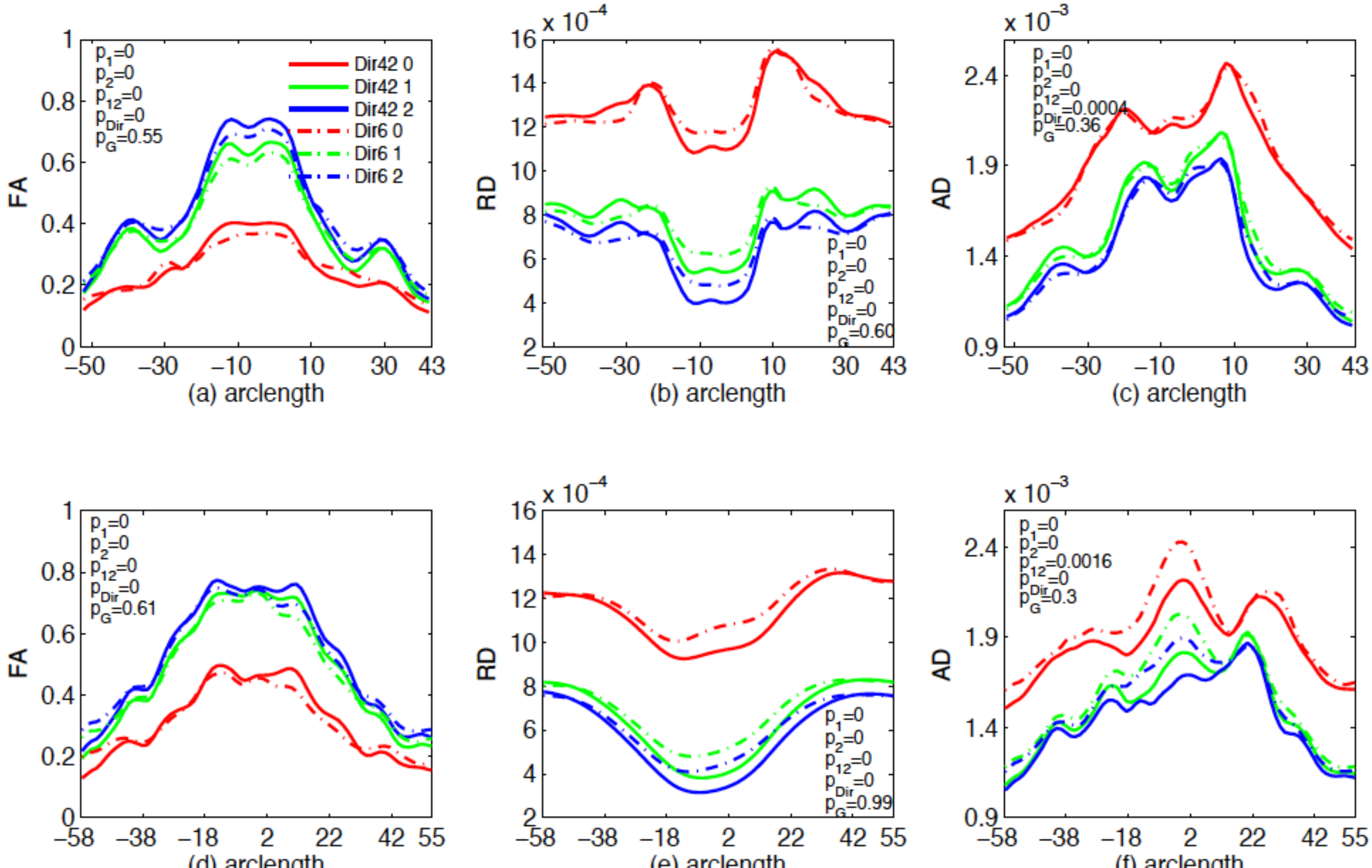

FA
RD
AD
x 10^−4
x 10^−3
Dir42 0
Dir42 1
Dir42 2
Dir6 0
Dir6 1
Dir6 2
p1=0 p2=0 p12=0 pDir=0 pG=0.55
p1=0 p2=0 p12=0 pDir=0 pG=0.60
p1=0 p2=0 p12=0 pDir=0.0004 pG=0.36
p1=0 p2=0 p12=0 pDir=0 pG=0.61
p1=0 p2=0 p12=0 pDir=0 pG=0.99
p1=0 p2=0.0016 p12=0 pDir=0 pG=0.3
(a) arclength
(b) arclength
(c) arclength
(d) arclength
(e) arclength
(f) arclength

FADTTS GUI Toolbox

Project IV: Structural and Functional Specialization

Real Data

ADHD200 NYU Data

Subjects: 174 subjects, 99 normal and 75 ADHD-combined
Response: RAVEN map
Covariates: age, gender, group, and whole brain volume
Goal: Group*Age and Group*Gender

Our goal of study is to detect the <u>location of structural atrophy</u> in ADHD patients.

Voxel Based Analysis (VBA)

SPM/FSL

- Images from Multiple Subjects
- Multiple Images from a single subject

$$Y_i(d) = x_i^T \beta(d) + \varepsilon_i(d)\sigma(d)_i$$

Subject $i = 1, \cdots, n$

Voxel $d \in D$

Inaccurate for both Prediction and Estimation

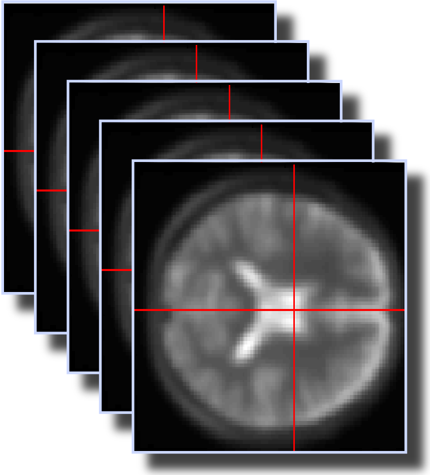

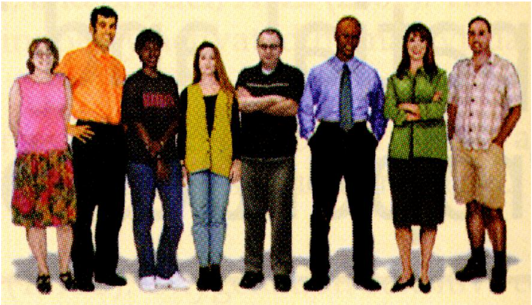

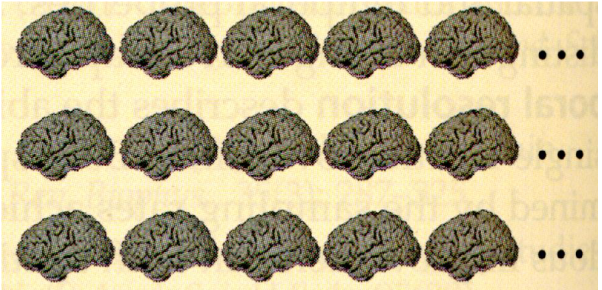

Huettel, Song, and McCarthy (2009)

VBA

Cons

Potential large smoothing errors.

Treat voxels as independent units/images as a collection of independent voxels.

Ignore spatial correlation and smoothness in statistical analysis.

Decrease statistical power.

Raw Images

Image Reconstruction

Image Registration

Multiple Comparisons

Models for Functional data

Statistical Analysis

Simulation

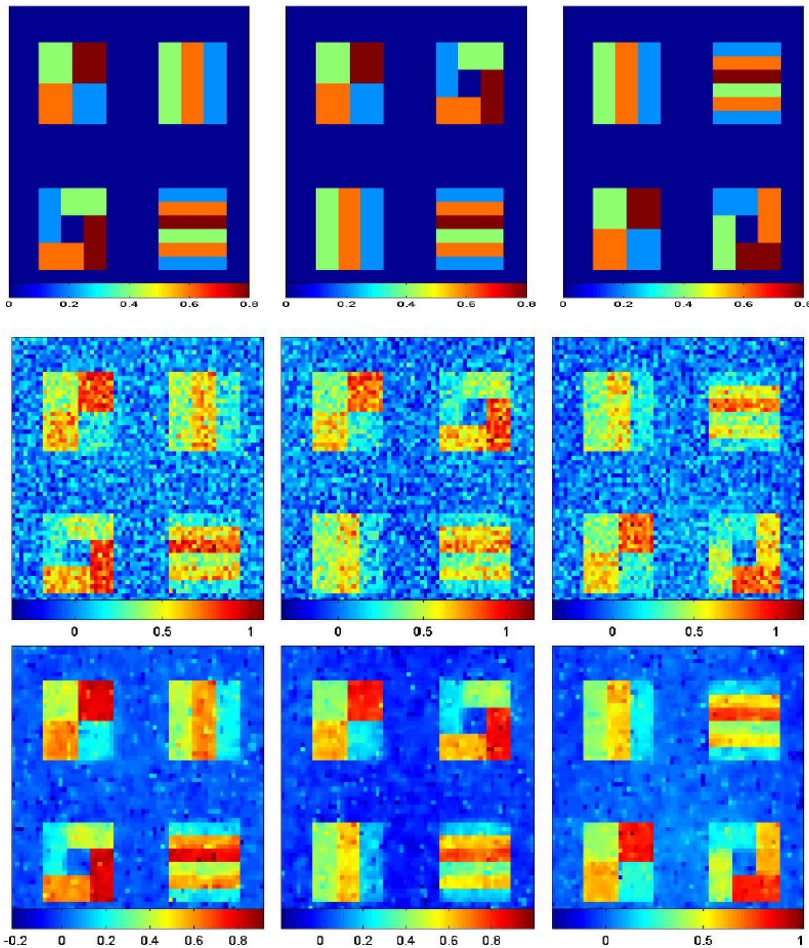

From up to down: initial and adaptive estimates; left to right: $\beta_1(d)$, $\beta_2(d)$, and $\beta_3(d)$.

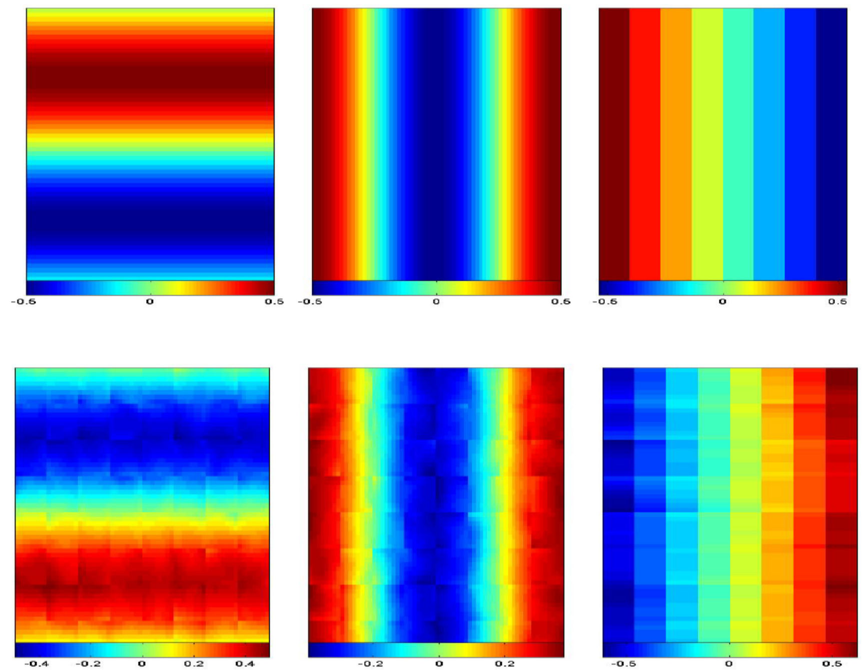

From left to right: $\psi_1(d)$, $\psi_2(d)$, and $\psi_3(d)$.

Simulation

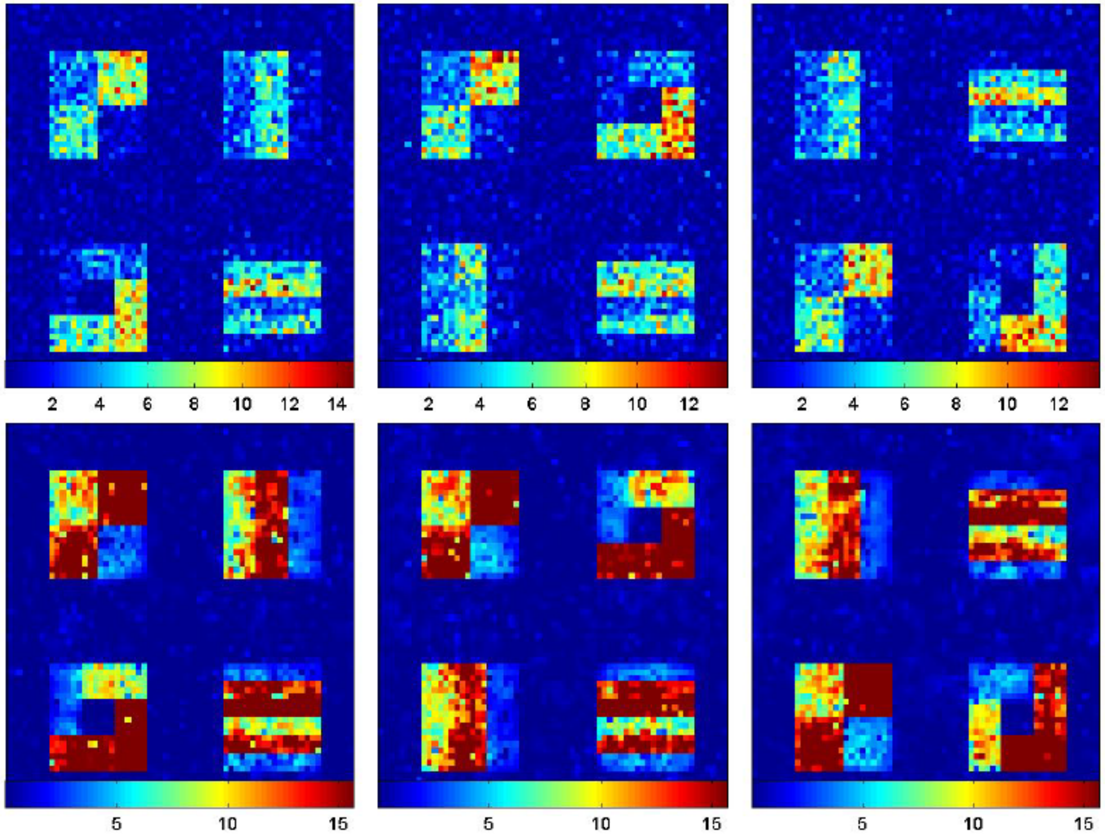

From up to down: $-log_{10}(p)$ of initial and adative estimates; left to right: $\beta_1(d)$, $\beta_2(d)$, and $\beta_3(d)$.

Interaction effect estimates

h_0

Age × Diagnotic Status

h_{10}

h_0

Gender × Diagnostic status

h_{10}

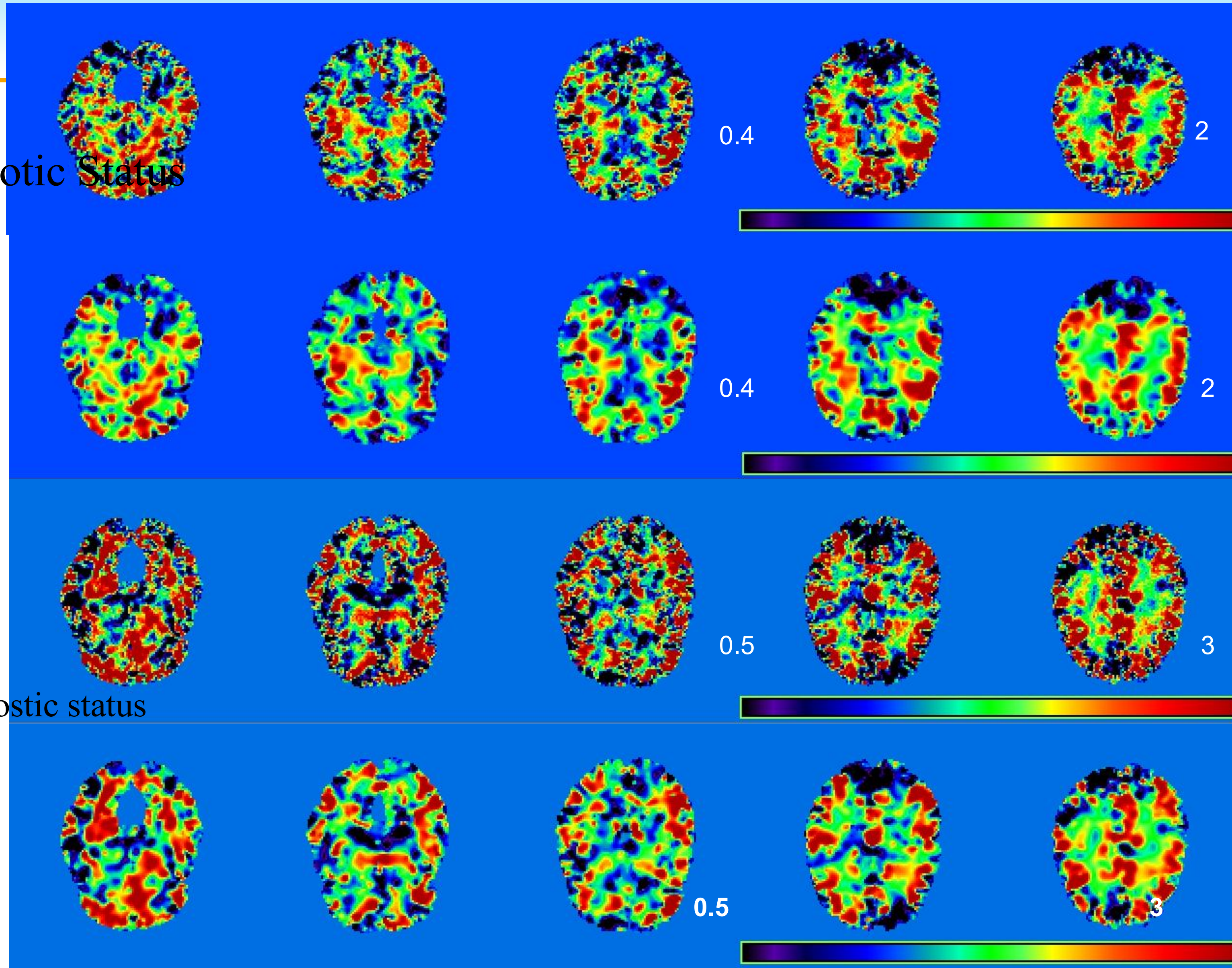

-log10(p) Maps

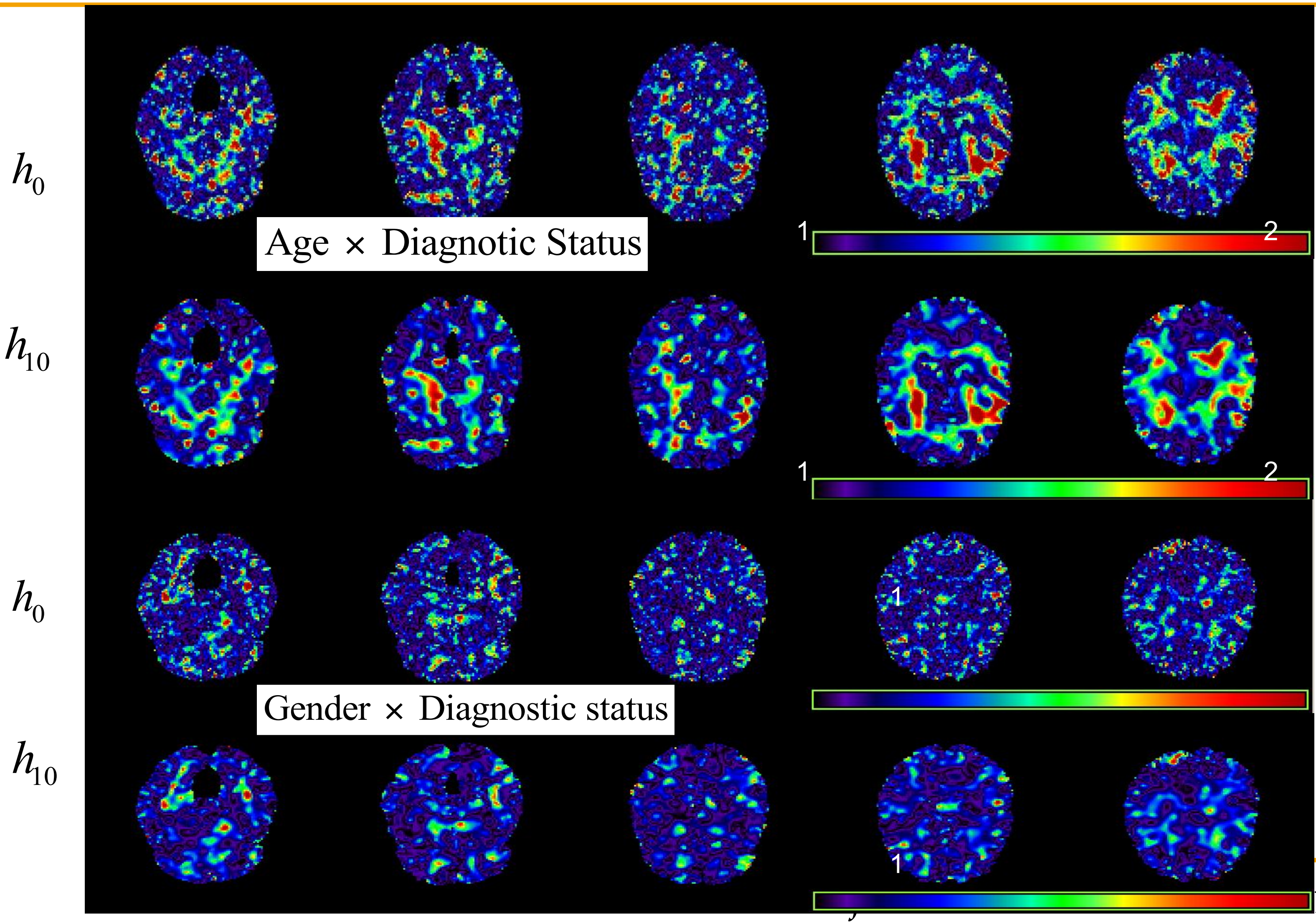

h_0
Age × Diagnotic Status
1
2
h_{10}
1
2
h_0
Gender × Diagnostic status
1
h_{10}
1

Significant Regions

Table 3: The first two largest significant regions of the first three largest significant blocks for hypothesis tests $H_0 : \beta_6(d) = 0$ and $H_0 : \beta_7(d) = 0$ with block and region voxel sizes. WM, L and R, respectively represent white matter, left and right.

			1st largest ROI		2nd largest ROI	
	block	size	ROI label	size	ROI label	size
$A \times D$	1	3954	frontal lobe WM L	1567	frontal lobe WM R	455
	2	2065	frontal lobe WM R	900	anterior limb of internal capsule R	220
	3	1642	nucleus accumbens L	1019	frontal lobe WM L	213
$G \times D$	1	228	temporal lobe WM L	184	middle temporal gyrus L	22
	2	216	frontal lobe WM R	163	superior frontal gyrus L	33
	3	95	temporal lobe WM R	66	lateral occipitotemporal gyrus R	21

Prediction

Raw Image

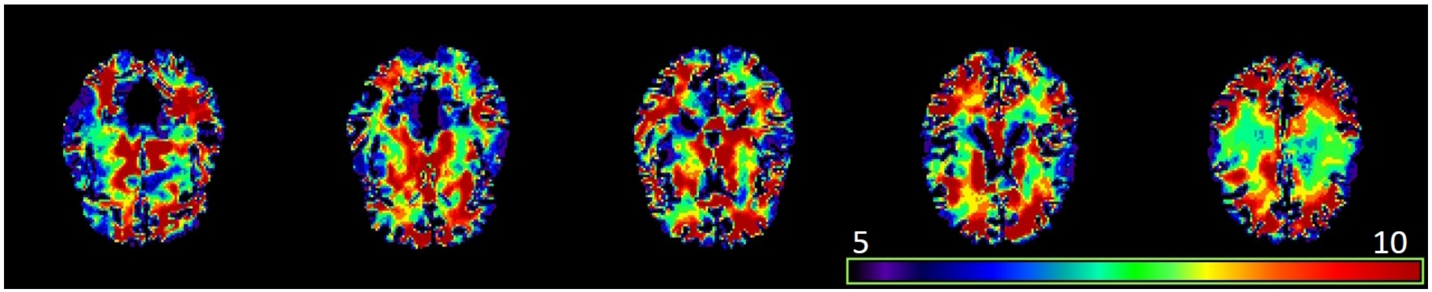

GLM

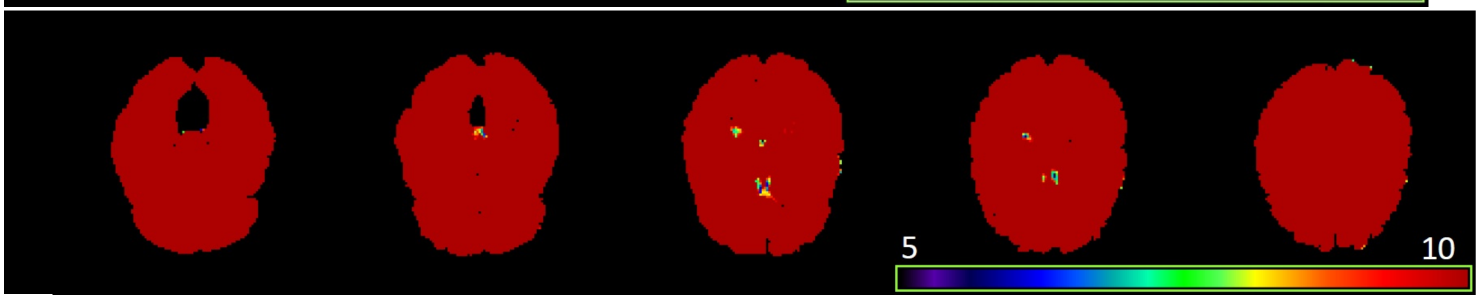

SVCM

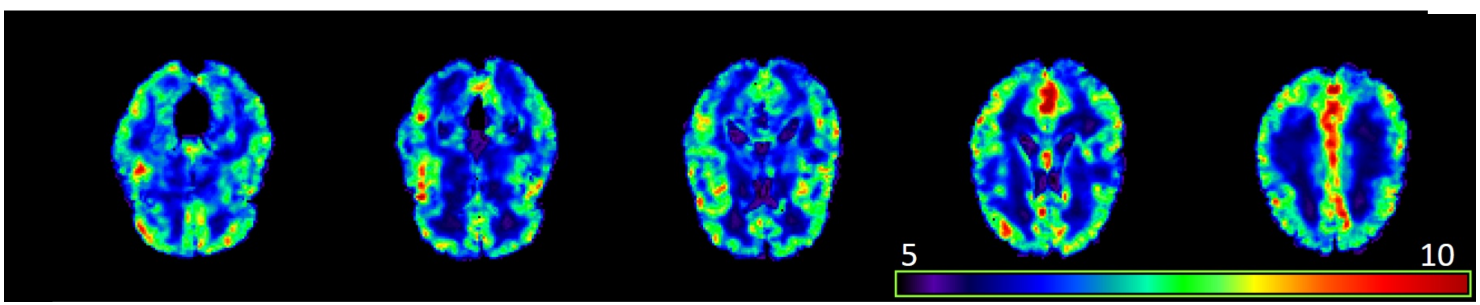

Project V: Functional Connectivity Comparisons

Functional Connectivity

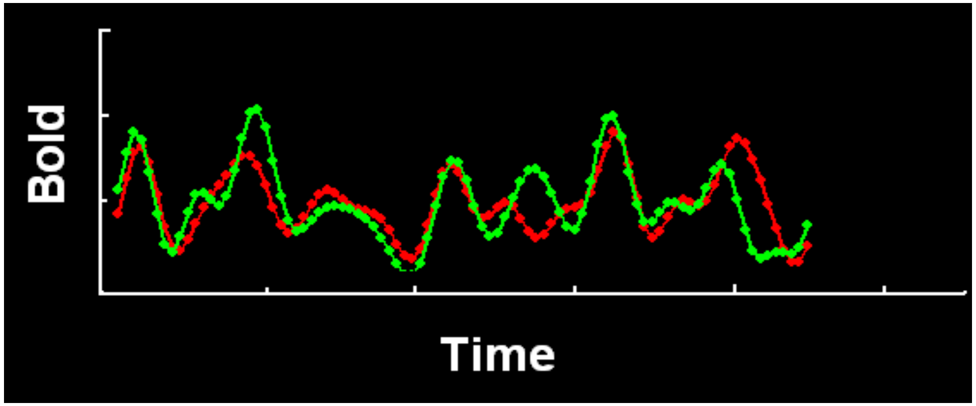

is the mechanism for the coordination of activity between different neural assemblies in order to achieve a complex cognitive task or perceptual process. (Fingelkurts, Fingelkurts, Seppo Kahkonen, Fingelkurts, 2005)

Resting-State Network

fMRI for finger tapping task;

fcMRI:

contralateral motor cortex showed activation and low frequency (<0.1 Hz) fluctuations in the signal of the resting brain, revealing a high degree of temporal correlation.

fMRI fcMRI

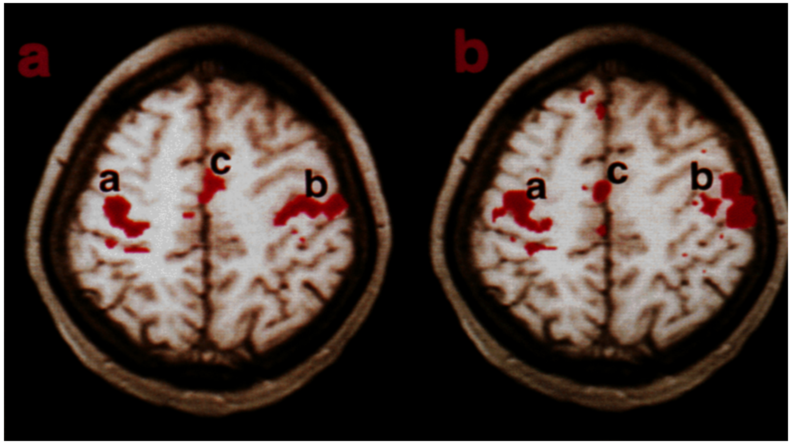

Biswal et al, JCBFM, 17:301-308, 1997

Functional Connectivity

Magnetoencephalography (**MEG**) is a technique for mapping brain activity by recording magnetic fields produced by electrical currents in the brain using very sensitive magnetometers.

Electroencephalography (**EEG**) is the recording of electrical activity along the scalp. EEG measures voltage fluctuations resulting from ionic current flows within the neurons of the brain.

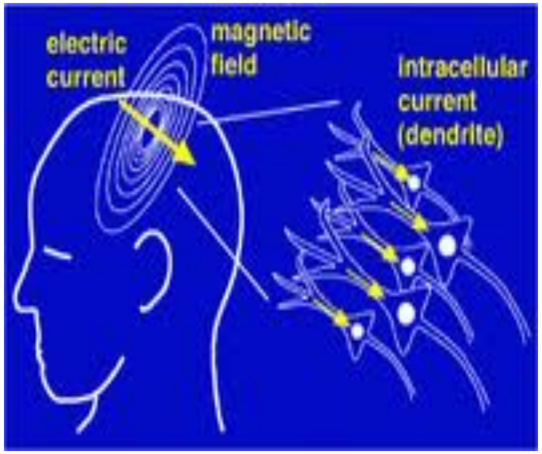

Development of the Default Network

6-12 months: It's another baby!
13-20 months: withdrawal, smile occasionally and make some noise
20-24 months: It's me!

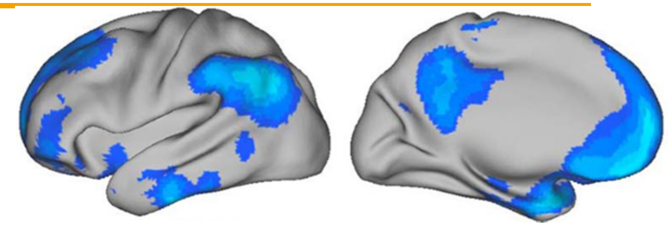

The "default-mode" network

Recollecting the past
Self-Concept
Thinking about future

an evolving trajectory of self-consciousness, essentially for self projection/referential

Functional Connectivity

- is to make inferences on the structure of relationships among brain regions and across groups or time.
- Interesting scientific questions include
  - ♦ "These ROIs form a network."
  - ♦ "ROIs are more connected during task A than B."
  - ♦ "Quantify the emergence and development of some brain networks."
  - ♦ "Connectivity pattern differs between groups A and B."

Standard Method

Average Correlation Map for YA

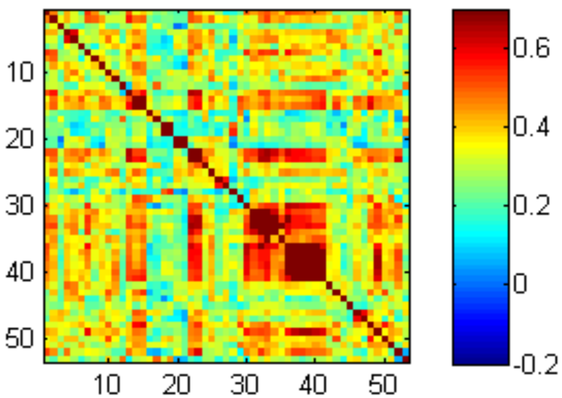

-log10(FDR-corrected p-value) Map for Testing YA

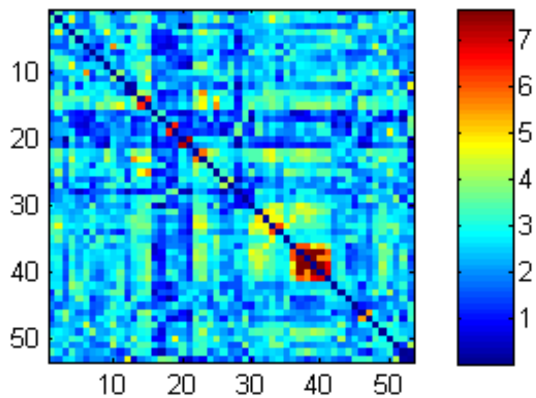

Test Significance Map for Testing YA (alpha=0.001)

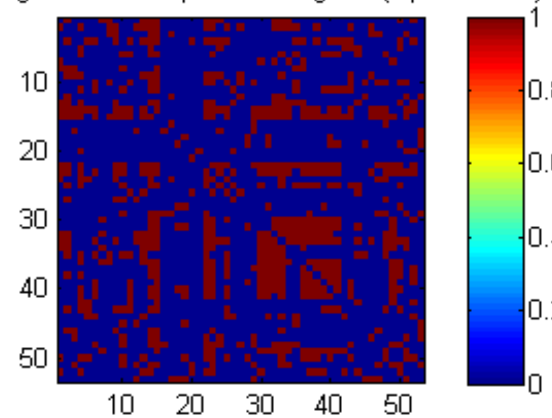

Graph

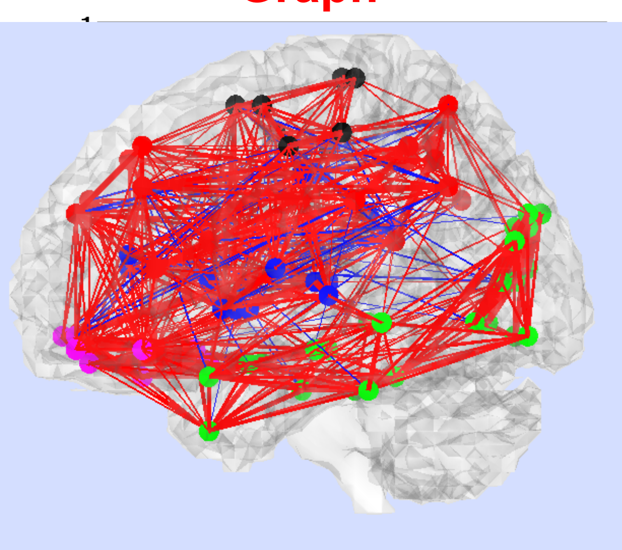

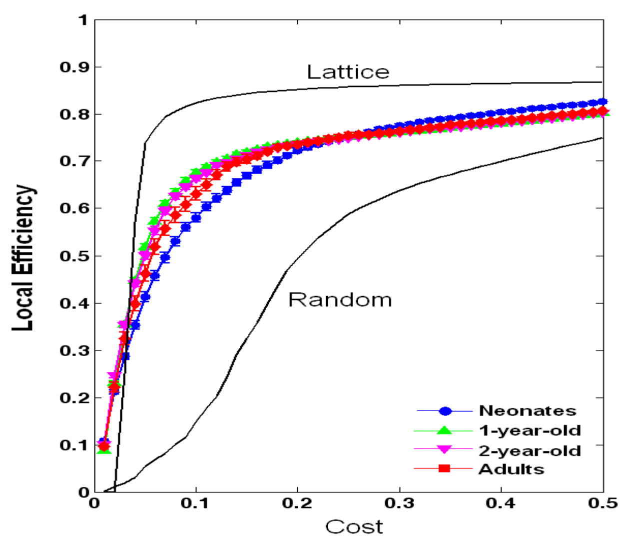

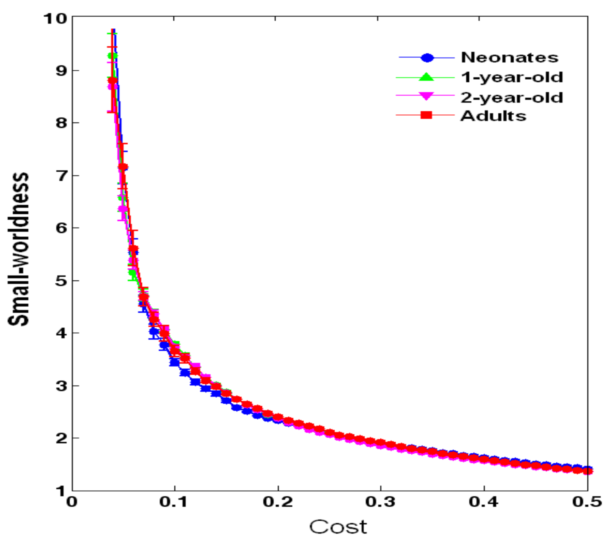

Spatial and Temporal Time Series Data

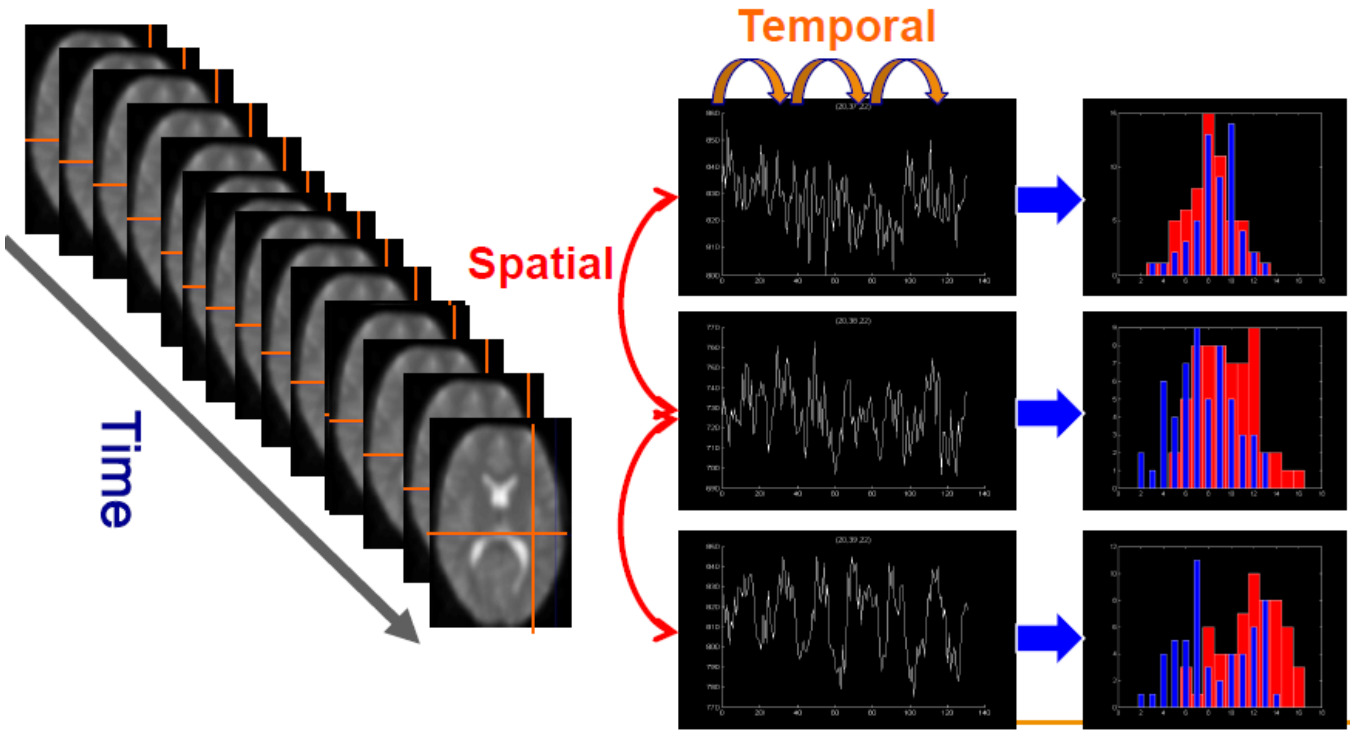

Covariates (e.g., age, gender, diagnostic, stimulus)

Motivation : The ADHD-200 Sample

- Global competition in 2011 to develop a predictive tool for ADHD diagnosis based on functional and structural MRI of the brain
- Data were collected from 8 institutions around the world
- There are 4 groups of subjects :

  Typically developing children (488)

  ADHD Combined type(158)

  ADHD Hyperactive/Impulsive type (11)

  ADHD Inattentive type (110)
- Our goals of study :

  Find group difference using time course data

  Find brain regions and time frequencies where ADHD groups show strong signals, compared with control group

Time course data

Region of interest

Time point

-0.076	-0.030	0.004	0.063	-0.109	-0.085	-0.020	0.039
-0.077	-0.017	-0.011	0.091	-0.211	-0.103	-0.030	0.083
-0.052	0.009	-0.011	0.088	-0.273	-0.109	-0.021	0.119
-0.016	0.034	0.012	0.049	-0.259	-0.104	0.004	0.122
0.011	0.040	0.052	-0.013	-0.175	-0.093	0.028	0.081
0.027	0.020	0.090	-0.074	-0.070	-0.087	0.038	0.009
0.042	-0.013	0.107	-0.113	-0.003	-0.094	0.033	-0.063
0.066	-0.038	0.100	-0.118	0.000	-0.111	0.026	-0.103
0.096	-0.037	0.082	-0.091	-0.033	-0.123	0.036	-0.097
0.116	-0.004	0.072	-0.042	-0.046	-0.111	0.067	-0.056
0.109	0.047	0.078	0.016	0.004	-0.063	0.107	-0.012
0.078	0.098	0.089	0.064	0.112	0.010	0.133	0.009
0.043	0.129	0.086	0.087	0.225	0.077	0.125	-0.002
0.030	0.135	0.056	0.072	0.280	0.107	0.084	-0.033
0.046	0.116	0.009	0.021	0.252	0.085	0.033	-0.067

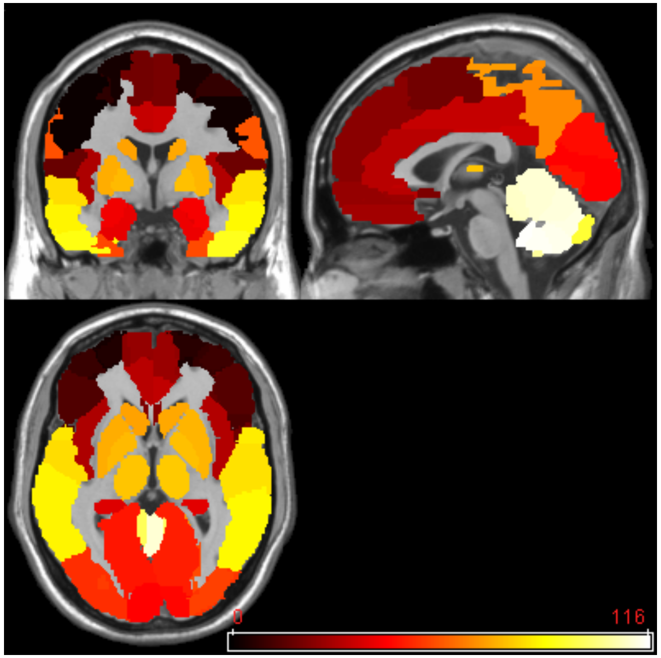

NYU data have 117 time points.
AAL atlas divides brain into 116 regions of interest.

Periodogram

We change the data into frequency domain

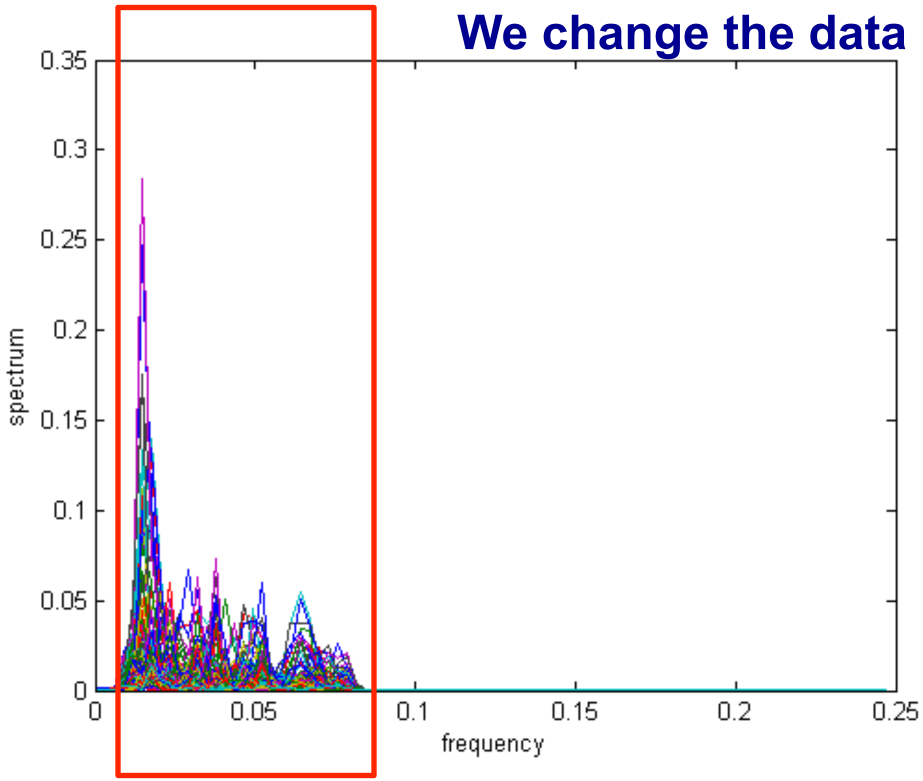

0.015	0.012	0.001	0.003	0.018	0.022	0.004	0.003
0.011	0.007	0.009	0.007	0.003	0.008	0.006	0.001
0.027	0.018	0.024	0.031	0.106	0.112	0.063	0.033
0.019	0.019	0.029	0.014	0.005	0.007	0.014	0.006
0.006	0.009	0.007	0.004	0.002	0.009	0.002	0.001
0.004	0.000	0.003	0.002	0.002	0.019	0.001	0.000
0.003	0.001	0.016	0.006	0.004	0.006	0.004	0.003
0.002	0.012	0.008	0.004	0.001	0.000	0.008	0.004
0.013	0.009	0.011	0.014	0.001	0.001	0.014	0.011
0.027	0.019	0.004	0.004	0.007	0.012	0.006	0.002
0.010	0.017	0.000	0.005	0.004	0.001	0.001	0.000
0.004	0.000	0.009	0.002	0.003	0.010	0.005	0.001
0.005	0.002	0.010	0.002	0.002	0.006	0.000	0.000
0.004	0.004	0.002	0.006	0.000	0.001	0.007	0.007
0.002	0.002	0.002	0.000	0.003	0.001	0.005	0.004

< An example of periodogram >

Band-pass filter (0.009<f<0.08 Hz) was used to exclude frequencies not implicated in resting state functional connectivity

Mean Spectrum

Control group

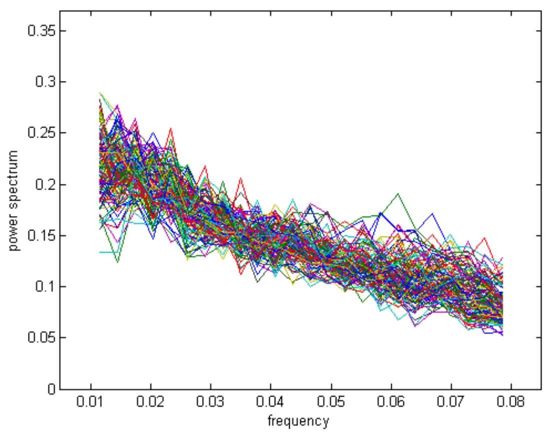

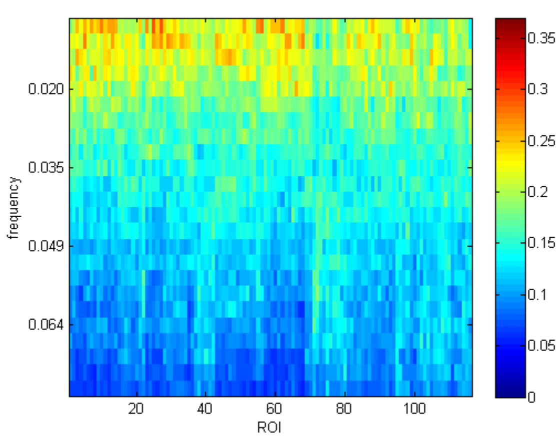

ADHD combined subtype

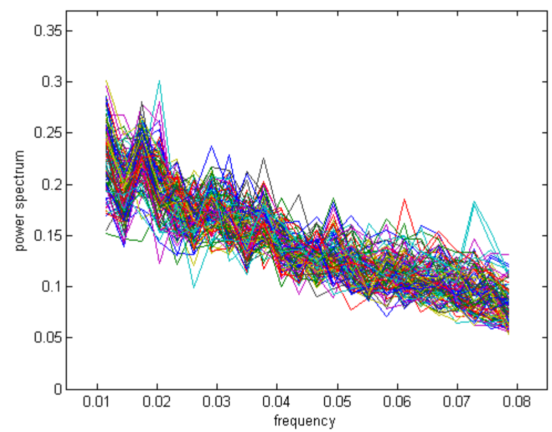

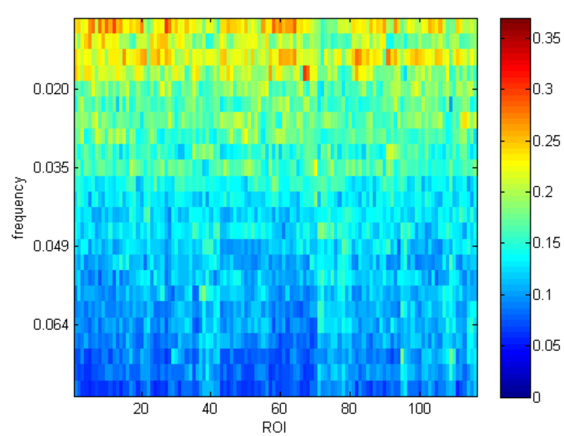

ADHD inattentive subtype

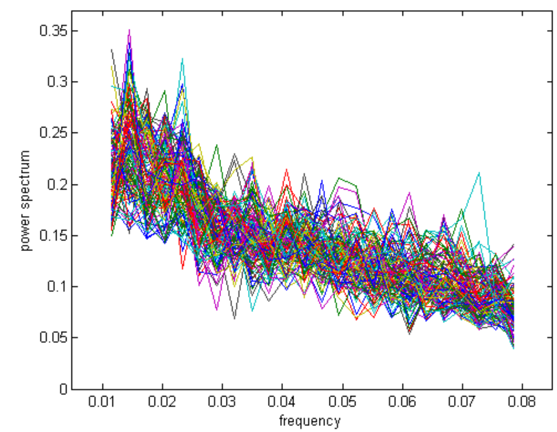

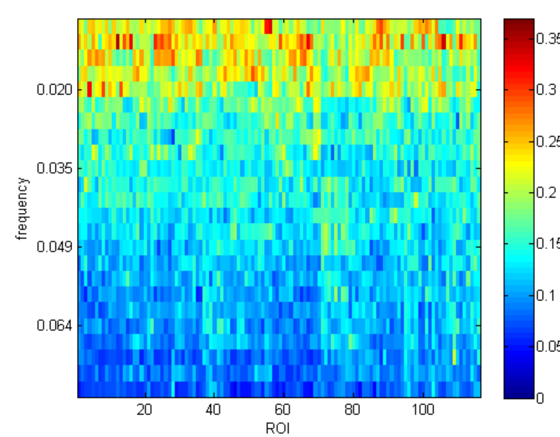

before

after penalization

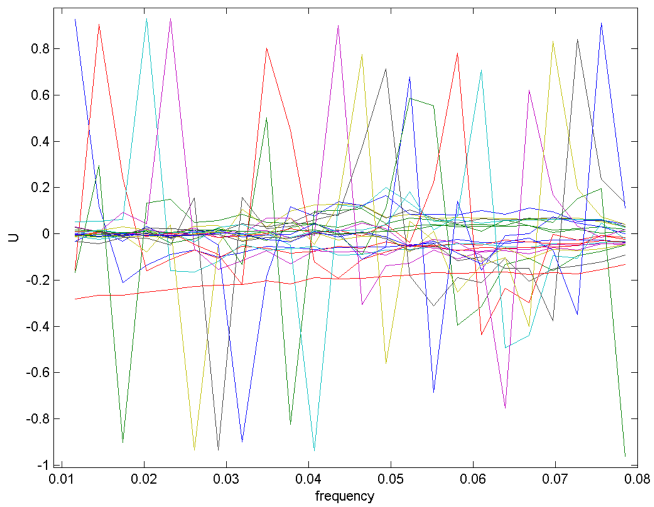

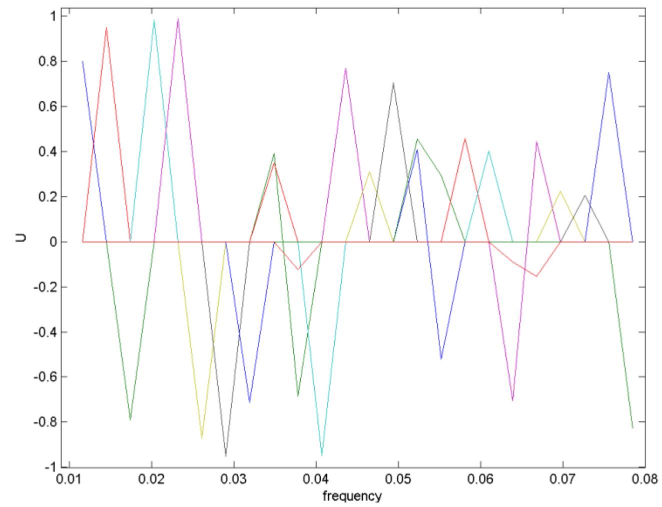

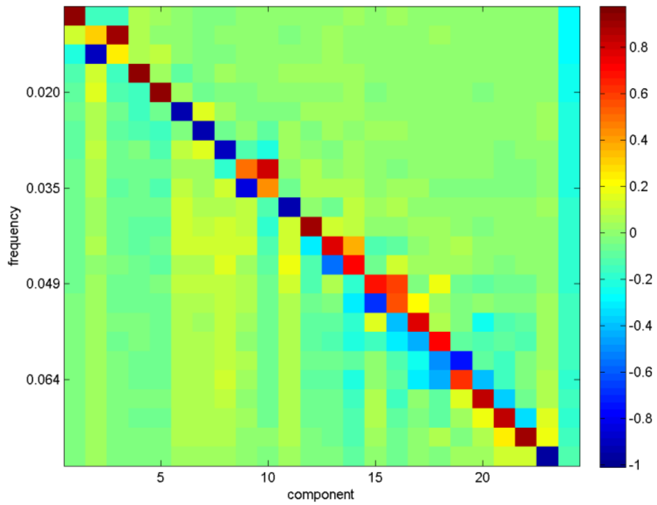

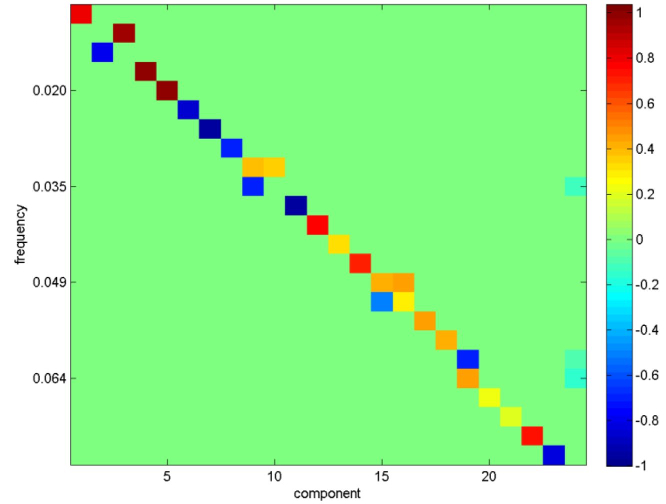

Testing differences among three groups

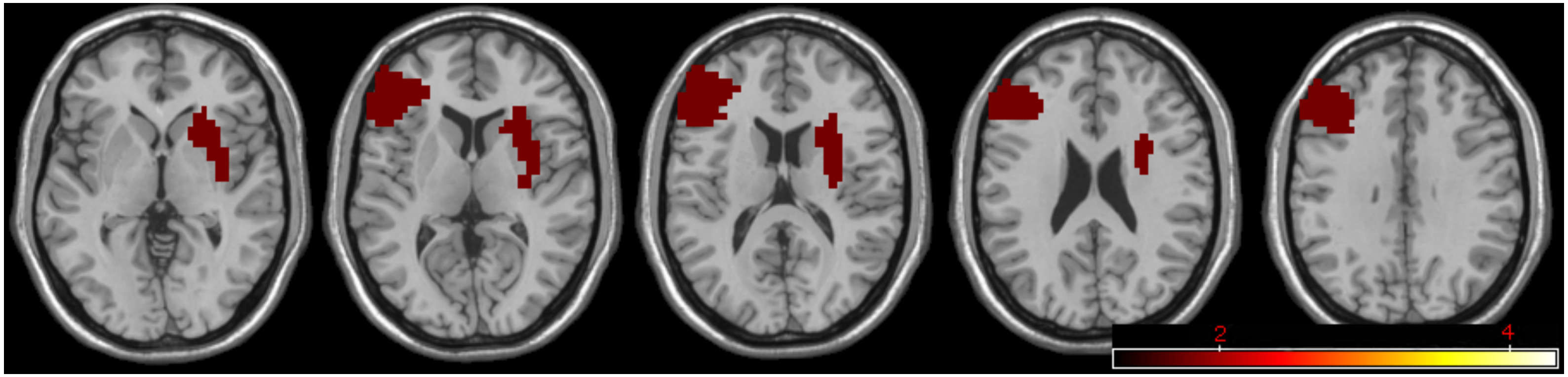

13th ROI : triangular part of inferior frontal gyrus (left)

⇨ **language**

74th ROI : right putamen

⇨ **movement regulation and some forms of learning**

Controls vs ADHD combined subtype

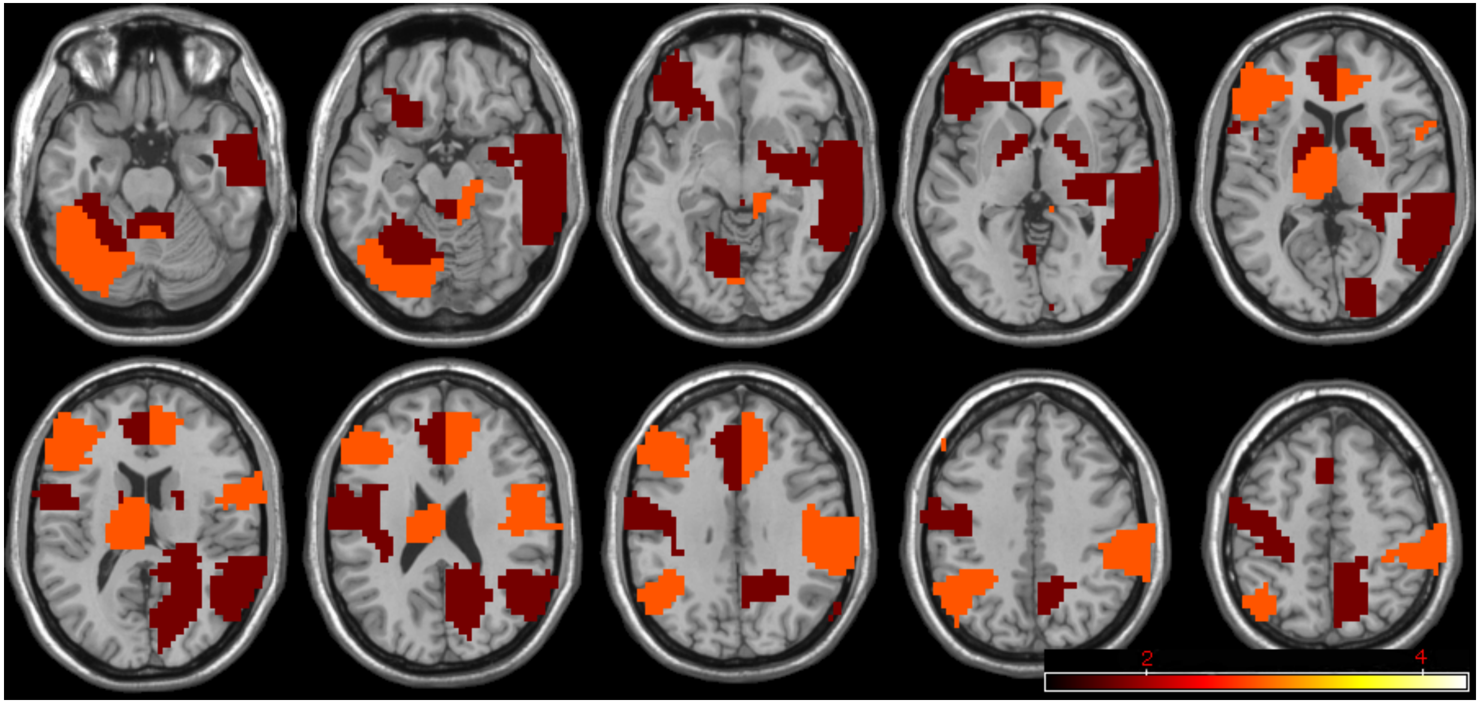

ROIs include:

Dorsolateral prefrontal cortex, Anterior prefrontal cortex, Inferior prefrontal gyrus, insular cortex, Motor cortex, Dorsal anterior cingulate cortex, Ventral anterior cingulate cortex, Visual cortex, Somatosensory cortex, Supramarginal gyrus, Temporal gyri (superior, middle, inferior), Parahippocampal gyrus , cerebellum

Controls vs ADHD inattentive subtype

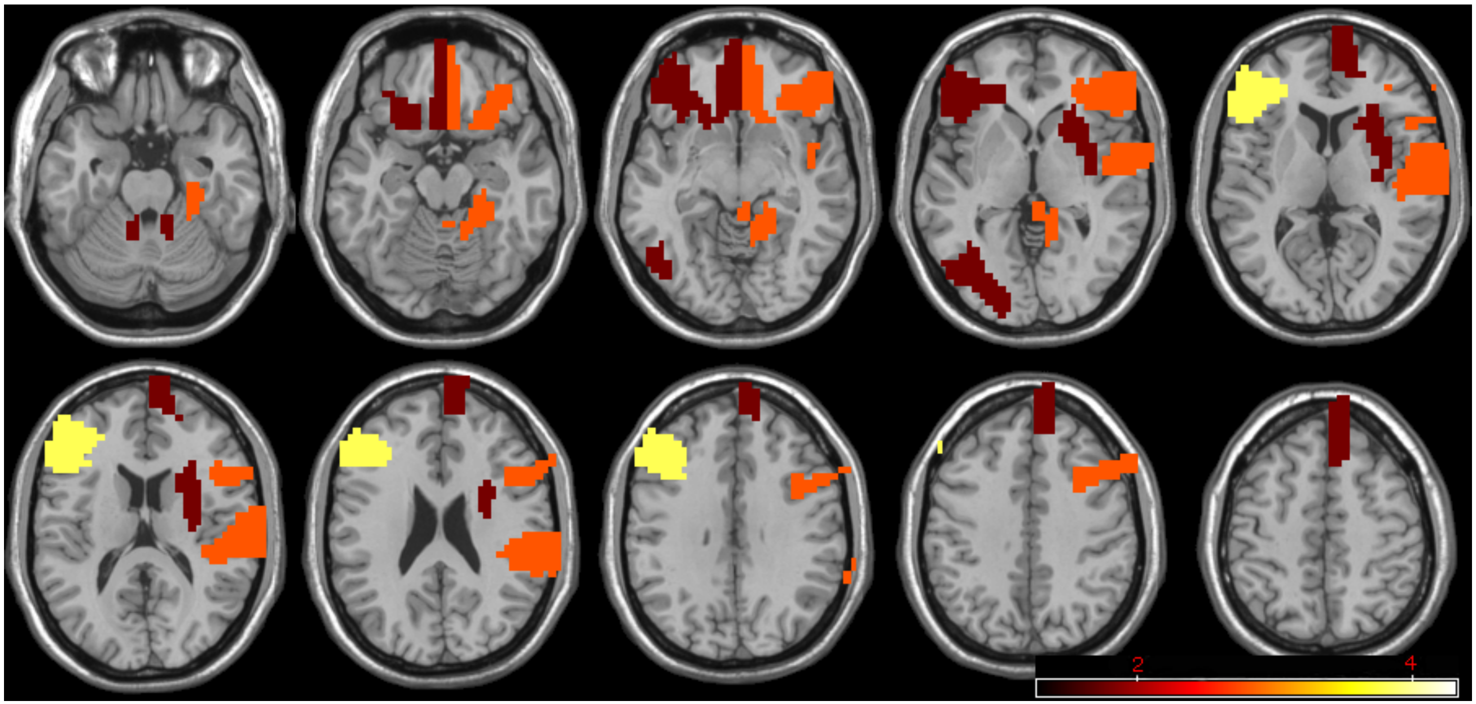

ROIs include:
Dorsolateral prefrontal cortex, Anterior prefrontal cortex, Inferior prefrontal gyrus, insular cortex, Motor cortex, Visual cortex, Somatosensory cortex, Temporal gyri (superior, middle), cerebellum

ADHD combined subtype vs inattentive subtype

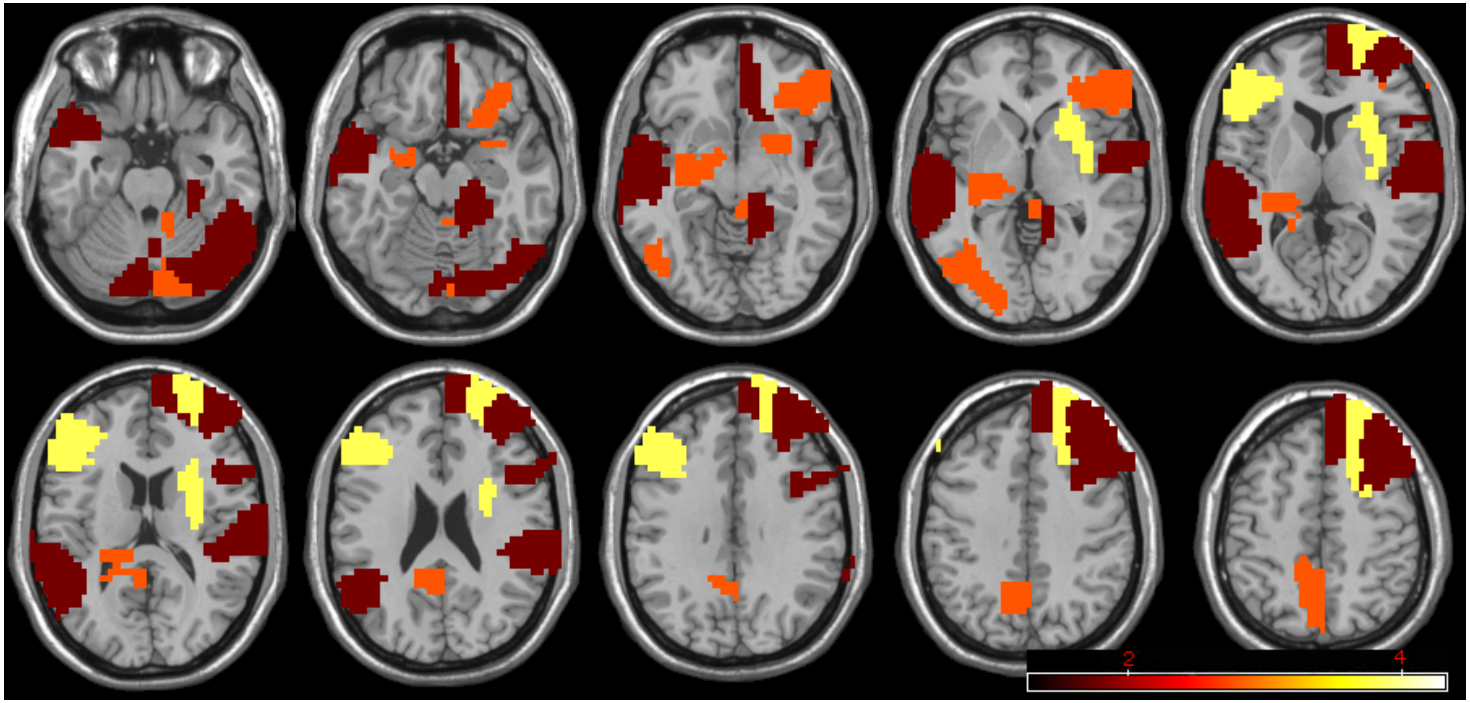

ROIs include:
Dorsolateral prefrontal cortex, Anterior prefrontal cortex, Inferior prefrontal gyrus, insular cortex, Motor cortex, Visual cortex, Somatosensory cortex, Temporal gyri (superior, middle), Parahippocampal gyrus , cerebellum

Conclusion

- In resting-state fMRI studies, abnormalities were found in anterior cingulate cortex, prefrontal cortex, putamen, temporal cortex, and cerebellum (Anderson et al, 2002; Tamm et al, 2004; Schulz et al, 2004; Valera et al, 2005; Tian et al, 2006; Cao et al, 2006; Cao et al, 2006; Toplak et al, 2006; Cherkasova and Hechtman, 2009)
- Especially, it is well-known that cerebellum, basal ganglia, and prefrontal cortex are important in ADHD.
- We found that normal controls and ADHD children show differences in several brain regions, including prefrontal cortex, motor cortex, cingulate cortex, visual cortex, somatosensory cortex, temporal gyrus, and cerebellum.
- We also identified some important frequencies by applying a penalization method (

Project VI. Imaging Genetics

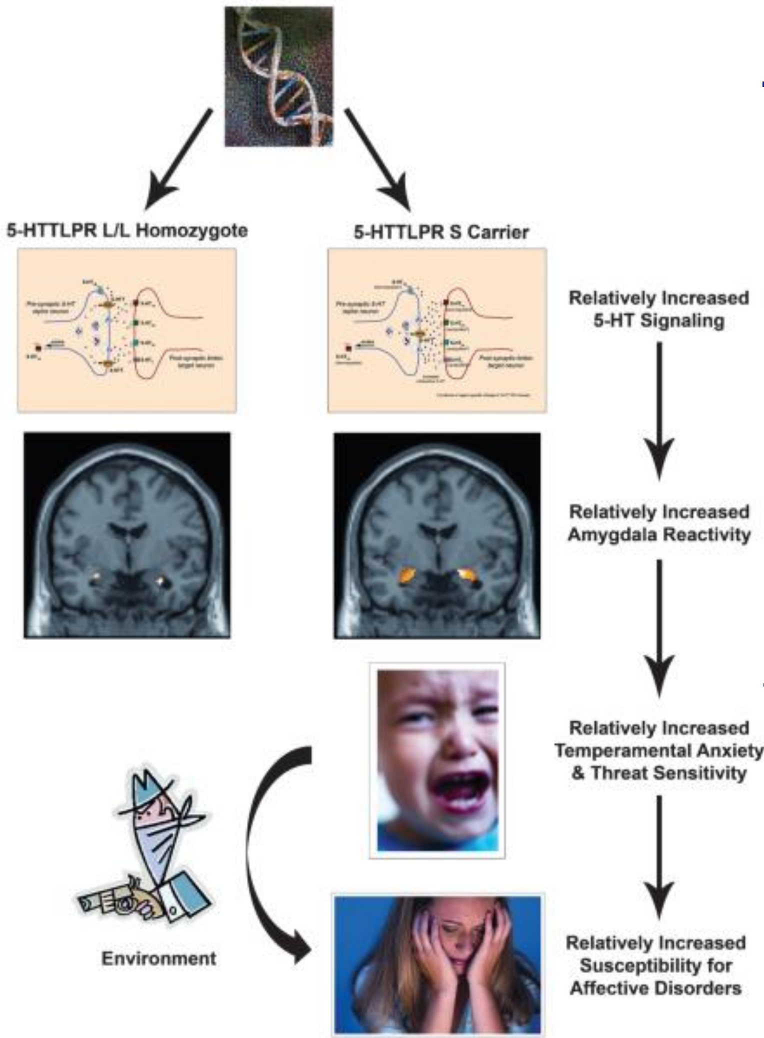

<u>Imaging genetics</u> allows for the identification of how common genetic polymorphisms influencing molecular processes (e.g., serotonin signaling), bias neural pathways (e.g., amygdala reactivity), mediating individual differences in complex behavioral processes (e.g., trait anxiety) related to disease risk in response to environmental adversity.

(Hariri AR, Holmes A.
Genetics of emotional regulation:
the role of the serotonin transporter in neural function.
Trends Cogn Sci. [10:182–191])

Directed Acyclic Graphs for Imaging Genetic Studies

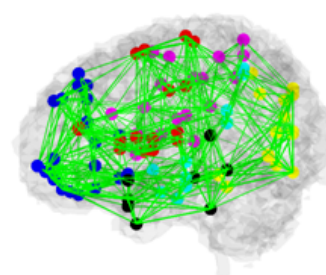

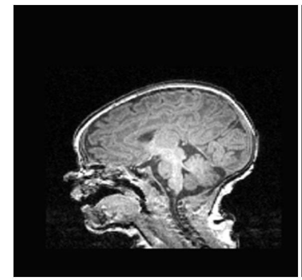

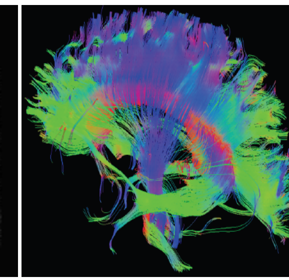

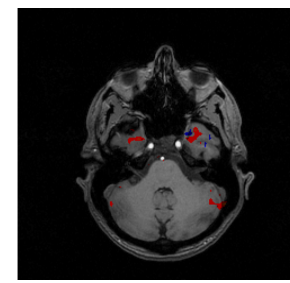

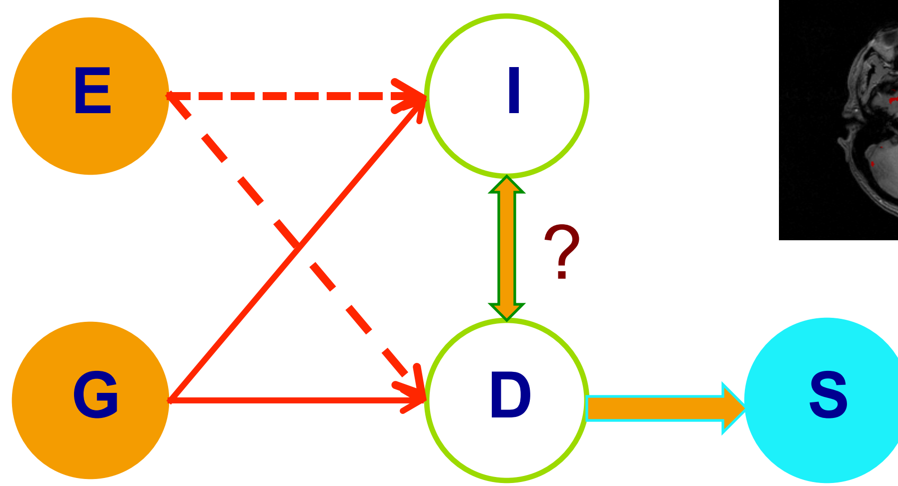

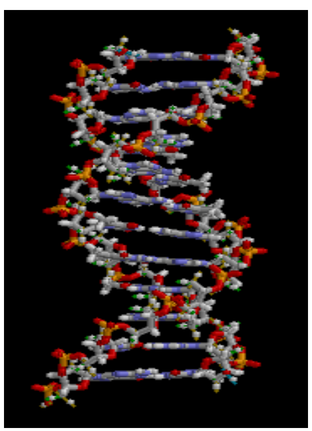

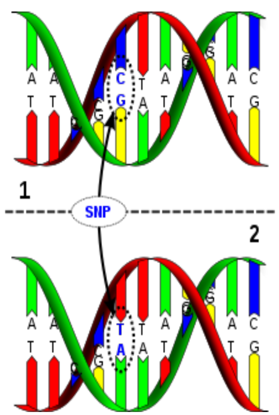

http://en.wikipedia.org/wiki/DNA_sequence

Neuroimaging Phenotype

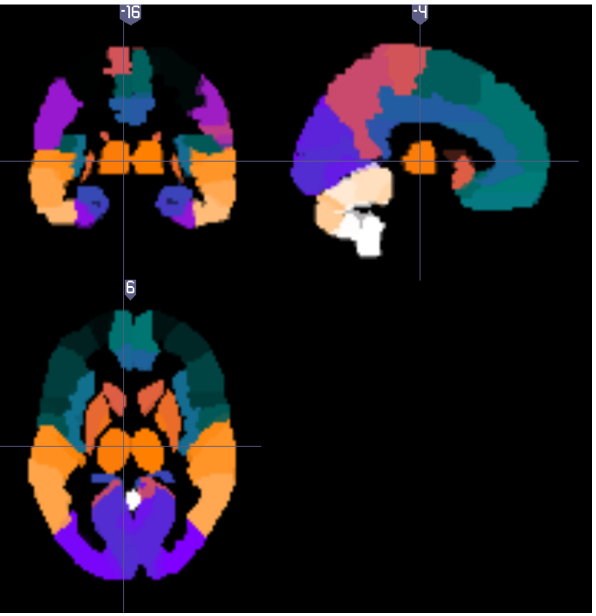

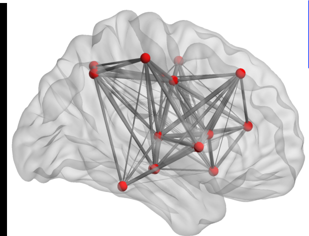

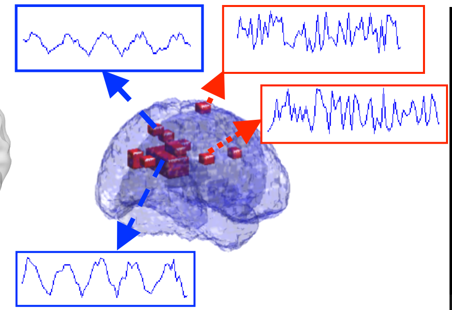

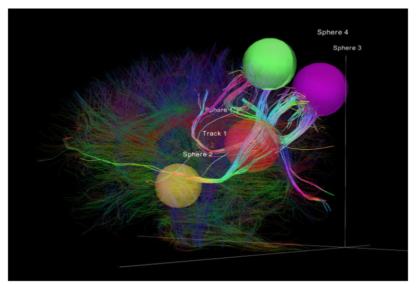

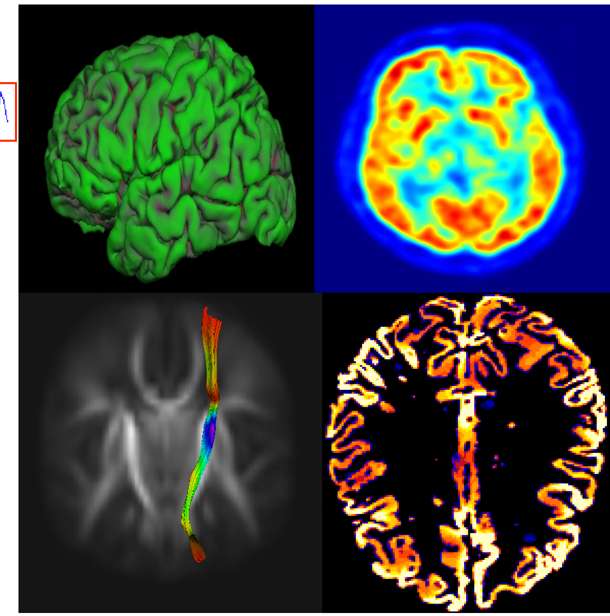

Multivariate, smoothed functions, and piecewisely smoothed functions

Dimension varies from 100~500,000.

Genetic Data

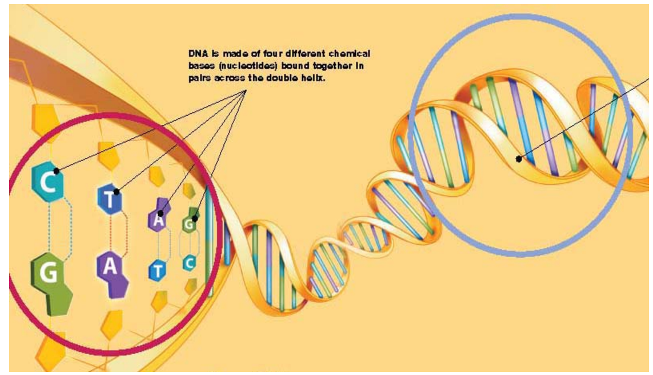

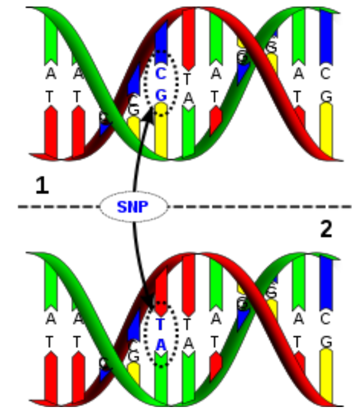

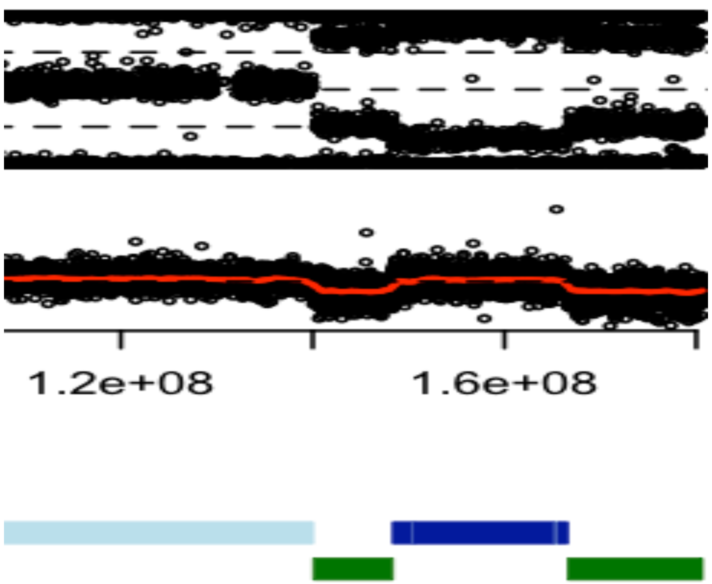

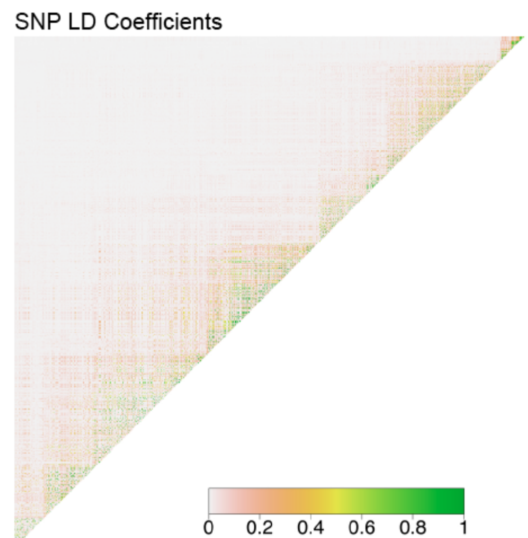

Imaging Genetics

Genetics \ Imaging	Candidate ROI 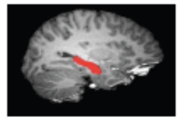	Many ROI 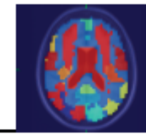	Voxelwise 
Candidate SNP 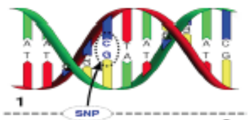	Imager	Imager	Imager
Candidate Gene 	Geneticist		
Genome-wide SNP rs661903 | rs59206197 rs11493920 | rs58524100 rs34984204 | rs11218322 rs55682479 | rs12279197 rs664238 | rs59966742 rs34898405 | rs617847	Geneticist		
Genome-wide Gene BUD13 | SCN4B | CBL BUD13 | SCN2B | MCAM BUD13 | AMICA1 | MCAM ZNF259 | AMICA1 | MFRP ZNF259 | AMICA1 | MFRP	Geneticist		

Hibar, et al. HBM 2012

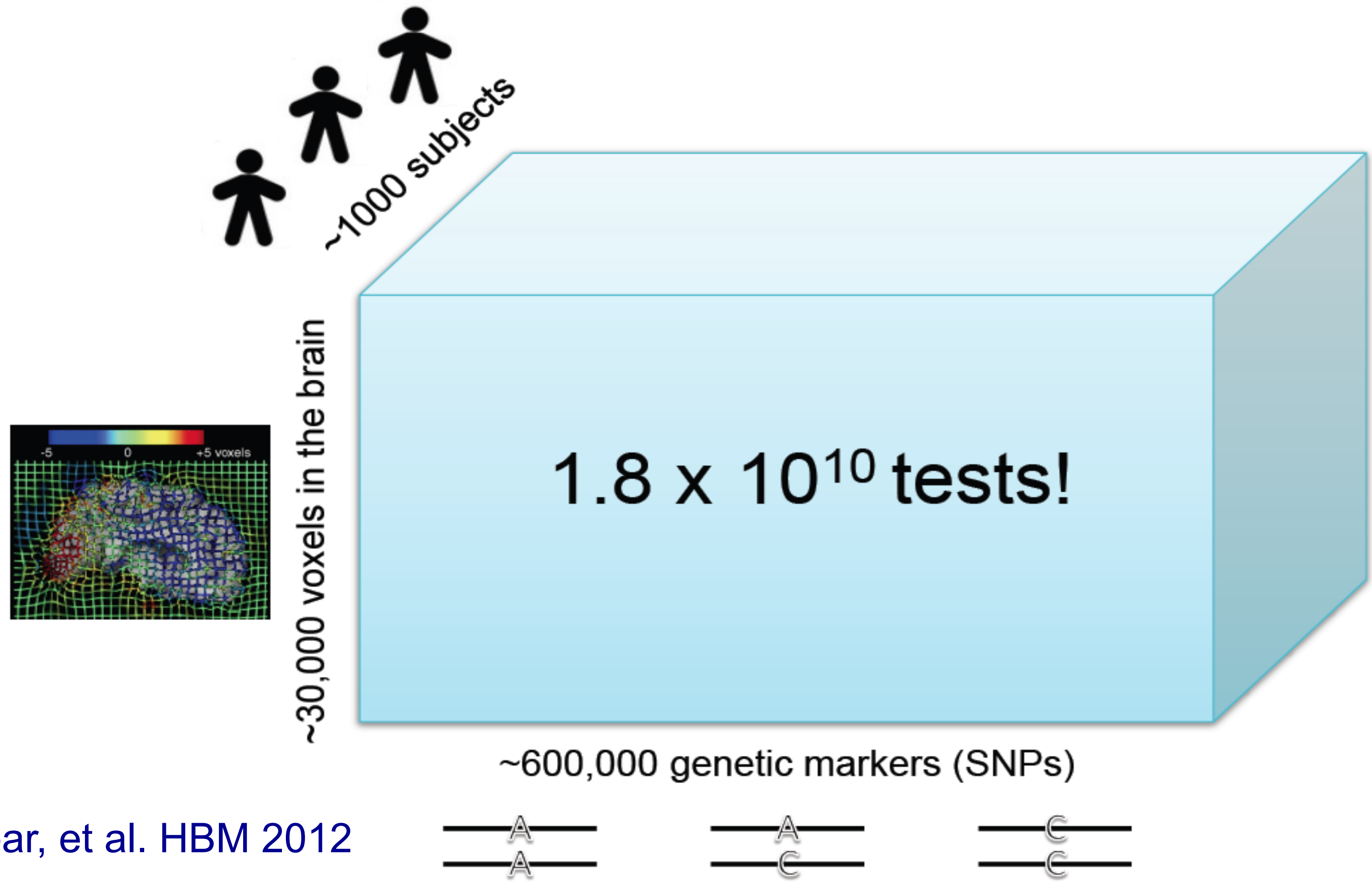

Hibar, et al. HBM 2012

Simulation I

N = 150, 200, 250, 300

q = 50, 100, 150, 200

$e_i \sim$ Normal $(0, Cov(e_i))$

$Var(e_{ij}) = 1$, $j = 1 \sim q$

$Cov(e_{i1}, e_{i2}) = 0.6$

$Cov(e_{i1}, e_{ij}) = 0.3$, $j = 3 \sim q$

$Cov(e_{ij}, e_{ik}) = 0.1$, $j = 2 \sim q$, $k = 3 \sim q$

$$y_i = B^t x_i + e_i$$

H_0: $(\beta_{1,SNP}, \ldots, \beta_{q,SNP}) = 0$

$\beta_{1,SNP} = 0.5$

$\beta_{2,diagnosis} = 0.5$

Others are **zero**

P = 5

Interest : Additive SNP

– MAF 0.05, 0.1, 0.2, 0.3, 0.4, 0.5

Diagnosis Status ~ Bernoulli (0.5)

3 Continuous covariates ~ Normal (0, V)

($v_{ii} = 1$ and $v_{ij} = 0.3$)

Results: Type I Error

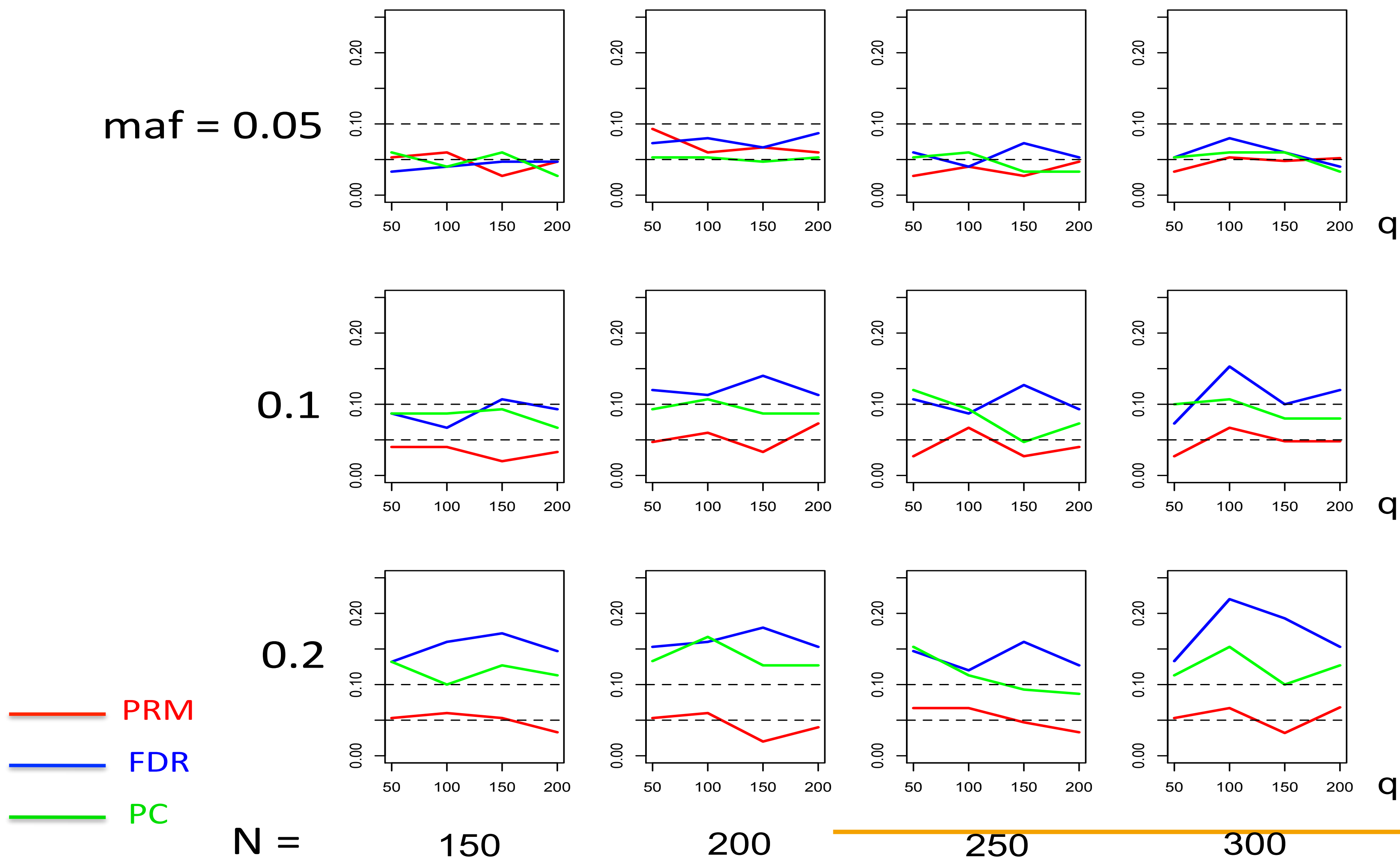

Results: Type I Error

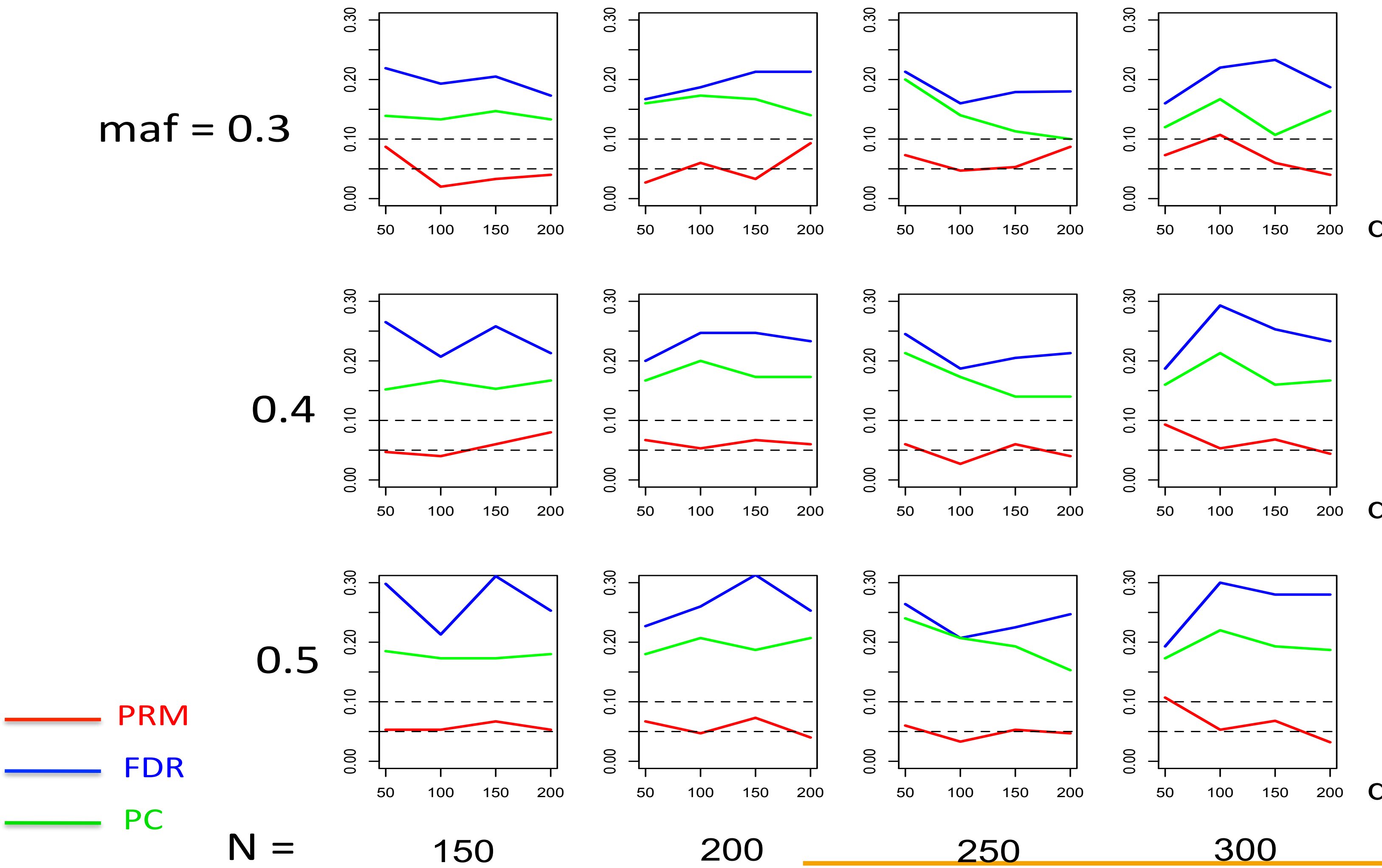

Results: Power

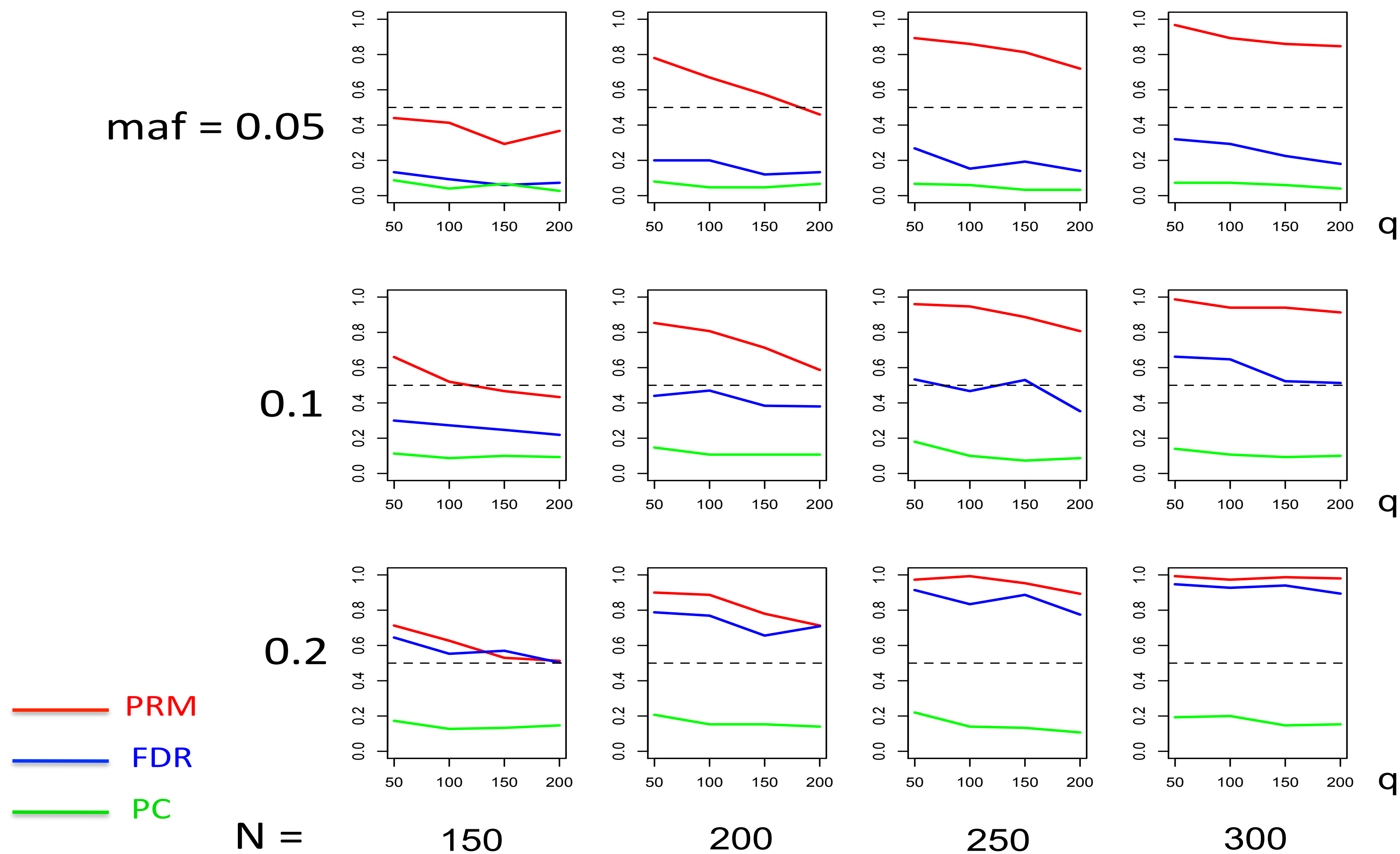

Results: Power

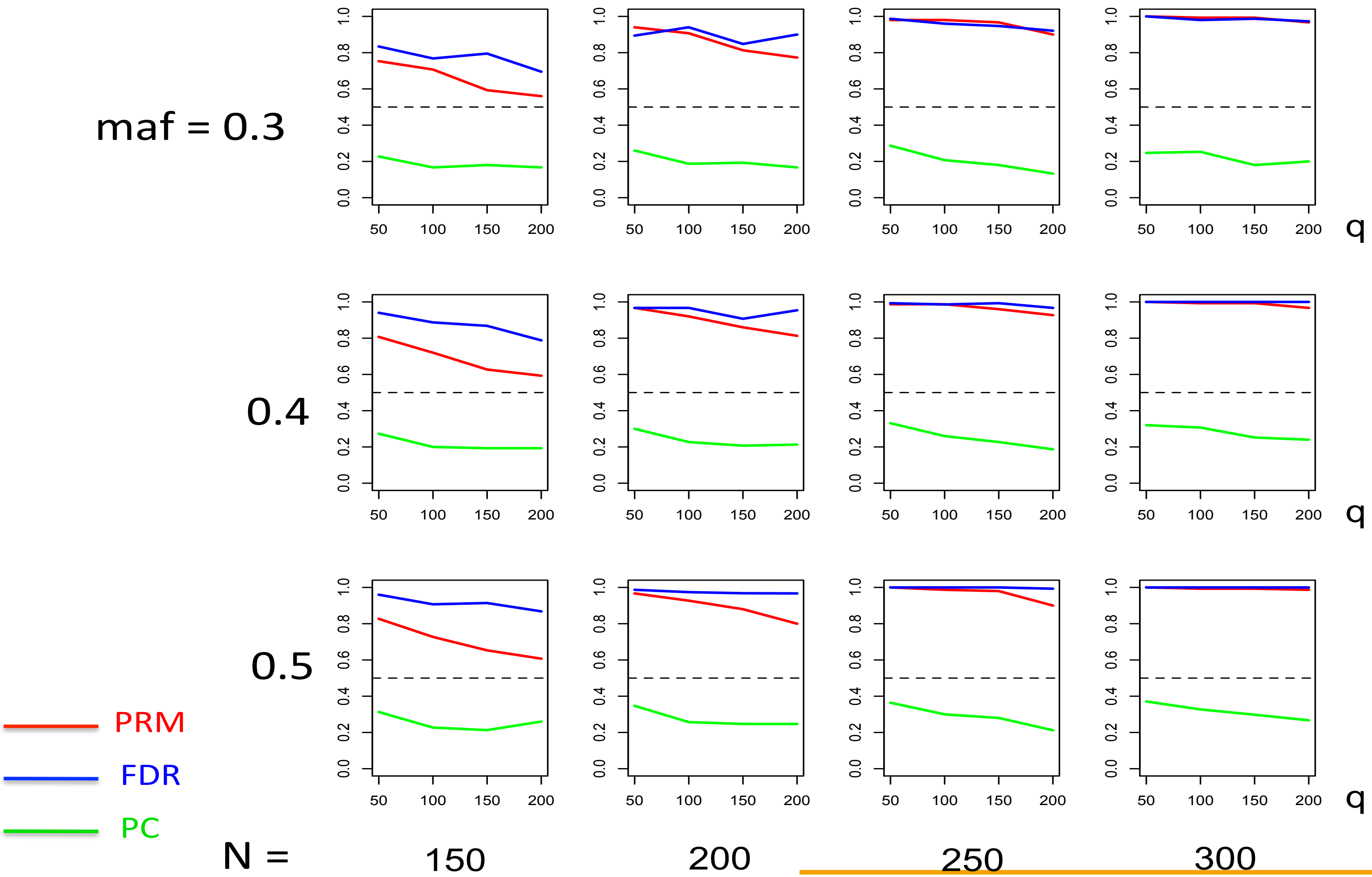

Simulation II

Voxed Based	True Value	Our Method
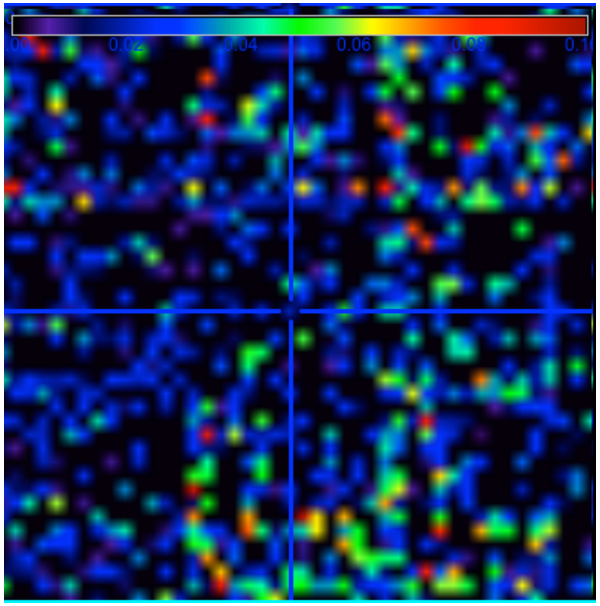	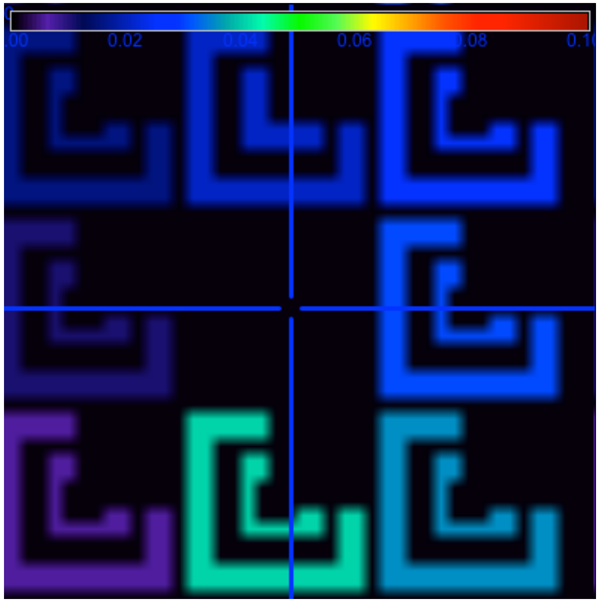	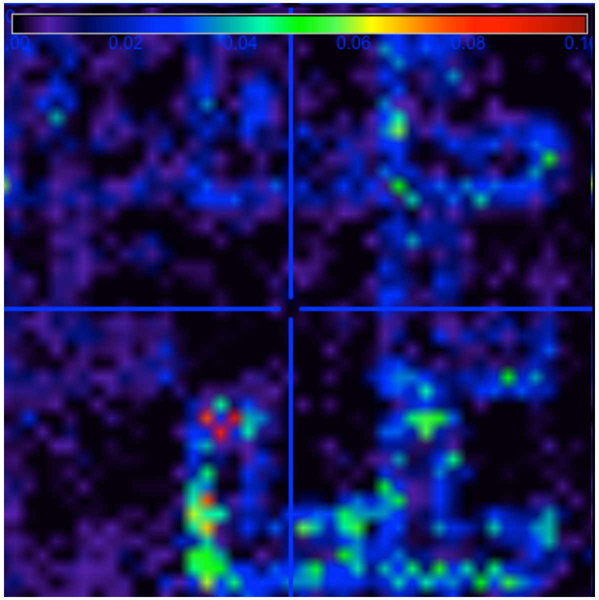

Results: Hypothesis Testing

$H_0 : \sigma^2_\gamma(v) = 0$ vs $H_1 : \sigma^2_\gamma(v) \neq 0$

Voxel Based **FMEM** **Voxel Based** **FMEM**

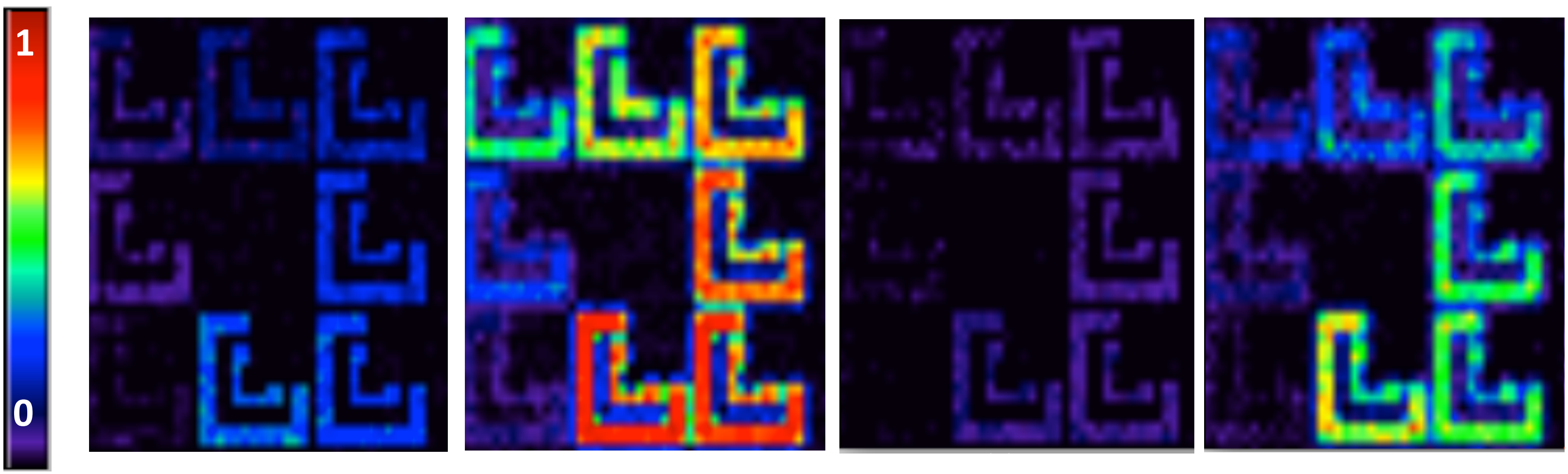

Neonatal Study

- **Objective:** Identify putative genes impacts early age brain development
- **Subject:** 237 infants (128 M, 109 F)
- **Image:** 47 ROIs from diffusion-weighted images and T1 weighted images which was assessed once for each subject
- **Demographic Info:** Gestational age (264.0 ± SD 18.91 days), Age after birth (30.2 ± SD 17.8 days), Gender, ICV (481799.9 ± SD 61528.96) , 9 SNPs
- **Method:** Projection Regression Method (PRM)

Neonatal Study

- **Null Hypothesis H_0** : the i^{th} SNP has no effects on the brain volume size, while adjusting for other SNPs and demographic information

Gene	Abbreviation	SNP	P-value
Catechol-O-methyltransferase	COMT	rs4680	0.88
Disrupted-in-schizophrenia-1	DISC1	rs821616	0.75
		rs6675281	**0.016**
Neuregulin 1	NRG1	**rs35753505**	**0.0136**
		rs6994992	0.51
Estrogen Receptor Alpha	ESR1	rs9340799	0.44
		rs2234693	0.57
Brain-derived Neurotrophic Factor	BDNF	rs6265	0.60
Glutamate Decarboxylase 1	GAD1 (GAD67)	rs2270335	0.39

ADNI Study

- **Objective:** Heritability of 93 Regional Brain Volumes explained by all common SNPs
- **Subject:** 818 elders/747
- **Genetic Data:** 620,901/512,905 SNPs
- **Demographic Info:** Gender, Baseline age, Diagnostic status, Handedness, Education Level, first ten eigenfunctions

Brain structure is highly heritable

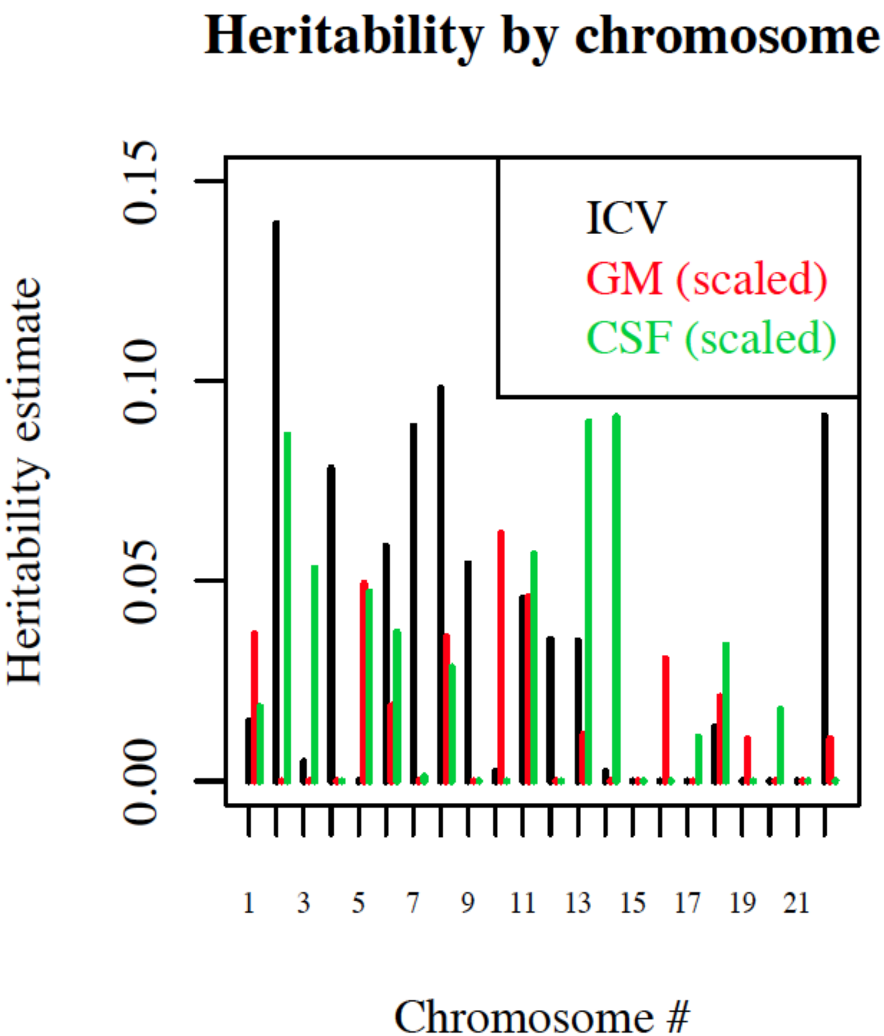

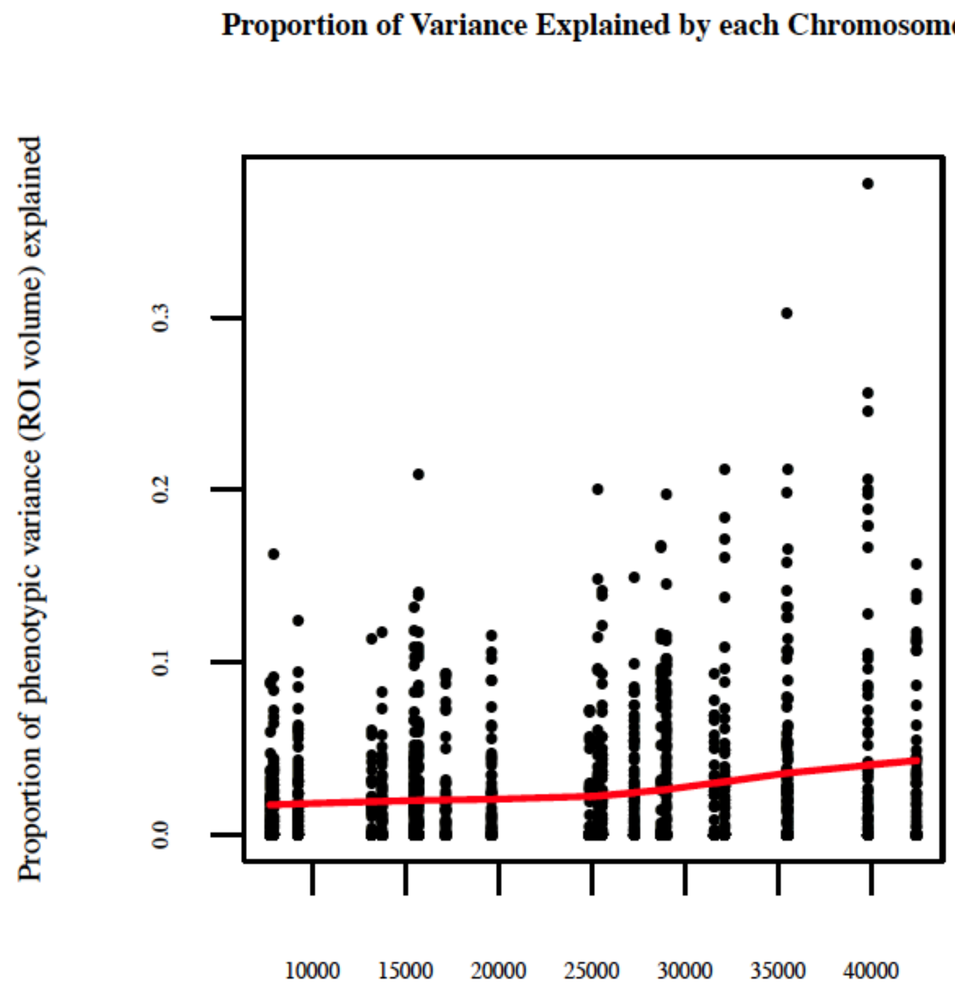

Highly heritable brain structures

Region	Estimated Heritability	LRT P-value
ICV	0.80331	0.0368
GM Volume	1.00E-06	0.5
WM Volume	1.00E-06	0.5
CSF Volume	0.60148	0.0965

ROI	Jakob ROI Label	Description	Estimated Heritability	LRT P-value	Cluster
39	53	caudate nucleus right	0.999999	0.0159	1
40	54	cuneus left	0.999999	0.00694	1
68	100	entorhinal cortex right	0.999999	0.000844	1
59	88	superior parietal lobule right	0.874851	0.0236	1
89	175	cuneus right	0.762135	0.0415	1
43	59	temporal lobe WM right	0.757369	0.0528	1
52	73	occipital lobe WM left	0.734196	0.0523	1
11	11	globus palladus right	0.710845	0.0591	1
58	86	perirhinal cortex right	0.695142	0.0685	1
8	8	lateral ventricle right	0.683006	0.0848	1
67	99	lateral occipitotemporal gyrus right	0.641683	0.0699	1
5	5	precentral gyrus right	0.620564	0.087	1

Acknowledgement